AD-A060 467 PRINCETON UNIV N J DEPT OF AEROSPACE AND MECHANICAL--ETC F/G 1/3
A STUDY OF LONGITUDINAL CONTROLLABILITY AND STABILITY REQUIREME--ETC(U)
AUG 78 D R ELLIS, C L GRIFFITH DOT-FA75WA-3679
UNCLASSIFIED AMS-1369 FAA-RD-78-113 NL

1 OF 2
AD A060 467

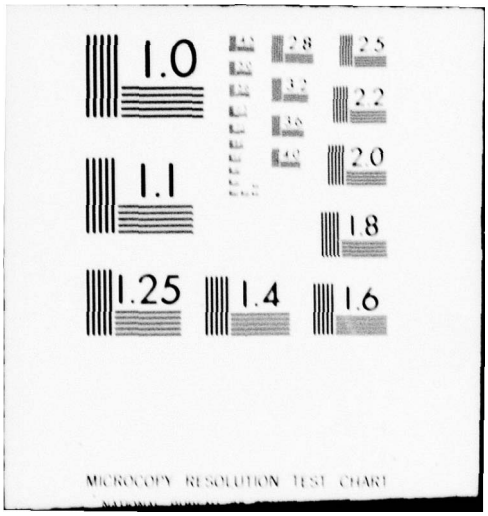
1.0
1.1
1.25
1.4
1.6
2.8
3.2
3.6
4.0
2.5
2.2
2.0
1.8
MICROCOPY RESOLUTION TEST CHART

Report No. FAA-RD-78-113

(12) LEVEL II

A STUDY OF LONGITUDINAL CONTROLLABILITY AND STABILITY REQUIREMENTS FOR SMALL GENERAL AVIATION AIRPLANES

David R. Ellis
Cornelius L. Griffith

August 1978
Final Report

Prepared for

U.S. DEPARTMENT OF TRANSPORTATION
Federal Aviation Administration
Systems Research & Development Service
Washington, D.C. 20590

NOTICE

This document is disseminated under the sponsorship of the Department of Transportation in the interest of information exchange. The United States Government assumes no liability for its contents or use thereof.

Technical Report Documentation Page

1. Report No.	2. Government Accession No.	3. Recipient's Catalog No.
FAA-RD-78-113		

4. Title and Subtitle

A Study of Longitudinal Controllability and Stability Requirements for Small General Aviation Airplanes

5. Report Date	
August 1978	
6. Performing Organization Code	
8. Performing Organization Report No.	
AMS-1369	

7. Author(s)

David R. Ellis, Cornelius L. Griffith

9. Performing Organization Name and Address

Flight Research Laboratory
Aerospace and Mechanical Sciences Department
Princeton University
Princeton, New Jersey 08540

10. Work Unit No. (TRAIS)	
11. Contract or Grant No.	DOT-FA75WA-3679
13. Type of Report and Period Covered	Final Report.
14. Sponsoring Agency Code	ARD-530

12. Sponsoring Agency Name and Address

Department of Transportation
Federal Aviation Administration
Systems Research and Development Service
Washington, D. C. 20591

15. Supplementary Notes

FAA Technical Monitors: Joseph W. Howell and Edward M. Boothe

146p.

16. Abstract

Several aspects of small airplane longitudinal stability and control were examined by means of analysis and in-flight simulation experiments. The influence of various levels of static stability in the context of approach, landing, and climb tasks was studied, with particular emphasis on the effects of force gradient augmentation by means of downsprings. Cases in which spring force varied with elevator deflection or with angle of attack were considered in addition to the classical constant-force type. Constant-force or increasing force with up-elevator springs were favored when the preferred natural (no device) gradient was not available.

Maneuvering stability tests focused on the effects of departure from linear force vs. normal acceleration characteristics; a local reduction in slope of 50 percent was detectable but considered to be acceptable.

17. Key Words	18. Distribution Statement
Static Stability Maneuvering Stability In-Flight Simulation Control System Devices	Document available to the public through the National Technical Information Service, Springfield, Virginia 22161.

19. Security Classif. (of this report)	20. Security Classif. (of this page)	21. No. of Pages	22. Price
UNCLASSIFIED	UNCLASSIFIED	145	

Form DOT F 1700.7 (8-72) Reproduction of completed page authorized

METRIC CONVERSION FACTORS

Approximate Conversions to Metric Measures

Symbol	When You Know	Multiply by	To Find	Symbol
		LENGTH		
in	inches	*2.5	centimeters	cm
ft	feet	30	centimeters	cm
yd	yards	0.9	meters	m
mi	miles	1.6	kilometers	km
		AREA		
in^2	square inches	6.5	square centimeters	cm^2
ft^2	square feet	0.09	square meters	m^2
yd^2	square yards	0.8	square meters	m^2
mi^2	square miles	2.6	square kilometers	km^2
	acres	0.4	hectares	ha
		MASS (weight)		
oz	ounces	28	grams	g
lb	pounds	0.45	kilograms	kg
	short tons (2000 lb)	0.9	tonnes	t
		VOLUME		
tsp	teaspoons	5	milliliters	ml
Tbsp	tablespoons	15	milliliters	ml
fl oz	fluid ounces	30	milliliters	ml
c	cups	0.24	liters	l
pt	pints	0.47	liters	l
qt	quarts	0.95	liters	l
gal	gallons	3.8	liters	l
ft^3	cubic feet	0.03	cubic meters	m^3
yd^3	cubic yards	0.76	cubic meters	m^3
		TEMPERATURE (exact)		
°F	Fahrenheit temperature	5/9 (after subtracting 32)	Celsius temperature	°C

*1 in = 2.54 (exactly). For other exact conversions and more detailed tables, see NBS Misc. Publ. 286, Units of Weights and Measures, Price $2.25, SD Catalog No. C13.10:286.

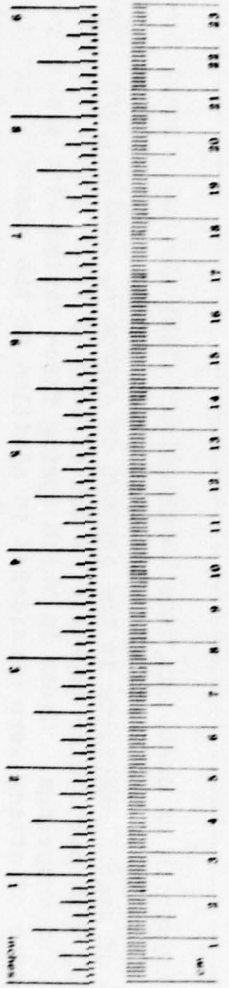

Approximate Conversions from Metric Measures

Symbol	When You Know	Multiply by	To Find	Symbol
		LENGTH		
mm	millimeters	0.04	inches	in
cm	centimeters	0.4	inches	in
m	meters	3.3	feet	ft
m	meters	1.1	yards	yd
km	kilometers	0.6	miles	mi
		AREA		
cm^2	square centimeters	0.16	square inches	in^2
m^2	square meters	1.2	square yards	yd^2
km^2	square kilometers	0.4	square miles	mi^2
ha	hectares (10,000 m^2)	2.5	acres	
		MASS (weight)		
g	grams	0.035	ounces	oz
kg	kilograms	2.2	pounds	lb
t	tonnes (1000 kg)	1.1	short tons	
		VOLUME		
ml	milliliters	0.03	fluid ounces	fl oz
l	liters	2.1	pints	pt
l	liters	1.06	quarts	qt
l	liters	0.26	gallons	gal
m^3	cubic meters	35	cubic feet	ft^3
m^3	cubic meters	1.3	cubic yards	yd^3
		TEMPERATURE (exact)		
°C	Celsius temperature	9/5 (then add 32)	Fahrenheit temperature	°F

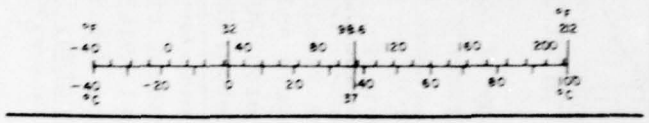

TABLE OF CONTENTS

LIST OF FIGURES

LIST OF SYMBOLS

A	Constant in control force equation.
a_t	Horizontal stabilizer lift curve slope, per rad.
a_w	Wing lift curve slope, per rad.
C_h	Hinge moment coefficient.
C_{h_b}	Elevator hinge moment parameter due to bobweight.
ΔC_{h_b}	Elevator hinge moment parameter due to elevator mass unbalance.
C_{h_e}	Elevator hinge moment coefficient.
C_{h_o}	Residual elevator hinge moment coefficient at zero angle of attack and zero elevator deflection.
C_{h_α}	Elevator floating tendency, $\frac{\partial C_h}{\partial \alpha}$, per rad.
C_{h_δ}	Elevator restoring tendency, $\frac{\partial C_h}{\partial \delta_e}$, per rad.
$C_{h_{\delta_t}}$	Trim tab effectiveness, $\frac{\partial C_h}{\partial \delta_t}$, per rad.
C_L	Lift coefficient, $\frac{L}{qS}$.
C_m	Pitching moment coefficient, $\frac{M}{qS\bar{c}}$.
C_{m_δ}	Elevator effectiveness, $\frac{\delta C_m}{\partial \delta_e}$, per rad.
$\bar{c}$	Wing mean aerodynamic chord, ft.
$\bar{c}_e$	Elevator mean aerodynamic chord, ft.
D_v	Drag damping derivative, $\frac{1}{m}\frac{\partial D}{\partial V}$, sec^{-1}.
D_α	Drag due to angle of attack, $\frac{1}{m}\frac{\partial D}{\partial \alpha}$, $ft/sec^2/rad$.
F_b	Control force due to bobweight, lb.
F_{b_o}	Residual control force due to bobweight with zero elevator deflection, lb.

F_c	Control force, lb.
F_d	Control force due to downspring, lb.
F_{d_o}	Residual control force due to downspring with zero angle of attack and zero elevator deflection, lb.
F_s	Stick force, lb.
G	Elevator gearing constant, rad/ft.
g	Acceleration of gravity, ft/sec^2.
H	Hinge moment, ft-lb.
H_e	Elevator hinge moment, ft-lb.
H_o	Elevator aerodynamic hinge moment in steady, equilibrium flight, ft-lb.
h_e	Elevator moment of intertia parameter.
h_i	Elevator bobweight and static balance parameter.
I_e	Elevator effective moment of inertia, $slug\text{-}ft^2$.
I_y	Airplane moment of inertia about lateral axis, $slug\text{-}ft^2$.
i_t	Horizontal stabilizer incidence angle, rad.
i_w	Wing incidence angle, rad.
j	$\sqrt{-1}$
K	Constant in control force equation, ft^2.
K_b	Slope of bobweight force vs. elevator deflection, lb/rad.
K_d	Slope of downspring force vs. elevator deflection, lb/rad.
K_e	Elevator radius of gyration, ft.
K_α	Slope of downspring force vs. angle-of-attack, lb/rad.

L	Lift, lb.
L_v	Lift/velocity derivative, $\frac{1}{m}\frac{\partial L}{\partial V}$, sec^{-1}.
L_α	Lift due to angle of attack, $\frac{1}{m}\frac{\partial L}{\partial \alpha}$, $ft/sec^2/rad$.
l_t	Tail length: distance from airplane center of gravity to horizontal stabilizer aerodynamic center, ft.
l_l	Elevator mass unbalance parameter.
m_e	Elevator mass, slug.
M_{ref}	Reference moment, ft-lb.
M_v	Speed stability, $\frac{1}{I_y}\frac{\partial M}{\partial V}$, $ft^{-1}\ sec^{-1}$.
M_α	Angle-of-attack static stability, $\frac{1}{I_y}\frac{\partial M}{\partial \alpha}$, sec^{-2}.
$M_{\dot{\alpha}}$	Angle-of-attack damping, $\frac{1}{I_y}\frac{\partial M}{\partial \dot{\alpha}}$, sec^{-1}.
M_δ	Elevator effectiveness, $\frac{1}{I_y}\frac{\partial M}{\partial \delta_e}$, sec^{-2}.
$M_{\dot{\theta}}$	Pitch damping derivative, $\frac{1}{I_y}\frac{\partial M}{\partial \dot{\theta}}$, sec^{-1}.
n	Load factor, $\frac{L}{W}$.
q	Dynamic pressure, $\frac{1}{2}\rho V^2$, lb/ft^2.
S	Wing area, ft^2.
S_e	Elevator area, ft^2.
S_t	Horizontal stabilizer area, ft^2.
s	Laplace transform variable.
T_{ph}	Period of phugoid mode, sec.
T_{sp}	Period of short period mode, sec.
T_v	Thrust/velocity derivative, $\frac{1}{m}\frac{\partial T}{\partial V}$, sec^{-1}.
V	Velocity, ft/sec.
$\bar{V}$	Tail volume coefficient, $\frac{S_t}{S}\frac{l_t}{\bar{c}}$.

V_o	Equilibrium velocity, ft/sec.
V_t	Trim velocity, ft/sec.
W	Weight, lb.
W_e	Elevator weight, lb.
x_e	Distance from elevator hinge line to elevator center of mass, ft.

Greek symbols

α	Angle of attack, rad.
α_o	Angle of attack for zero lift, rad.
α_t	Angle of attack of horizontal stabilizer, rad.
α_w	Angle of attack of wing, rad.
γ	Flight path angle, rad.
δ_e	Elevator deflection, rad.
δ_{e_o}	Elevator deflection at zero lift, rad.
δ_t	Trim tab deflection, rad.
ε	Downwash angle of airflow, rad.
ζ_{ph}	Damping ratio of phugoid mode.
ζ_{sp}	Damping ratio of short period mode.
η_t	Tail efficiency.
θ	Pitch attitude, rad.
μ	Airplane relative density factor, $\frac{m}{\rho S \bar{c}}$.
ρ	Density, slug/ft^3.
τ	Aerodynamic time, $\frac{m}{\rho s V}$, sec.

τ	Elevator effectiveness parameter, $\frac{d\alpha_t}{d\delta_e}$.
ω_{ph}	Frequency of phugoid mode, rad/sec.
ω_{sp}	Frequency of short period mode, rad/sec.

A dot "$\dot{}$" above a quantity indicates the time derivative of that quantity.

A STUDY OF LONGITUDINAL CONTROLLABILITY AND STABILITY REQUIREMENTS FOR SMALL GENERAL AVIATION AIRPLANES

D. R. Ellis and C. L. Griffith

1. INTRODUCTION

1.1 OBJECTIVE AND TOPICS COVERED

The objective of this study is to examine existing longitudinal stability-and-control criteria for small airplanes, giving special attention to the influence of commonly-used control system devices such as downsprings and bobweights. Although the operating principles of such devices have long been understood - bobweights were used on several World War II fighters to increase stick force per g - and some generalized research was undertaken in the 1950's (Refs. 1 and 2), there still exists little in the way of quantitative guidelines to aid in their use and design. In practice, the devices are usually developed on a cut-and-try basis, and installation considerations often dictate that the idealized constant-force springs and weights of the textbooks are not realized; both factors can influence the performance of the control system.

The study includes both analysis and in-flight simulation experiments; the topics covered in subsequent sections of the report are:

- A brief review of existing civil and military standards for longitudinal stability and control of small airplanes
- Factors in compliance with FAR Part 23 standards

- Review and analysis of longitudinal stability and control, with emphasis on the effect of downsprings and bobweights
- Description and results of in-flight simulation experiments
- Conclusions

1.2 EXISTING CONTROLLABILITY AND STABILITY STANDARDS

Civil Standards- Basic standards for controllability and stability of small general aviation airplanes are stated in Part 23 of the Federal Air Regulations (Ref. 3), Articles 23.41 through 23.253. The requirements for longitudinal controllability are generally qualitative in nature; they stipulate that without exceptional skill, alertness, or strength on the part of the pilot, it should be possible to safely maneuver the airplane during normal flight phases and to transition smoothly between those phases without exceeding operating limitations, such as limit load factor.

Longitudinal static stability of a type termed "stick free" in most textbooks is required. This stable control force gradient (a pull force to maintain speeds below the trim speed, a push force for higher speeds) must be evident outside of the friction band for ± 15 percent variations about the trim speed, and must be demonstrated for specific climb, cruise, and approach and landing conditions. No particular minimum gradient is specified for Part 23 airplanes, but there is the qualitative requirement that any substantial speed change from trim will result in a clearly perceptible stick force. (For transport category airplanes FAR Part 25 stipulates a minimum gradient of 1 pound for each 6 kt.)

Positive stick-free maneuvering stability is required through Article 23.155, which defines the minimum control forces needed

to reach limit load factor. This requirement, in contrast to those for controllability and static stability, is quantitative, with minimum forces being related to airplane weight and differing for wheel- and stick-type controllers. Since the requirement is linked to positive limit load factor, the minimum permissible gradient of stick force per "g" (assuming a linear variation of stick force with increasing load factor) will differ for normal, utility, and acrobatic category airplanes.[1] If cast in the form of equivalent linear stick force gradient (F_s/n, lb per g), the requirement may be summarized as follows for wheel controls:

Airplane Category	Minimum F_s/n , lb per g
Normal	$7.14 \leq \frac{W}{280} \leq 17.85$
Utility	$5.88 \leq \frac{W}{340} \leq 14.7$
Acrobatic	$4.0 \leq \frac{W}{500} \leq 10.0$

(The bounding values appear because the regulation stipulates that the force required to reach limit load factor must be at least 20 lb, but need not be more than 50 lb, regardless of airplane weight.) The requirement must be met with maximum cruise power and at speeds greater than the minimum at which limit load factor may be achieved without stalling.

Longitudinal dynamics receive only brief mention in Part 23 (Article 23.181); the article simply specifies that any short period oscillations must be heavily damped with both fixed and free controls.

---

[1] Positive limit load factor varies as follows for airplane categories:
Normal category - 3.8g
Utility category - 4.4g
Acrobatic category - 6.0g

No quantitative definitions of "short period" or "heavily damped" are given. Longer period (phugoid) oscillations are not mentioned and presumably are allowed to be undamped or unstable.

To summarize, the civil requirements for longitudinal controllability are qualitative in nature and stress safe operability throughout the normal flight envelope. The static stability requirement is also qualitative; it specifies stable force feel ("stick-free" stability) but does not rule out unstable control deflection vs. velocity ("stick-fixed") characteristics. Positive maneuvering stability is required, and quantitative limits are stated. Short period dynamics must be heavily damped (no quantitative specification); long period oscillations are not treated in the requirements.

Military Standards - Small, light (Class I) airplanes are covered in the military specification for flying qualities (Ref. 4). Although a close reading of the background document (Ref. 5) will confirm that the orientation is toward the larger, faster classes of aircraft, and that recent experimental data for small airplanes is sparse, it is instructive to compare the civil and military standards.

First, it should be noted that the military specification defines both clearly adequate and minimum safe levels of flying qualities, whereas the civil standards are generally oriented toward definition of minimum acceptable (and, hence, safe) conditions. Although it is not clear that the lowest military flying qualities level (Level 3) truly corresponds to the civilian case, since it alludes to "excessive pilot workload" and "inadequate mission effectiveness", it will be used as the basis of discussion here.

In the military specification, controllability throughout the normal flight envelope is called for, as in the civil standards, but it deals in somewhat more detail with such items as attainable load

factor and force limits in various maneuvers.

Longitudinal static stability is specified, but whereas FAR Part 23 calls only for stick-free stability, the military specification requires both force and elevator deflection gradients to be in a stable sense (increasing pull forces and aft motion of the elevator control to maintain slower airspeeds and the opposite to maintain higher airspeeds). This applies over a range about trim speed of ±15 percent (or ±50 kt EAS, whichever is less); no quantitative requirement is placed on the gradient.

In contrast to the civil standards, the military specification places quantitative requirements on dynamic stability in connection with maneuvering flight. Both frequency and damping ratio of the short period mode are specified, the frequency requirement being related to the lift-response parameter, n/α. Specific requirements depend on the flight phase and are not simply stated. For example, small airplanes are required to have ω_{sp} greater than 0.6 rad/sec to meet Level 3 during landing; the corresponding minimum short period damping ratio is $\zeta_{sp} = 0.15$.

Long period (phugoid) oscillations also are treated in the military specification. The mode may be unstable, but the time to double amplitude must be at least 55 sec.

Positive maneuvering stability is called for, in terms of both increasing control force and aft control deflection for increasing load factor. The variation in force with steady-state normal acceleration is specified to be approximately linear, with "local" gradient departures from linearity of more than 50 percent considered to be excessive. Both maximum and minimum force gradients, F_s/n, are specified; for the lowest level of flying qualities (Level 3), these are 240 lb/g and 6 lb/g, respectively, for wheel controllers (the equivalent Part 23 minimum

gradient would be 4 lb/g for acrobatic category airplanes).

Thus the civil and military requirements for small airplanes are seen to be similar in many respects. The major differences may be summarized as follows:

- The military specification requires both stick-force and stick-position ("stick-free") static stability; the civil standards require only stick-force stability.
- The military specification places quantitative requirements on short period frequency and damping: FAR Part 23 contains the qualitative stipulation that short period motions be heavily damped.
- The military specification has quantitative requirements for long-period phugoid oscillations; FAR Part 23 does not cover the phugoid mode.

1.3 FAR PART 23 COMPLIANCE AND RELATED FACTORS

Achieving Stable Force Gradients - The requirement for stable stick force vs. velocity characteristics is often difficult to meet in modern light planes with large center of gravity (c.g.) range and relatively high installed power. The critical condition is often the aft-c.g., climb case, where the destabilizing effects of power tend to be most evident; even if a small stable gradient is obtainable near trim, it will tend to deteriorate and become unstable at the lowest speeds within the required range.

A downspring is commonly installed to restore the necesaary stable gradient. Although this is often a simple, low-cost approach to compliance with the regulation, there are several related factors which are more or less disadvantageous:

- The long-period (phugoid) oscillation will be shortened in period and more lightly damped, sometimes

even divergent. Although this is allowed by the regulations, it appears as a tendency for the airplane to wander in speed, pitch attitude, and altitude, and the need for constant stabilization adds to the pilot workload, particularly when flying on instruments.

- Control system friction in small airplanes is frequently large enough to interfere with proper small-amplitude operation of the device, requiring it to be over-sized in order to produce much effect for small speed changes; this tends to accentuate the dynamics problems when operating outside of the friction band.

- Transient control motions and forces due to the down-spring can be distracting; an example is the large increase in stick force experienced in some twins as power is reduced for landing, causing the dynamic pressure at the horizontal tail to decrease suddenly.

- Very large forces may be encountered if up-elevator deflections are required at below-flight speed, such as for nose wheel lift-off or hold-off in soft-field operations.

Maneuvering Stability Tests- Compliance with the maneuvering stability requirements of Article 23.155 of FAR Part 23 may be demonstrated in either of two ways:

- Measurement of load factor achieved with the specified limiting stick force.

- Determination of the stick force per "g" gradient at low load factor, with extrapolation to limit load factor.

The second method carries the implication that the change in load factor will be essentially linear, and in most normally configured airplanes it is. However, non-linear cases of the type sketched below in Fig. 1-1 have been documented.

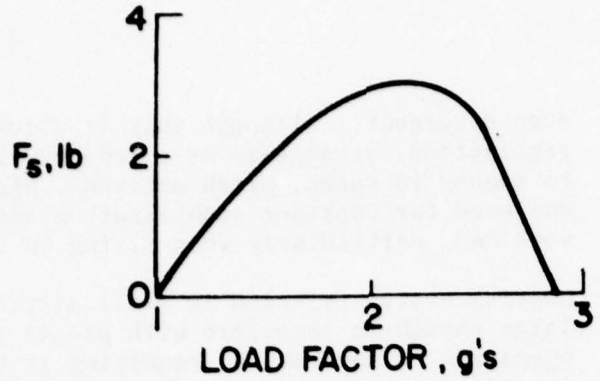

Figure 1-1. Stick Force vs. Load Factor

The flattening and eventual reversal of the curve are known to be dangerous, and certainly would not be allowed under the general requirement that the airplane be safely controllable and maneuverable throughout its normal flight envelope (Ref. 3).
However, there are two important points to be noted concerning the linearity of the curve:

- The F_s vs n curve is not always linear, and extrapolation from low-g conditions can be misleading.
- Although flattening to zero or negative stick force gradient is clearly undesirable, some local flattening (up to 50 percent) has been found acceptable in military practice (Ref. 4).

A bobweight can, of course, be used to augment low natural stick-force per g, though a simple form will not cope with nonlinearities.

Classical versus Non-Classical Devices - Downsprings and bobweights are now commonly encountered in small airplanes, but practical installations usually exhibit somewhat different operating characteristics from their textbook progenitors. Classical downsprings and bobweights are considered to exert constant force into the control system. The spring is considered to be very long compared to the amount by which it is deflected, and the mass of the bobweight is considered to be close to the center of gravity and to move vertically (i.e. parallel to the Z axis).

In practice, springs are usually quite short for convenience of installation and low weight, and the force exerted varies markedly with elevator deflection; some common variations are sketched in Fig. 1-2, where F_d represents the force required at the control column to hold the elevator in a given position at zero airspeed.

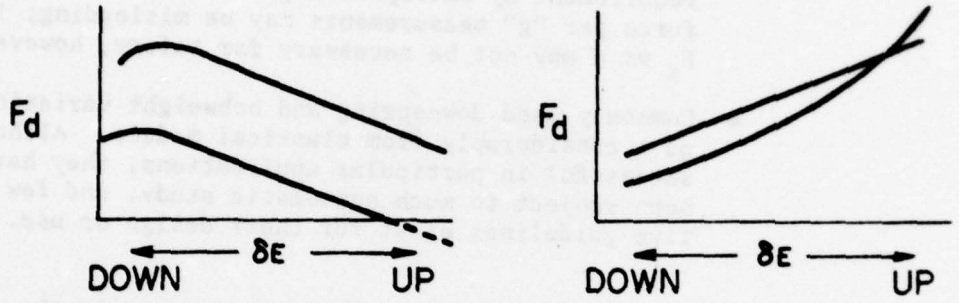

Figure 1-2. Commonly Found Downspring Force Characteristics.

Similarly, practical bobweights often turn out to vary with elevator deflection and occasionally are arranged to go over center for large deflections; often they are located considerably ahead of or behind the center of gravity, which influences their operation.

Recently another downspring variation has appeared which differs considerably in operation from the classical form, namely, a spring attached to a servoactuator which is driven by an angle-of-attack signal. The α-tensioned downspring works in the sense of increasing the down-elevator force on the control system at high angle of attack, the servo being in the extended (least spring tension) position for high speed operation. This scheme permits the force gradient to be increased over particular speeds of interest, such as the low end of the climb range. However, actuator rate is obviously important, even though the basic function is to increase the static stick force gradient; a fast actuator could lead to gust sensitivity and distracting elevator transients.

1.4 SCOPE OF STUDY

The foregoing discussion may be summarized as follows:

- Compliance with the existing static stability standards of FAR Part 23 by use of downsprings may have certain disadvantageous side effects.

- Demonstrating compliance with the maneuvering stability requirement by extrapolating from low load factor stick force per "g" measurements may be misleading; linear F_s vs. n may not be necessary for safety, however.

- Commonly used downspring and bobweight variations depart considerably from classical models. Although successful in particular applications, they have not been subject to much systematic study, and few quantitative guidelines exist for their design or use.

Various aspects of these issues are addressed in the subsequent sections of the report. In particular, the analysis section extends the classical treatment of downsprings and bobweights to include some of the elevator deflection dependent variations mentioned above.

The in-flight simulator tests explored the piloting implications of the increasing- and decreasing-force springs and the α-tensioned downspring. In addition, limited testing was carried out with nonlinear stick force per "g" characteristics.

2. REVIEW AND ANALYSIS OF LONGITUDINAL STABILITY AND CONTROL

2.1 GENERAL INTRODUCTION

This chapter describes an analytical study of several design parameters affecting airplane longitudinal stability and control. Emphasis is on those airframe and control system parameters which are available to the designer for adjusting stability and control characteristics. The discussion is oriented toward general aviation airplanes, and the baseline configuration selected for analysis is representative of airplanes in this class. Both static and dynamic longitudinal stability are discussed, and much of the discussion is cast in terms of control force trim curves. These trim curves are plots of control force as a function of airspeed, and they conveniently illustrate the control force required to fly at an off-trim airspeed.

The discussion is divided into basic airframe design parameters and control system design parameters. Basic airframe parameters discussed are angle of attack static stability M_α, elevator floating tendency C_{h_α}, and elevator restoring tendency C_{h_δ}. The control system design parameters discussed include downsprings and bobweights, commonly used for augmenting the stick-free longitudinal static stability of an airplane. The discussion herein reviews classical downspring and bobweight theory, and then extends the classical theory to consider downspring and bobweight implementations which yield a device force that varies with elevator deflection or angle of attack.

To allow illustrative calculations of the effect of the study parameters on stability-and-control characteristics, a baseline airplane configuration is defined. These parameter values and stability derivatives are typical of those encountered in small general aviation airplanes.

The nomenclature and conventions are generally those of Ref. 6.

TABLE 2-1

PARAMETERS DEFINING BASELINE AIRPLANE

a_t	= 3.88 per rad	k_e	= 0.66 ft.
a_w	= 4.71 per rad	l_t	= 16.4 ft.
$\bar{c}$	= 5.7 ft.	m_e	= 0.84 slug
$\bar{c}_e$	= 1.07 ft.	S	= 184 ft^2
G	= 1.00 per ft.	S_e	= 14.1 ft^2
I_e	= 0.366 slug-ft^2	$\bar{V}$	= 0.67
I_y	= 2773 slug-ft^2	W	= 3100 lb
i_t	= -3 deg.	x_e	= 0.057 ft
i_w	= 0.5 deg.	τ	= 0.53

TABLE 2-2

NOMINAL STABILITY DERIVATIVES OF BASELINE AIRPLANE AT 70-KT TRIM SPEED

$(D_V - T_V)$	= 0.16 sec^{-1}	$M_{\dot{\theta}}$	= -1.7 sec^{-1}
$(D_\alpha - g)$	= 12.0 $\frac{ft/sec^2}{rad}$	M_{δ_e}	= -8.7 sec^{-2}
L_V	= 0.58 sec^{-1}	$\frac{\partial H}{\partial \alpha_t}$	= -45.2 $\frac{ft\text{-}lb}{rad}$
L_{α/V_o}	= 1.2 sec^{-1}	$\frac{\partial H}{\partial \delta_e}$	= -129.2 $\frac{ft\text{-}lb}{rad}$
M_V	= 0		
M_α	= -6.0 sec^{-2}	$\frac{\partial H}{\partial \dot{\delta}_e}$	= -3.91 $\frac{ft\text{-}lb}{rad/sec}$
$M_{\dot{\alpha}}$	= 0.82 sec^{-1}		

2.2 BASIC AIRFRAME DESIGN PARAMETERS

Angle-of-Attack Static Stability (M_α) - A negative value of the angle-of-attack stability parameter, M_α, indicates longitudinal static stability, with a nose-down (negative) pitching moment resulting from a positve angle-of-attack perturbation. The most important factors influencing the size of M_α are tail design and center-of-gravity (c.g.) location. The value of M_α becomes more negative (i.e. more stable) with increasing horizontal tail area S_t , tail length l_t (the distance from wing aerodynamic center to horizontal tail aerodynamic center), and horizontal tail lift-curve slope, a_t . It also becomes more negative as airplane c.g. moves forward, and vice versa; thus,the operators of the airplane can exert an overriding influence on static stability through load distribution.

Figures 2-1 and 2-2 show control force trim curves for control-fixed M_α equal to + 1.25, -1.25, -6.0, and -12.0. The trim curve for M_α = -1.25 is plotted alone in Figure 2-2, since this plot requires an expanded control force axis. As M_α becomes more negative, the increase in stability is illustrated by the increasing control force gradient through trim, dF_c/dV. The more stable the airplane, the larger the control force required to hold a given off-trim airspeed. Note that for the statically unstable airplane (M_α = +1.25), the pilot is confronted with the unfamiliar situation of holding a pull force to fly faster than the trim speed.

The trim curve in Figure 2-2 illustrates an interesting phenomenon. Although the airplane is slightly stable control-fixed (M_α = -1.25),note that the control force trim curve is unstable. This is because the baseline configuration on which the trim curves are based has a negative value of the elevator floating tendency, $\partial H/\partial \alpha_t$ (= -45.2 ft-lb/rad). The tendency of the elevator to float with the

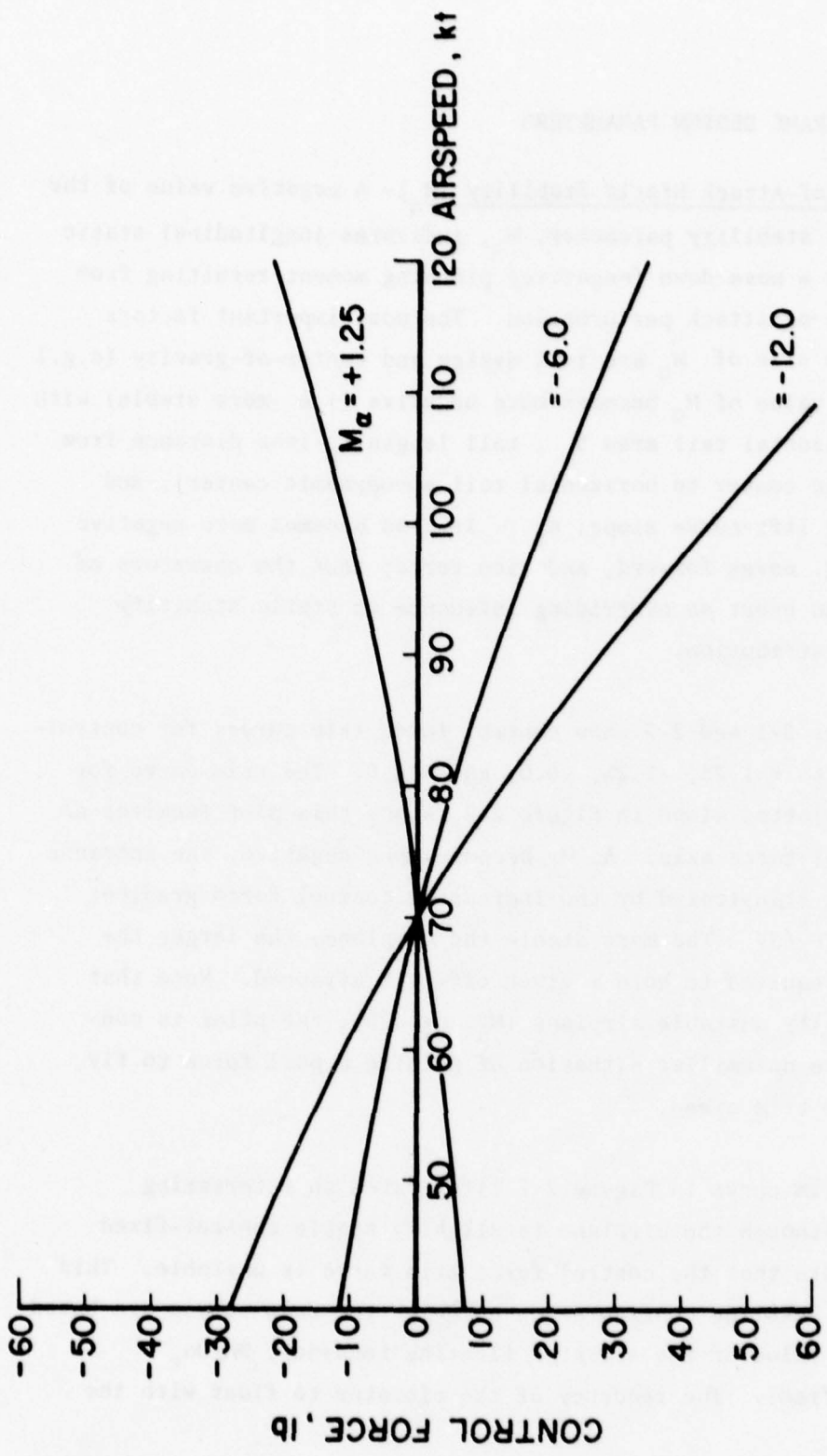

Figure 2-1. Basic Airframe Trim Curves with M_α as Parameter.

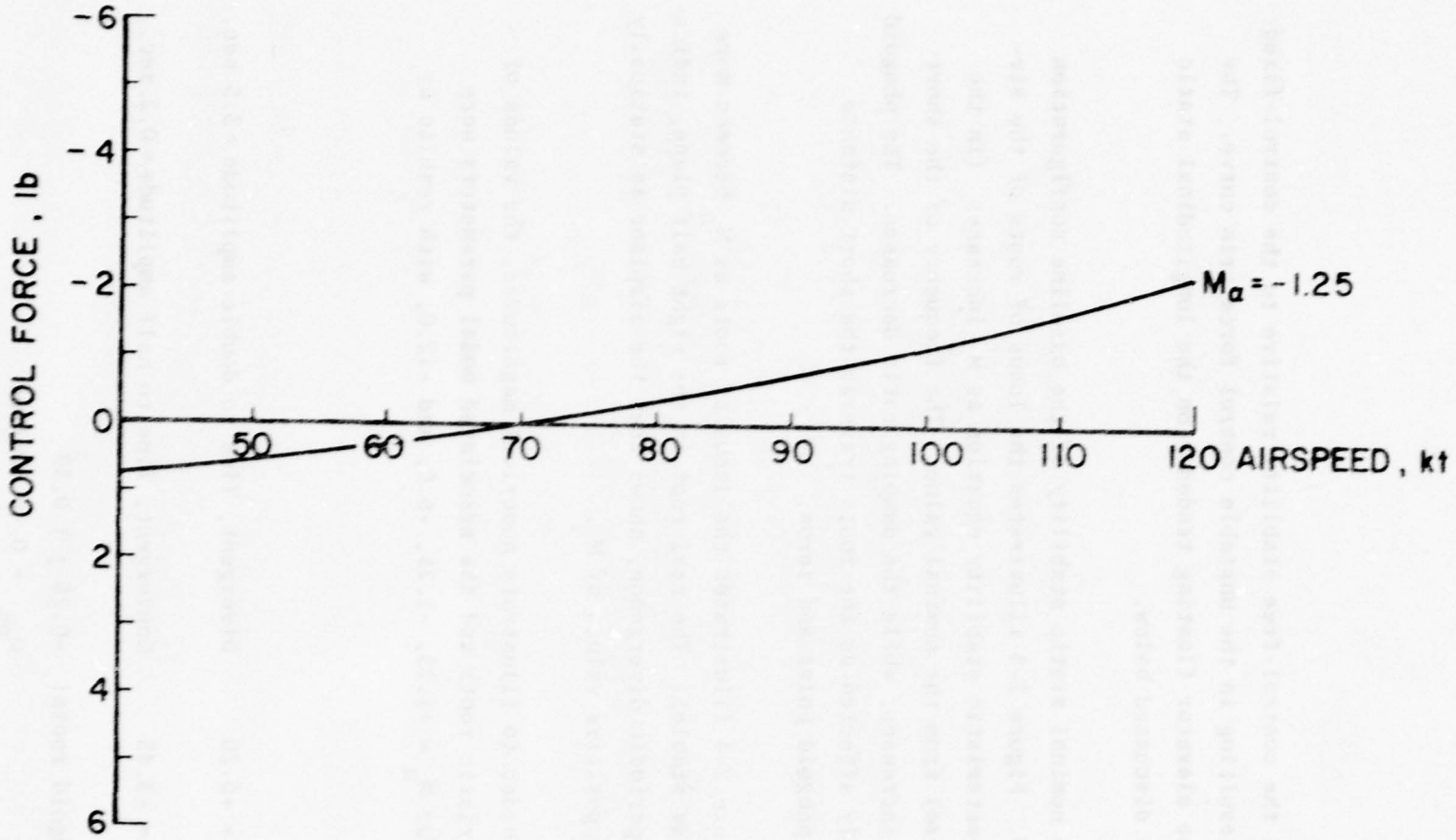

Figure 2-2. Basic Airframe Trim Curve, $M_\alpha = -1.25$.

wind reduces the control-free stability relative to the control-fixed stability, resulting in the unstable control force trim curve. The effect of the elevator floating tendency on the longitudinal static stability is discussed below.

The nominal static stability of the baseline configuration is $M_\alpha = -6.0$. Figure 2-3 illustrates the locus of roots of the airplane's characteristic stability equation as M_α increases (in the negative sense) from the nominal value. The frequency of the short period mode increases, while the damping ratio decreases. The phugoid mode is hardly affected as the roots traverse the short distance between the phugoid poles and zeros.

Figure 2-4 illustrates the locus of roots as M_α becomes more positive (less stable). The real root in the right half plane, indicative of an aperiodic divergence, shows that the airplane is statically unstable for positive values of M_α.

In order to illustrate numerical magnitudes, the values of the characteristic roots and the associated modal parameters were calculated for $M_\alpha = +1.25, -1.25, -6.0$, and -12.0, with results as follows:

$M_\alpha = +1.25$:

$r_1 = +0.20$ Divergent, Time to double amplitude = 3.5 sec.

$r_2 = -3.45$ Convergent, Time to half amplitude = 0.2 sec.

Phugoid roots: $-0.25 \pm j\ 0.39$

$\omega_{ph} = 0.40$ rad/sec

$T_{ph} = 14$ sec

$\zeta_{ph} = 0.54$

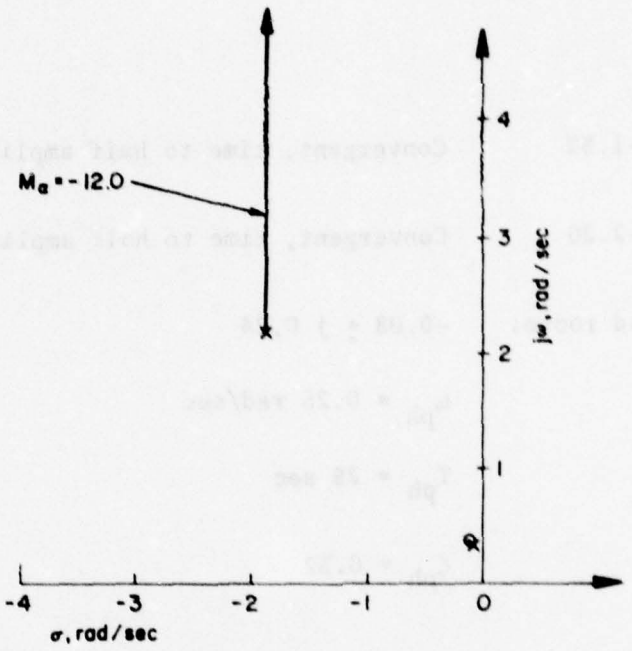

Figure 2-3. M_α Root Locus: Negative ΔM_α (Increasing Static Stability)

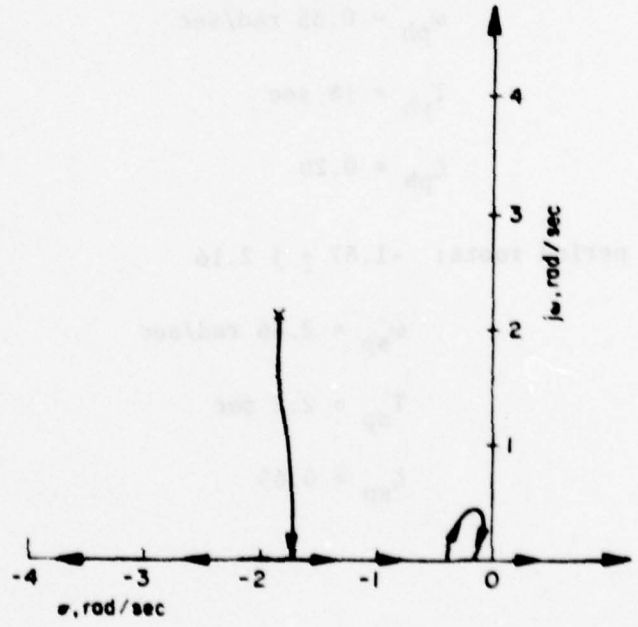

Figure 2-4. M_α Root Locus: Positive ΔM_α (Decreasing Static Stability)

$M_\alpha = -1.25$:

$r_1 = -1.52$ Convergent, time to half amplitude = 0.46 sec.

$r_2 = -2.20$ Convergent, time to half amplitude = 0.32 sec.

Phugoid roots: $-0.08 \pm j\ 0.24$

$\omega_{ph} = 0.25$ rad/sec

$T_{ph} = 25$ sec

$\zeta_{ph} = 0.32$

$M_\alpha = -6.0$:

Phugoid roots: $-0.07 \pm j\ 0.34$

$\omega_{ph} = 0.35$ rad/sec

$T_{ph} = 18$ sec

$\zeta_{ph} = 0.20$

Short period roots: $-1.87 \pm j\ 2.16$

$\omega_{sp} = 2.86$ rad/sec

$T_{sp} = 2.2$ sec

$\zeta_{sp} = 0.65$

$M_\alpha = -12.0$

Phugoid roots $-0.07 \pm j\ 0.36$

$\omega_{ph} = 0.37$ rad/sec

$T_{ph} = 17$ sec

$\zeta_{ph} = 0.19$

Short period roots: $-1.87 \pm j\ 3.26$

$\omega_{sp} = 3.75$ rad/sec

$T_{sp} = 1.7$ sec

$\zeta_{sp} = 0.50$

Elevator Floating Tendency (H_α) - Elevator Floating Tendency, H_α, accounts for the difference between the control-fixed and control-free static stability of the airplane. A tendency of the elevator to float upward with increasing angle of attack (negative H_α) reduces the pitching moment contribution of the horizontal tail with elevator free, reducing the control-free static stability from the control-fixed level. Conversely, positive H_α increases control-free stability relative to the control-fixed condition.

These H_α effects can also be explained in terms of neutral point behavior. The control-fixed neutral point is the c.g. location for neutral control-fixed static stability. Analogously, the control-free neutral point is the c.g. location for neutral control-free static stability. An increase in stability is represented by aft mevement of the neutral point. Hence, for the case of negative H_α, the control-free point is forward of the control-fixed neutral point, while for positive H_α the control-free neutral point is aft of the control-fixed neutral point.

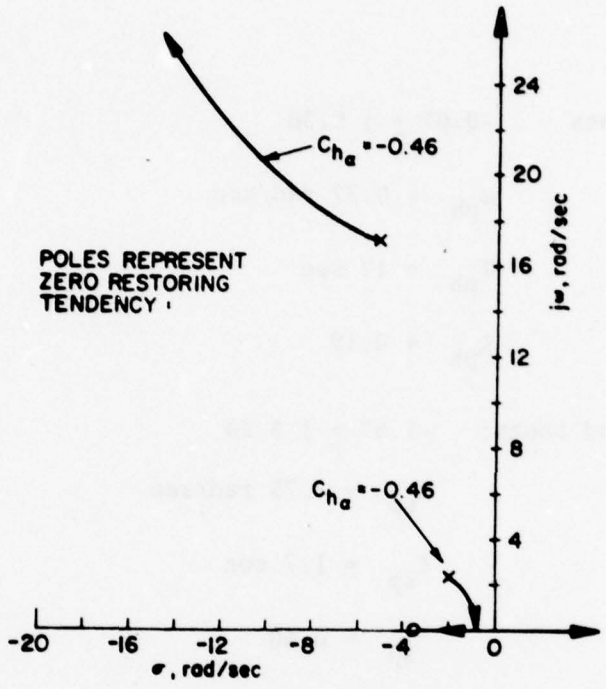

Figure 2-5. Root Locus: Negative Floating Tendency, C_{h_α}.

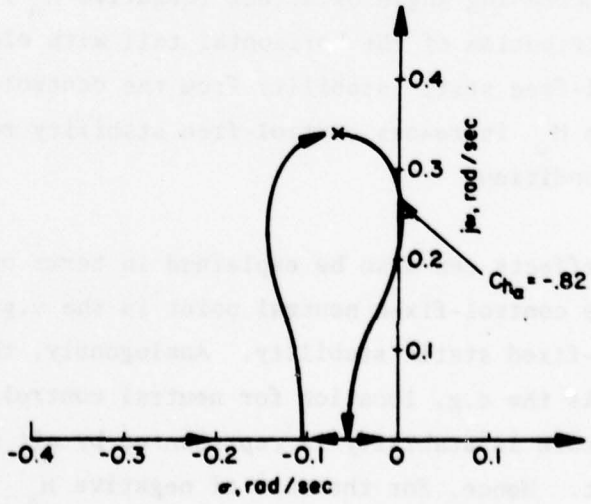

Figure 2-6. Root Locus: Negative Floating Tendency, C_{h_α}. Expansion of Phugoid Region of Figure 2.5.

In addition to its effects on static stability, H_α also has important effects on the dynamic response of the airplane. Positive H_α can cause undesirable control feel characteristics during transient maneuvers. Due to the phase relationship between elevator deflection and control force for the positive floating tendency case, the build-up of control force lags elevator deflection for rapid control movements (Ref. 7). This effect can be disconcerting to the pilot, and may cause a tendency to overcontrol.

Reference 6 points out that positive H_α, coupled with friction and a small value of the restoring tendency, can result in limit cycle oscillations. Due to such undesirable transient and dynamic effects, positive H_α should generally be avoided in conventional control system design.

The root locus plots in Fig. 2-5 and 2-6 show that good dynamic characteristics can be achieved for a considerable range of negative floating tendency. The poles of the root locus plots represent zero floating tendency. The nominal value for the baseline configuration, $H_\alpha = -0.21$, is in the region of good short period and phugoid characteristics.

The limiting factor on negative H_α may be the reduction in control-free static stability associated with negative floating tendency. For the baseline airplane with a nominal control-fixed static stability of $M_\alpha = -6.0$, a value of $C_{h_\alpha} = -0.82$ (3.9 times the nominal) would completely obviate the control-fixed stability of the airplane, giving neutral control-free stability. Such a large negative value of C_{h_α} is unlikely to occur in practice, but for aft-c.g. locations, relatively less negative floating tendency would be required to cause control-free static instability.

Elevator Restoring Tendency (H_δ) - The derivative H_δ represents

the restoring hinge moment resulting from elevator deflection; it clearly must be negative to avoid control system instability. The root loci of Fig. 2-7 and 2-8 illustrate the paths of the characteristic roots as C_{h_δ} varies from its baseline nominal value of -0.6 per radion. The root locus shows that H_δ must be sufficiently negative to insure adequately high control system natural frequency. Once these requirements are met, there are few dynamics difficulties associated with larger negative values of H_δ . For extreme negative H_δ , the control system damping ratio may become unacceptably small (Ref .6).

Since the static control forces are directly proportional to H_δ , and since H_δ can vary over a wide range of negative values without dynamics complications, this parameter is available to the designer for adjusting control forces to desirable levels.

2.3 DOWNSPRINGS AND THEIR EFFECTS ON LONGITUDINAL STABILITY AND CONTROL

2.3.1 Classical Constant-Force Downspring

Background Discussion - The downspring is a familiar device for augmenting the static stability of an airplane, and, as noted in Chapter 1, downsprings are used in many current general aviation airplanes. Physically, the downspring is a spring attached to the longitudinal control system so as to exert a stick-forward (i.e. elevator-down) force. The extra control force due to the downspring is nulled with a downward trim tab deflection. Due to the trim tab deflection, an increase in airspeed from trim causes the elevator to float upward, giving a nose-up pitching moment tending to reduce the airspeed back to the trim value. Similarly, a reduction in airspeed from trim causes a nose-down pitching moment tending to restore the airspeed to its trim value. The net result of the installation of a downspring is an increase in the airplane's control-free static stability, or in terms of neutral point an aft movement of the control-free neutral point.

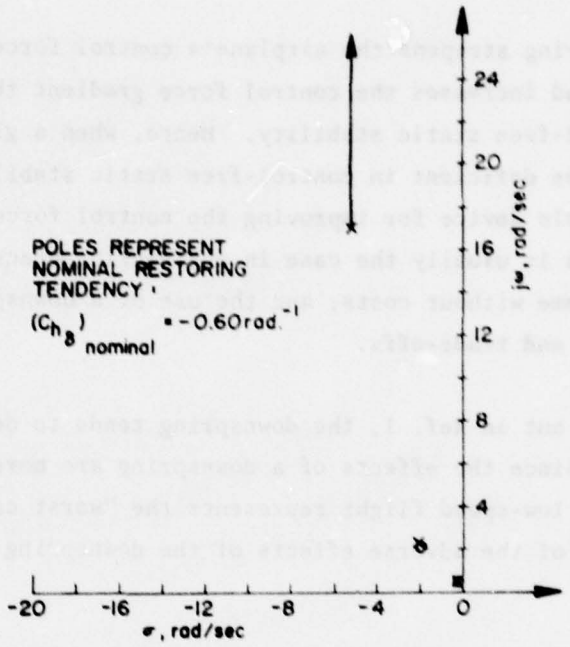

Figure 2-7. Root Locus: Increasingly Negative C_{h_δ}.

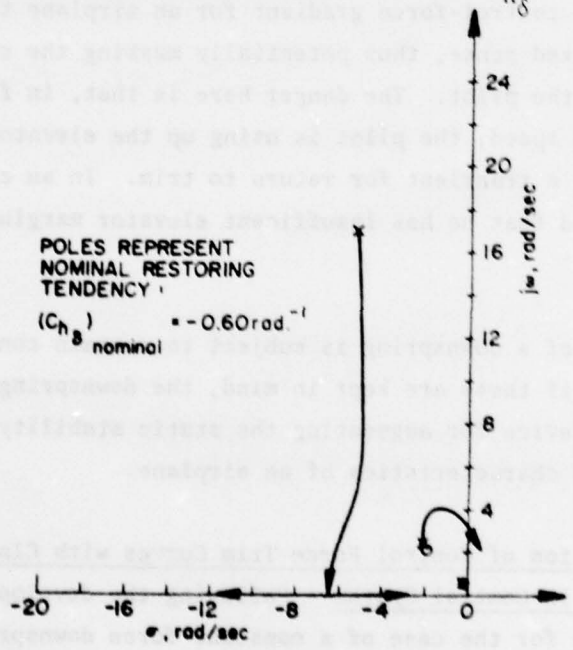

Figure 2-8. C_{h_δ} Root Locus: Positive Increments From Nominal.

The downspring steepens the airplane's control force vs. airspeed trim curve, and increases the control force gradient through trim, a measure of control-free static stability. Hence, when a given airplane design is found to be deficient in control-free static stability, the downspring is a simple device for improving the control force characteristics. However, as is usually the case in engineering practice, these advantages do not come without costs, and the use of a downspring entails certain compromises and trade-offs.

As pointed out in Ref. 1, the downspring tends to destabilize the phugoid mode. Since the effects of a downspring are more pronounced at low trim speeds, low-speed flight represents the "worst case" condition for evaluation of the adverse effects of the downspring on the phugoid mode.

Another point to be noted in employing a downspring is that it can give a stable control-force gradient for an airplane that is unstable in the control-fixed sense, thus potentially masking the control-fixed instability from the pilot. The danger here is that, in flying above or below the trim speed, the pilot is using up the elevator margin he needs to initiate a transient for return to trim. In an extreme case, the pilot may find that he has insufficent elevator margin to return to trim.

The use of a downspring is subject to certain constraints and limitations, but if these are kept in mind, the downspring can be a very convenient device for augmenting the static stability and improving the control force characteristics of an airplane.

Calculation of Control Force Trim Curves with Classical Constant-Force Downspring in Control System - Following the development of Ref. 7, the control force for the case of a constant force downspring in the longitudinal control system may be expressed,

$$F_c = -GH_e - F_d \tag{2-1}$$

Introducing the elevator hinge moment coefficient,

$$F_c = -GS_e\bar{c}_e q\eta_t C_{h_e} - F_d$$

$$= -GS_e\bar{c}_e q\eta_t (C_{h_o} + C_{h_\delta}\delta_e + C_{h_\alpha}\alpha_t + C_{h_{\delta_t}}\delta_t) - F_d \tag{2-2}$$

The horizontal tail angle of attack is

$$\alpha_t = \alpha_o + \frac{C_L}{a_w}\left(1 - \frac{\partial\varepsilon}{\partial\alpha}\right) - i_w + i_t \quad , \tag{2-3}$$

and the elevator angle is

$$\delta_e = \delta_{e_c} - \left(\frac{\partial C_m}{\partial C_L}\right)\Bigg|_{\text{fixed}} \frac{C_L}{C_{m_\delta}} \quad , \tag{2-4}$$

The control-free static stability is given by

$$\frac{\partial C_m}{\partial C_L}_{\text{free}} = \frac{\partial C_m}{\partial C_L}\Bigg|_{\text{fixed}} + \left(\frac{C_{h_\alpha}}{C_{h_\delta}}\frac{a_t}{a_w}\right)\bar{V}\eta_t\tau\left(1 - \frac{\partial\varepsilon}{\partial\alpha}\right) \quad , \tag{2-5}$$

so the control force equation may be written,

$$F_c = \tfrac{1}{2}K\rho V^2\left(A + C_{h_{\delta_t}}\delta_t\right) - K\frac{W}{S}\frac{C_{h_\delta}}{C_{m_\delta}}\frac{\partial C_m}{\partial C_L}\Bigg|_{\text{free}} - F_d \tag{2-6}$$

where $K = - GS_e \bar{c}_e \eta_t$

$$A = C_{h_o} + C_{h_\alpha} (\alpha_o - i_w + i_t) + C_{h_\delta} \delta E_o$$

Setting $F_c = 0$ and $V = V_t$, Eq. (2-6) can be solved for the trim tab setting giving zero control force at the trim airspeed:

$$(A + C_{h_{\delta_t}}) = \frac{2(W/S)}{\rho V_t^2} \frac{C_{h_\delta}}{C_{m_\delta}} \left.\frac{\partial C_m}{\partial C_L}\right|_{free} + \frac{2F_d}{K\rho V_t^2} \qquad (2\text{-}7)$$

Substituting this expression for $(A + C_{h_{\delta_t}} \delta_t)$ into the control force equation (Eq. 2-6) and simplifying yields a particularly convenient form of the control-force equation:

$$F_c = \left[K\left(\frac{W}{S}\right) \frac{C_{h_\delta}}{C_{m_\delta}} \left.\frac{\partial C_m}{\partial C_L}\right|_{free} + F_d\right] \left(\frac{V^2}{V_t^2} - 1\right) \qquad (2\text{-}8)$$

Equation (2-8) is applicable when the trim tab is set to give $F_c = 0$ at $V = V_t$. The equation gives the control force as a function of airspeed for the case of a constant force downspring of force F_d in the control system.

Using Eq. (2-8), control force vs. airspeed trim curves were calculated for the case of no downspring, a 15-lb constant force downspring, and a 30-lb constant force downspring. The curves were calculated for four levels of control fixed static stability: M_α = + 1.25, - 1.25, - 6.0, and - 12.0. The resulting curves are displayed in Fig. 2-9 through 2-12. Figure 2-9 clearly illustrates the ability of the downspring to yield a stable control force gradient for a statically unstable basic airframe.

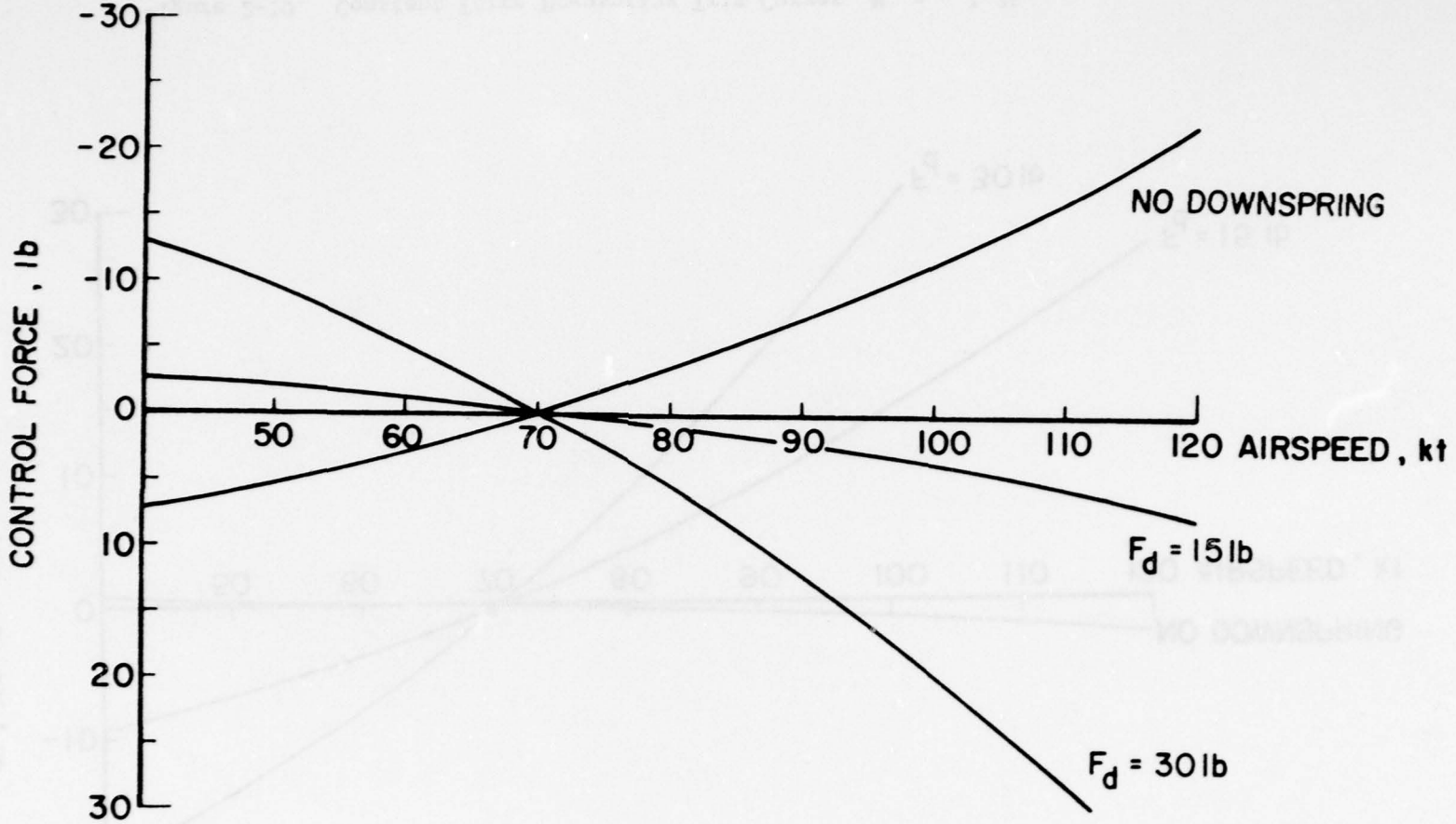

Figure 2-9. Constant Force Downspring Trim Curves, M_α = + 1.25.

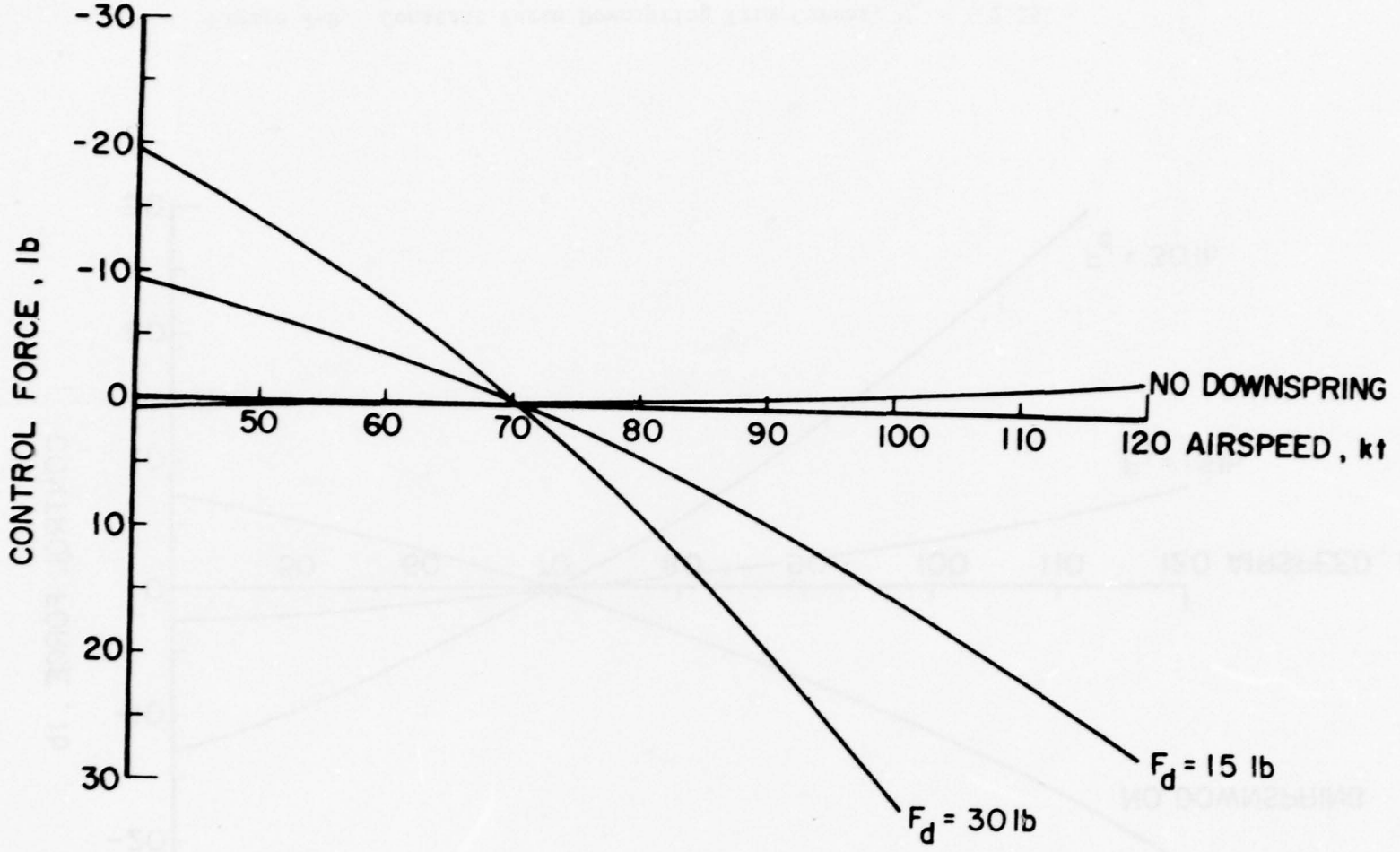

Figure 2-10. Constant Force Downspring Trim Curves, M_α = - 1.25.

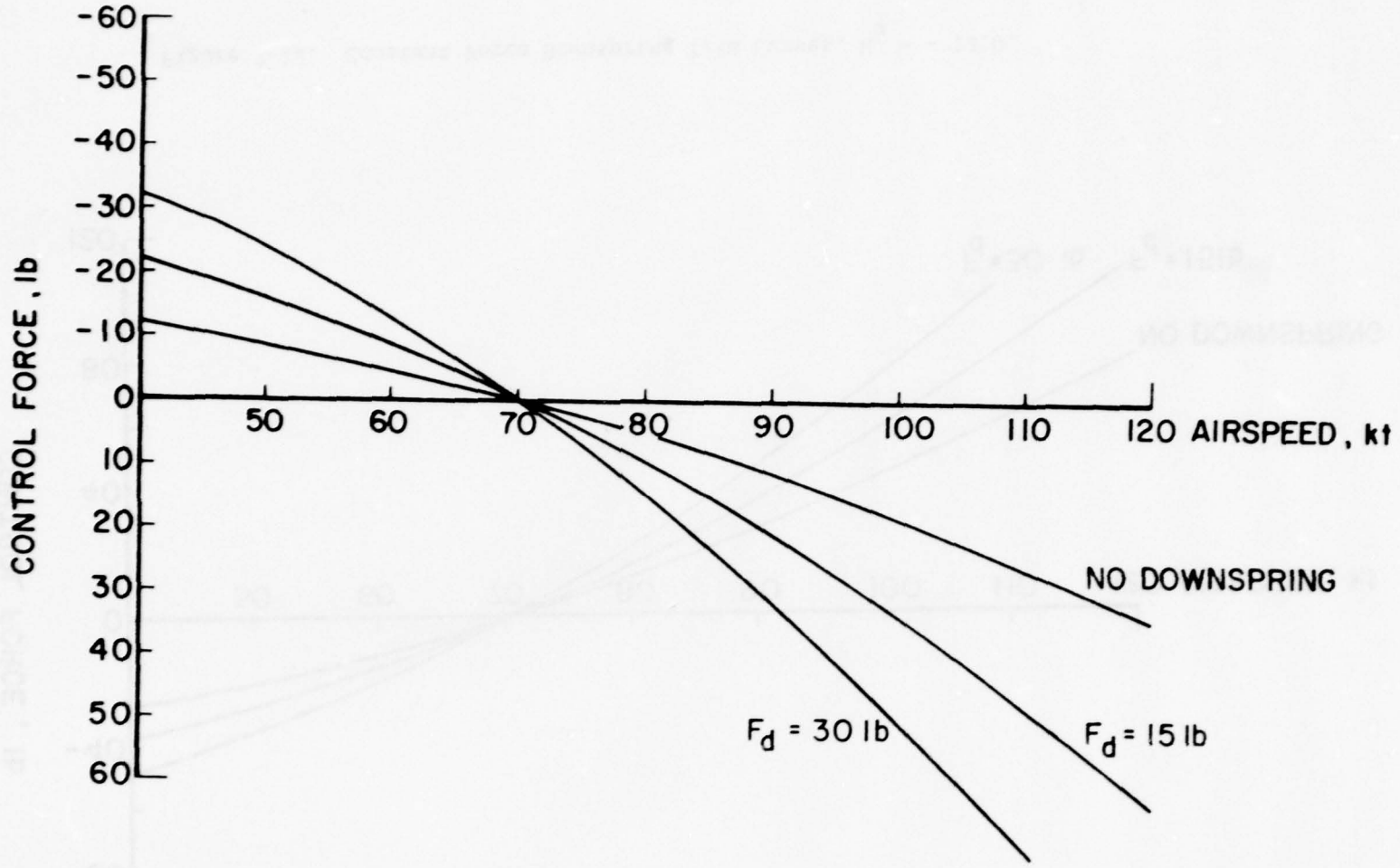

Figure 2-11. Constant Force Downspring Trim Curves , M_α = - 6.0.

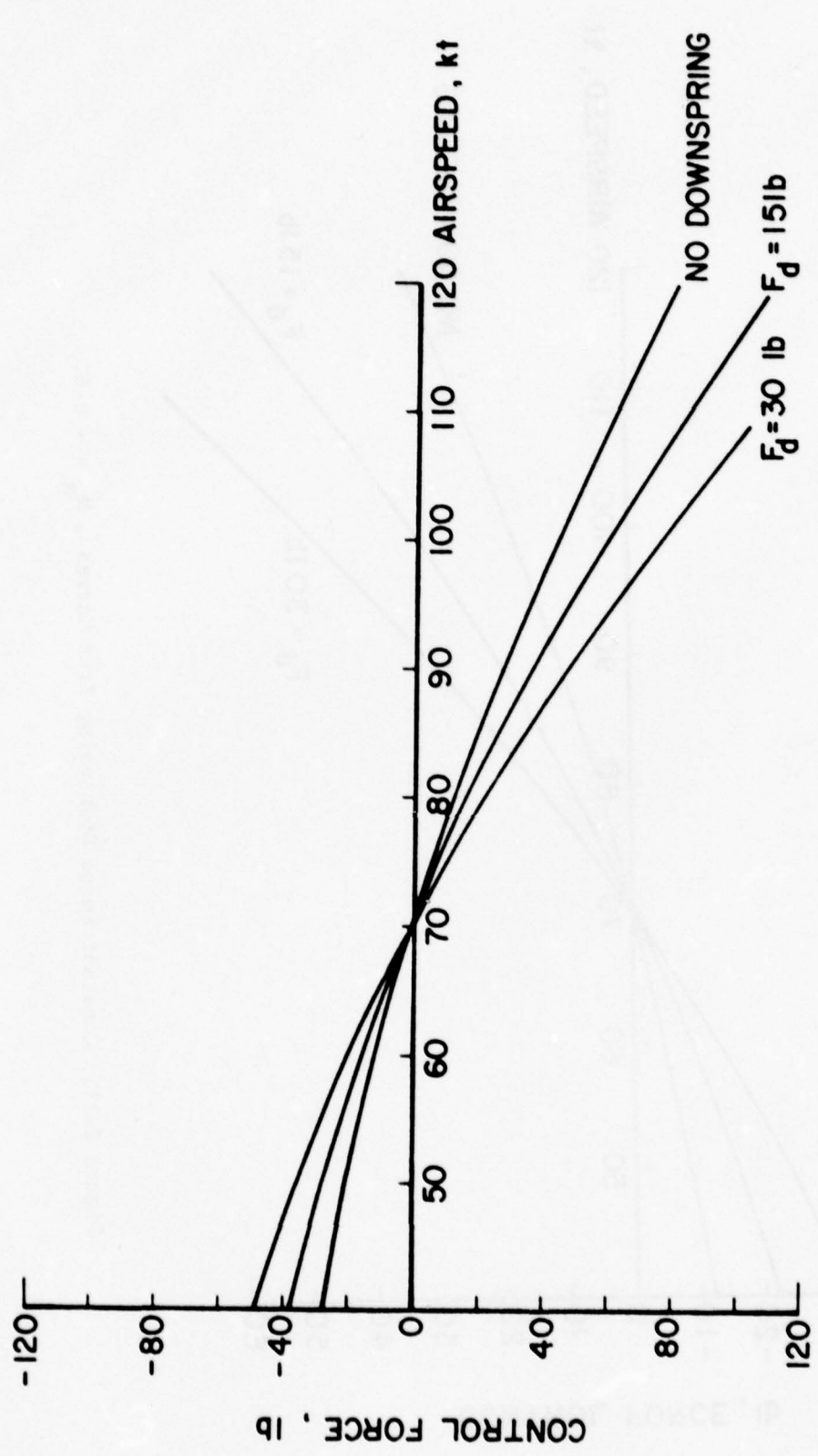

Figure 2-12. Constant Force Downspring Trim Curves, M_α = - 12.0.

Dynamics Considerations Pertaining To Downsprings - The four degree-of-freedom, longitudinal equations of motion for an airplane may be written in generalized Laplace notation in the form,

$$
\begin{aligned}
X_V\Delta V + X_\alpha\Delta\alpha + X_\theta\Delta\theta + X_\delta\Delta\delta &= 0 \\
L_V\Delta V + L_\alpha\Delta\alpha + L_\theta\Delta\theta + L_\delta\Delta\delta &= 0 \\
M_V\Delta V + M_\alpha\Delta\alpha + M_\theta\Delta\theta + M_\delta\Delta\delta &= 0 \\
H_V\Delta V + H_\alpha\Delta\alpha + H_\theta\Delta\theta + H_\delta\Delta\delta &= -\Delta H_{\text{control}}
\end{aligned}
\qquad (2\text{-}9)
$$

where the generalized coefficients appearing in these equations are defined in Table 2-3. The equations are represented in block diagram form in Fig. 2-13; the transfer functions for the block diagram are defined in Table 2-4. The block diagram representation explicitly identifies the feedback paths via which airplane motions feed forces back to the control column.

In the block diagram, the effect of a downspring is contained in the term H_V. The trim tab deflection which balances the downspring force at the trim condition results in a change of elevator hinge moment with airspeed. The generalized derivative H_V is defined by the equations,

$$H_V = \frac{zH_o}{M_{ref}V} + \frac{\partial C_h}{\partial V} \qquad (2\text{-}10)$$

where H_o is the initial elevator aerodynamic hinge moment given by,

$$H_o = -gm_eX_e - \frac{F_d + F_b}{G} \qquad (2\text{-}11)$$

Here, F_d is the downspring force, and the damping contributes to a non-zero initial elevator hinge moment. The initial elevator hinge moment,

TABLE 2-3

DEFINITIONS OF GENERALIZED STABILITY DERIVATIVES

$$X_v = s + (D_v - T_v)$$

$$X_\alpha = D_\alpha - g$$

$$X_\theta = g$$

$$X_\delta = 0$$

$$L_v = L_{v/V_o}$$

$$L_\alpha = s + L_{\alpha/V_o}$$

$$L_\theta = - s$$

$$L_s = 0$$

$$M_v = -M_v$$

$$M_\alpha = -M_{\dot{\alpha}} s - M_\alpha$$

$$M_\theta = s^2 - M_{\dot{\theta}} s$$

$$M_\delta = -M_{\delta_e}$$

$$H_v = \frac{2H_o}{M_{ref} V} + \frac{\partial C_h}{\partial V}$$

$$H_\alpha = \frac{1}{M_{ref}} \left(1 - \frac{\partial \epsilon}{\partial \alpha} \right) \frac{\partial H}{\partial \alpha_t} + \tau \left(\frac{1}{M_{ref}} \frac{1}{\mu} \frac{1t}{\bar{c}} \frac{\partial \epsilon}{\partial \alpha} \frac{\partial H}{\partial \alpha_t} - h_1 \right) s$$

$$H_\theta = \tau \left(\frac{1}{M_{ref}} \frac{1}{\mu} \frac{1t}{\bar{c}} \frac{\partial H}{\partial \alpha_t} + h_1 \right) s - \tau^2 (h_e + l_1) s^2$$

$$H_\delta = - \tau^2 h_e s^2 + \tau \left(\frac{1}{M_{ref}} \frac{1}{2\mu} \frac{2V}{\bar{c}} \frac{\partial H}{\partial \dot{\delta}_e} \right) s + \frac{1}{M_{ref}} \frac{\partial H}{\partial \delta_e}$$

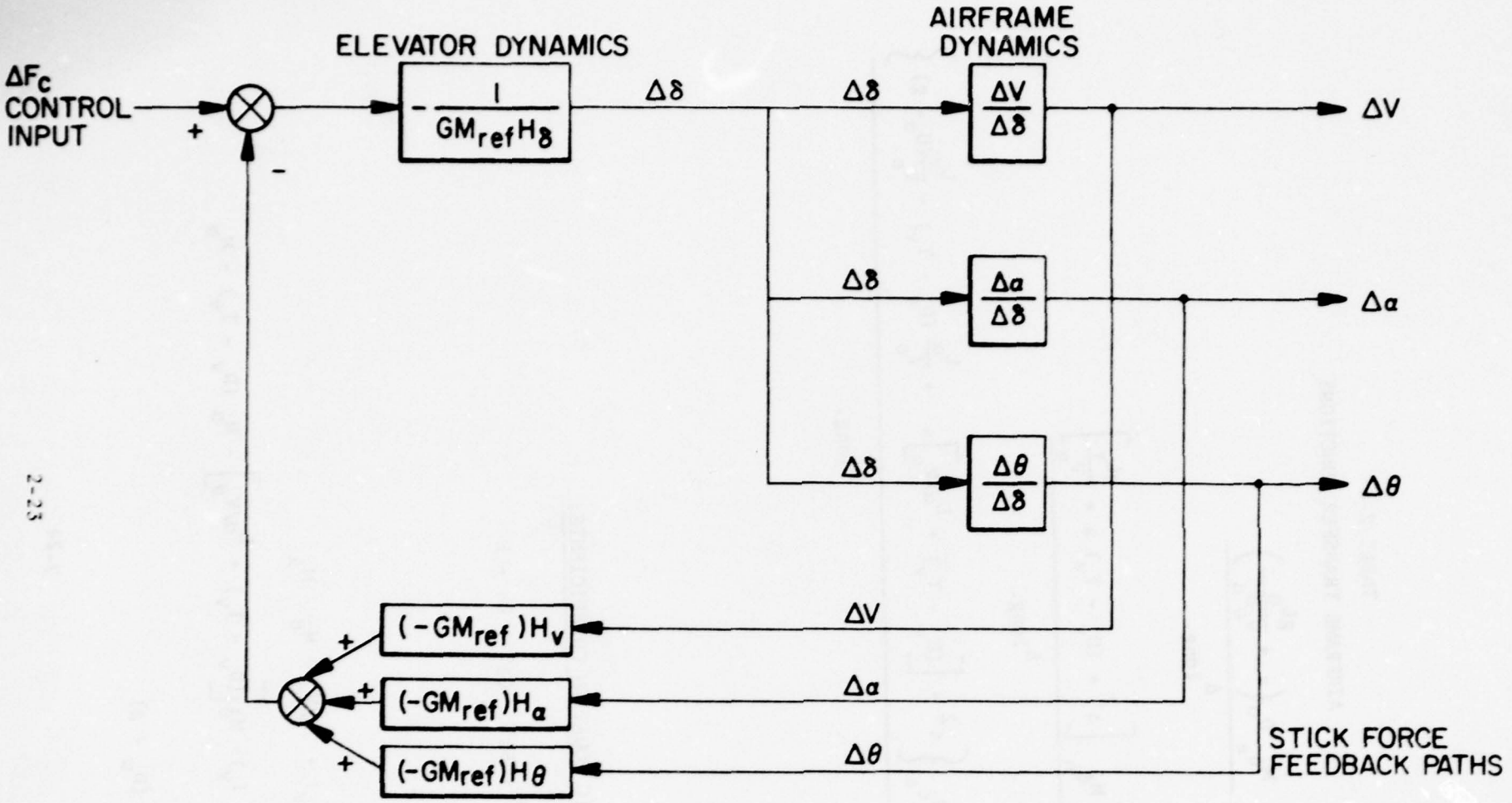

Figure 2-13. Block Diagram of Longitudinal Equations of Motion (Four Degrees of Freedom)

TABLE 2-4

AIRFRAME TRANSFER FUNCTIONS

$$\frac{\Delta V(s)}{\Delta \delta_e(s)} = -\frac{M_{\delta_e} D_\alpha \left(s + \frac{gL_\alpha}{V_o D_\alpha} \right)}{\Delta_{long.}}$$

$$\frac{\Delta \alpha\ (s)}{\Delta \delta_e(s)} = \frac{M_{\delta_e} \left[s^2 + (D_V - T_V)\, s + \frac{gL_V}{V_o} \right]}{\Delta_{long.}}$$

$$\frac{\Delta \theta\ (s)}{\Delta \delta_e(s)} = \frac{M_{\delta_e} \left\{ s^2 + \left[(D_V - T_V) + L_{\alpha/V_o} \right] s + \frac{L_\alpha}{V_o} (D_V - T_V) - \frac{L_V}{V_o} (D_\alpha - g) \right\}}{\Delta_{long.}}$$

CHARACTERISTIC EQUATION COEFFICIENTS:

$$\Delta_{long.} = As^4 + Bs^3 + Cs^2 + Ds + E$$

where:

$$A = 1.$$

$$B = (D_V - T_V) + L_{\alpha/V_o} - M_{\dot{\theta}} - M_{\dot{\alpha}}$$

$$C = \frac{L_\alpha}{V_o}(D_V - T_V) - M_{\dot{\theta}} \left[(D_V - T_V) + L_{\alpha/V_o} \right] - M_{\dot{\alpha}} (D_V - T_V) - M_\alpha - \frac{L_V}{V_o} (D_\alpha - g)$$

TABLE 2-4, continued

$$D = -M_{\dot{\theta}}^{\cdot}(D_v - T_v)\frac{L_\alpha}{V_o} + M_v(D_\alpha - g) - M_{\dot{\alpha}}^{\cdot}\frac{gL_v}{V_o} + gM_v$$

$$- M_\alpha (D_v - T_v) + M_{\dot{\theta}}^{\cdot}\frac{L_v}{V_o}(D_\alpha - g)$$

$$E = -M_\alpha \frac{gL_v}{V_o} + M_v \frac{gL_\alpha}{V_o}$$

HINGE MOMENT DERIVATIVES:

$$H_\delta = \tau^2 h_e s^2 + \tau\left(\frac{1}{M_{ref}}\ \frac{1}{2\mu}\ \frac{2V}{\bar{c}}\ \frac{\partial H}{\partial \dot{\delta}_e}\right) s + \frac{1}{M_{ref}}\ \frac{\partial H}{\partial \delta_e}$$

$$H_v = \frac{2\,H_o}{M_{ref} V} + \frac{\partial C_h}{\partial V}$$

$$H_\alpha = \frac{1}{M_{ref}}\left(1 - \frac{\partial \varepsilon}{\partial \alpha}\right)\frac{\partial H}{\partial \alpha_t} + \left(\frac{1}{M_{ref}}\ \frac{1}{\mu}\ \frac{l_t}{\bar{c}}\ \frac{\partial \varepsilon}{\partial \alpha}\ \frac{\partial H}{\partial \alpha_t} - h_1\right) s$$

$$H_\theta = \tau\left(\frac{1}{M_{ref}}\ \frac{1}{\mu}\ \frac{l_t}{\bar{c}}\ \frac{\partial H}{\partial \alpha} + h_1\right) - \tau^2 (h_e + l_1) s^2$$

H_o , appears in the derivative $\frac{\partial H_e}{\partial V}$, representing a change in elevator hinge moment with airspeed.

The root locus plot in Fig. 2-14 illustrates the path of the airplane's characteristic roots as the downspring force increases. The plot is for the baseline airplane with nominal control fixed static stability, M_α = - 6.0. The downspring has very little effect on short period characteristics, a downspring forces of 200-lb (many times larger than any value likely to occur in practice) causes a barely perceptible movement of the short period roots. The main effect of the downspring on the airplane's dynamics appears in the phugoid mode. Figure 2-15 is an expansion of the phugoid region of the previous root locus, where the downspring is seen to reduce the damping and increase the frequency of the phugoid mode. Despite this unfavorable trend, for the nominal value of M_α illustrated, a moderately strong downspring can be introduced (F_d = 20 lb) without seriously degrading the airplane's dynamic response characteristics.

The real potential of the downspring to introduce dynamics difficulties is revealed in the case of relaxed static stability, corresponding to an aft-c.g. location. The root locus in Fig. 2-16 shows the effect of a downspring when basic airframe M_α = + 1.25. Figure 2-17 is an expansion of the phugoid region, and here it can be seen that any downspring force greater than 10 lb means an unstable phugoid.

If the baseline airplane, equipped with a 20-lb downspring, were loaded so as to reduce the control-fixed static stability level to M_α = + 1.25, the phugoid would be unstable due to the downspring. It should be noted that although the phugoid is unstable in this situation (a dynamic instability), the downspring does render the airplane statically stable, moving the divergent real root into the left half plane.

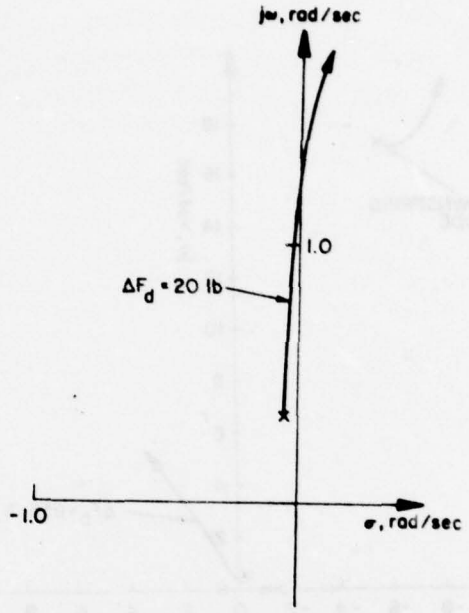

Figure 2-14. Root Locus For Positive ΔF_d.

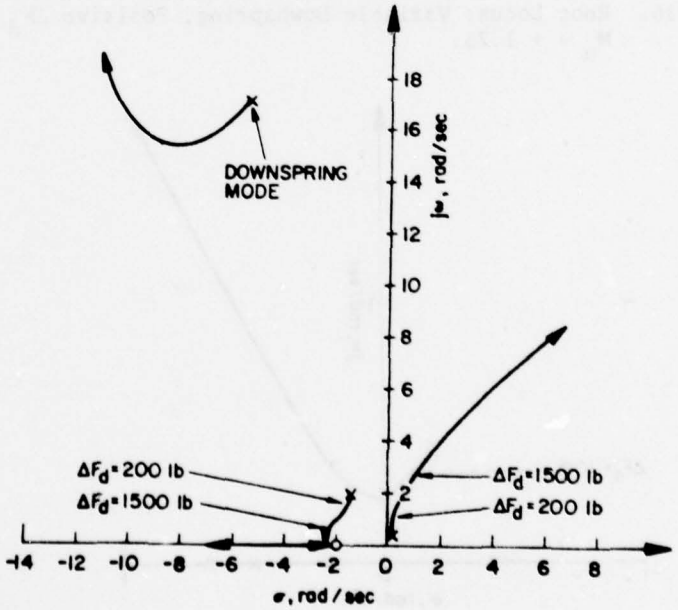

Figure 2-15. Root Locus For Positive ΔF_d. Expansion of Phugoid Region of Figure 3.6.

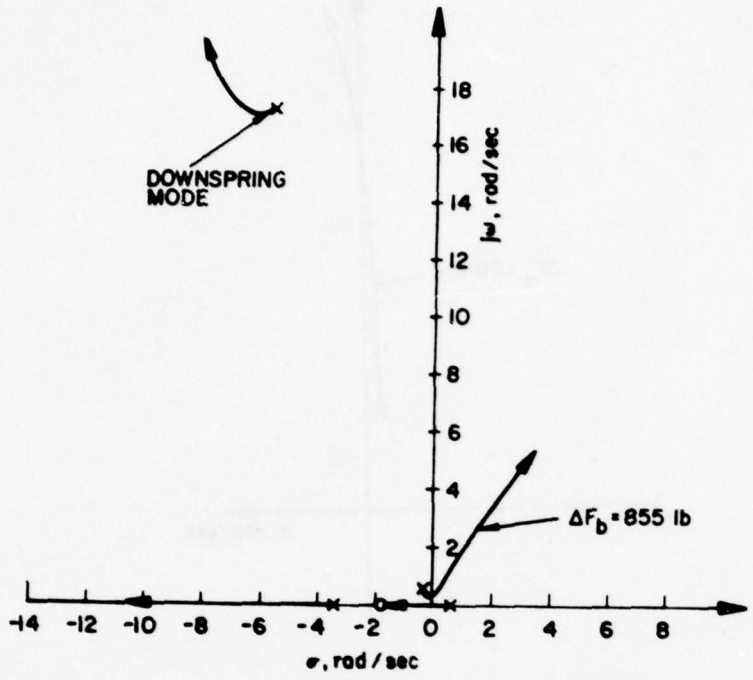

Figure 2-16. Root Locus: Variable Downspring, Positive ΔF_d, M_α = + 1.25.

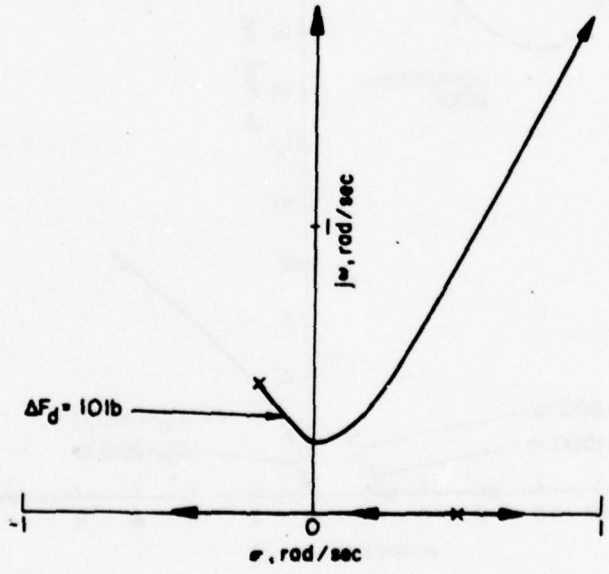

Figure 2-17. Root Locus: Variable Downspring, Positive ΔF_d, M_α = + 1.2. Expansion of Phugoid Region of Figure 3.8.

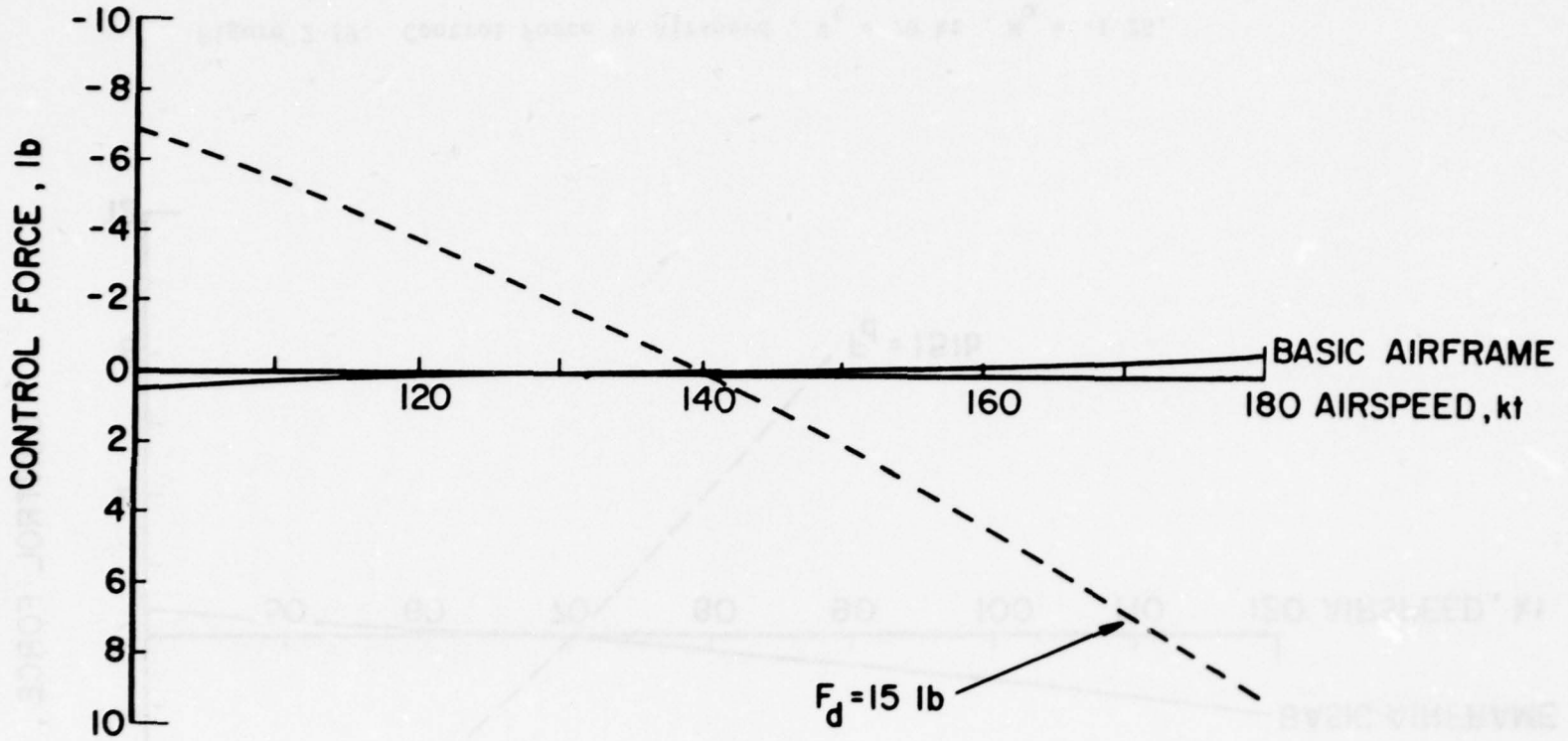

Figure 2-18. Control Force vs Airspeed, V_t = 140 kt , M_α =-5.0.

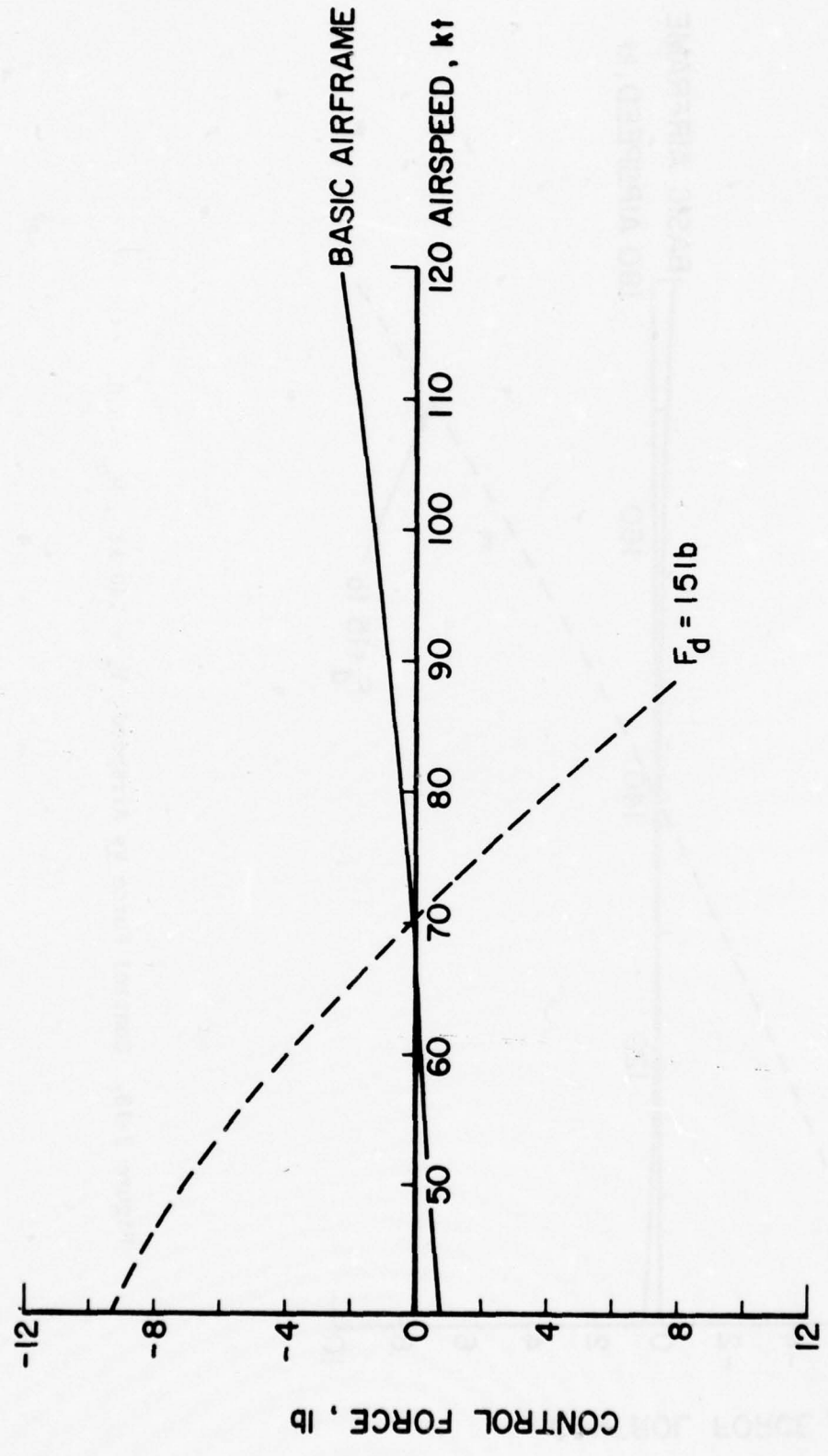

Figure 2-19. Control Force vs Airspeed , V_t = 70 kt , M_α = -1.25.

Downsprings: Effect of Trim Speed - A downspring of given tension will have a more pronounced effect on elevator hinge moment, and hence on control force, as the trim airspeed is reduced. This can be seen in the block diagram representation of the equations of motion (Fig.2-13). The generalized derivative $H_V = \frac{2H_o}{M_{ref}V} + \frac{\partial C_h}{\partial V}$ represents the note of change of elevator hinge moment with airspeed. Since the downspring contribution to H_V is contained in H_o, the initial aerodynamic hinge moment, the effect of downspring is inversely proportional to trim speed. Consequently, a downspring that gives good control-force characteristics and favorable dynamic response at high trim speed, might seriously destabilize the phugoid at a lower trim speed.

To illustrate this phenomenon, phugoid characteristics and trim curves were calculated for the baseline airplane, equipped with a 15-lb downspring, for trim speeds of 140 kt and 70 kt. The calculations were for an aft c.g. location corresponding to M_α = - 5.0 at 140 kt, and M_α = - 1.25 at 70 kt (note: $M_\alpha \propto V^2$). The trim curves are shown in Fig. 2-18 and 2-19, and the beneficial effects of the downspring on the control force trim curves are obvious. The phugoid characteristics are also satisfactory for the 140-kt trim speed. The phugoid is stable, with a period of 34 sec, a damping ratio of 0.9, and a time to half amplitude of 4.1 sec. At the 70-kt trim speed, even though the static control force characteristics are satisfactory, the phugoid is unstable, with a period of 13 sec, a negative damping ratio of - 0.068, and a time to double amplitude of 20 sec. When static stability is augmented by use of a downspring, the designer should be aware of potentially unfavorable phugoid characteristics for aft c.g. positions and low trim speeds.

2.3.2 Non-Classical Downspring: Downspring Force a Function of Elevator Deflection

Background Discussion - The downsprings discussed up to now have been idealized cases where the downspring force is assumed independent of elevator deflection. If the installed downspring is sufficiently long, this idealized situation may be approached in actual practice, but there are several other possibilities. Many downsprings encountered in practice are actually short springs whose force varies strongly with spring extension and, therefore, with elevator deflection. Figure 2-20 illustrates this situation with downspring force data for an actual airplane, taken from Ref. 8. Also, downspring installations may be intentionally geared for a particular variation of downspring force with control position, in order to tailor the control force trim curve to desired specifications.

To illustrate the implications of such non-classical downspring installations, five configurations were considered in which downspring force, F_d, varies with elevator position in a linear or piecewise-linear fashion. The slope of downspring force with elevator deflection is denoted by the symbol K_d. The downspring configurations selected for study are described below, and are illustrated in Fig. 2-21 through 2-25. Trim curves were calculated for each downspring case, for each of the four levels of M_α used in this study. The trim curve equation is developed in the next section.

The downspring configurations selected for study are:

- Case 1 (Figure 2-21)

  Centering spring. $F_d = 0$ for $\delta_e = 0$.

  Downspring force varies linearly with elevator deflection, of a sense to resist elevator deflection.

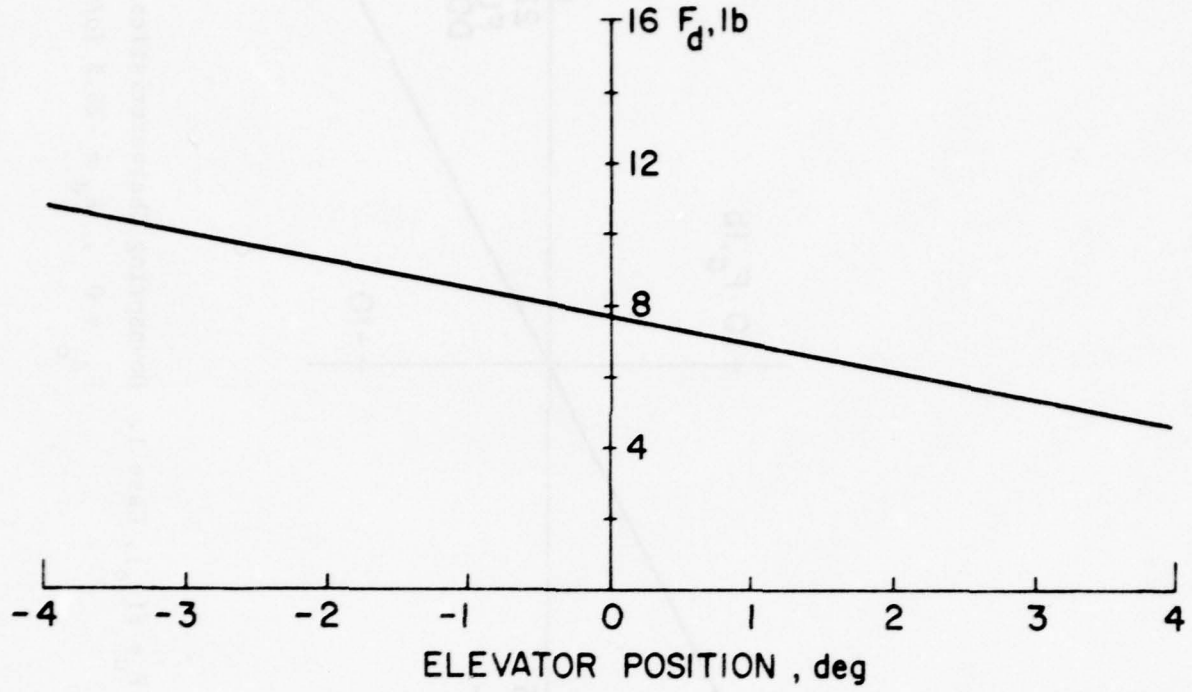

Figure 2-20. Downspring Force vs Elevator Position with $F_d = F(\delta_e)$.

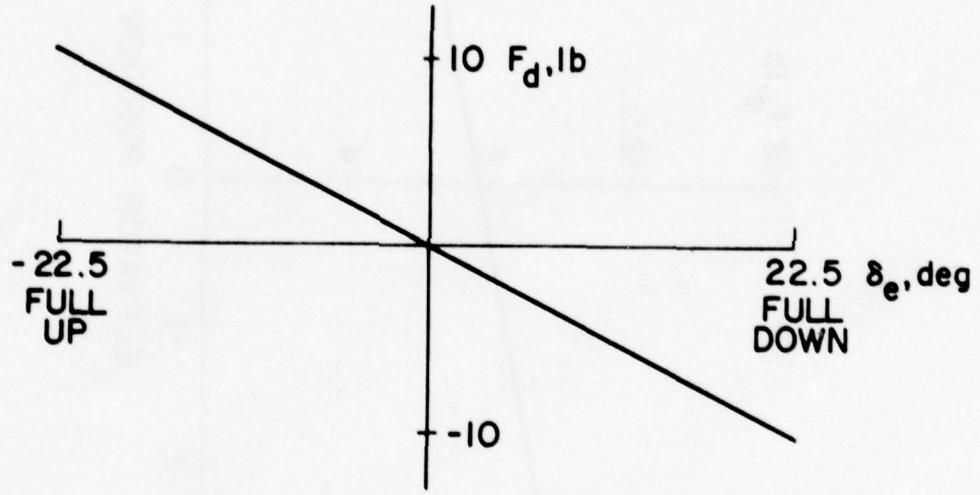

Figure 2-21. $F_d = f(\delta_e)$, Case 1. Downspring Characteristics:
$F_{d_o} = 0$, $K_d = -25.5$ lb/rad .

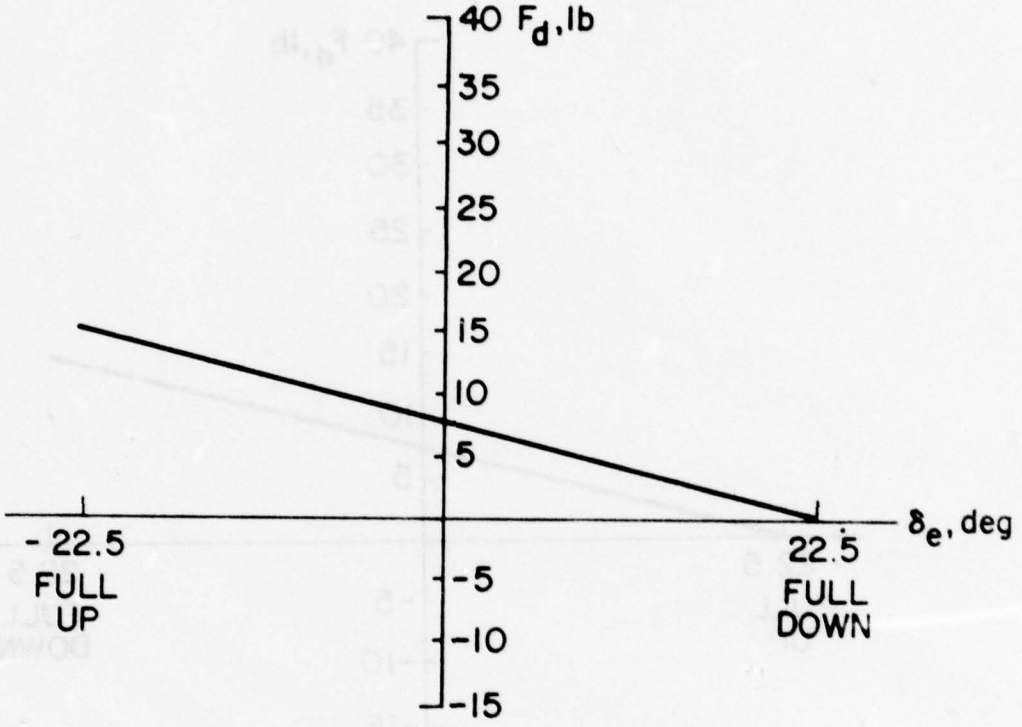

Figure 2-22. $F_d = f(\delta_e)$, Case 2., Downspring Characteristics: $F_{d_o} = 7.5$ lb , $K_d = -19.1$ lb/rad.

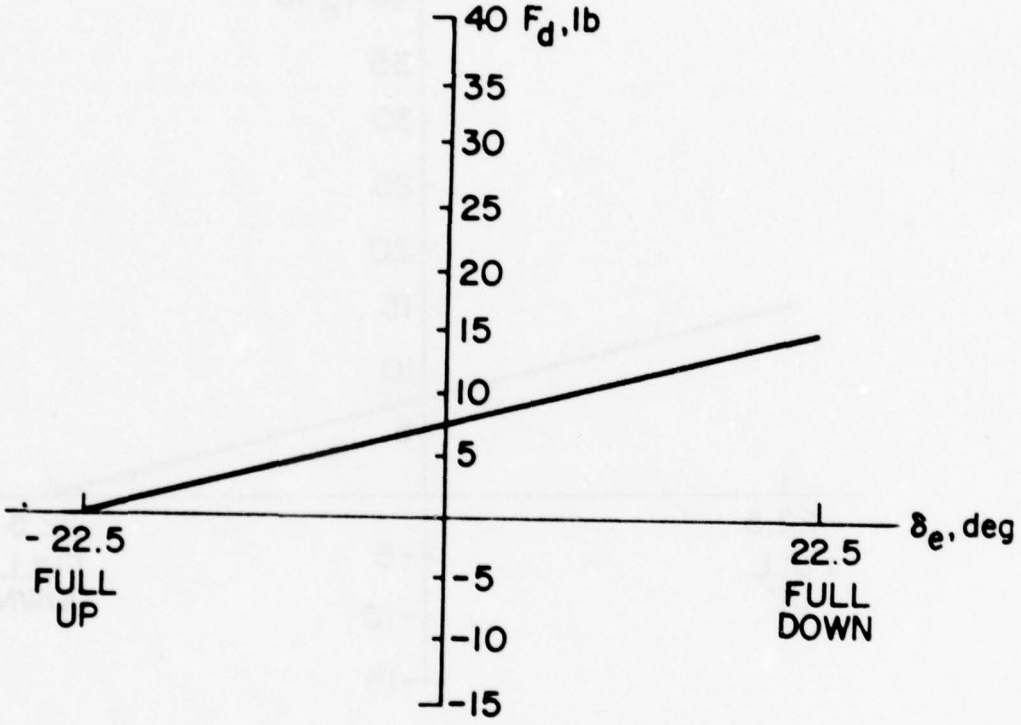

Figure 2-23. $F_d = f(\delta_e)$ Case 3. , Downspring Characteristics:
$F_{d_o} = 7.5$ lb , $K_d = 19.1$ lb/rad.

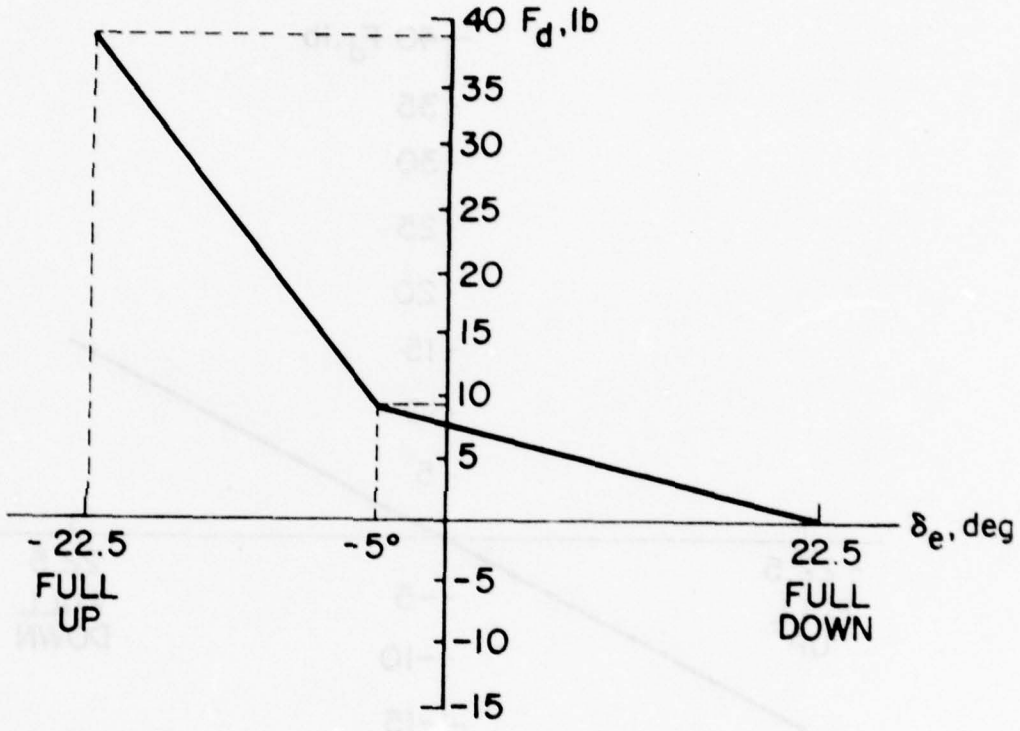

Figure 2-24. $F_d = f(\delta_e)$, Case 4. Downspring Characteristics:

$\delta_e < -5^o$: $F_{d_o} = 0.815$ lb , $k_d = -95.7$ lb/rad.

$\delta_e < -5^o$: $F_{d_o} = 7.5$ lb , $k_d = -19.1$ lb/rad.

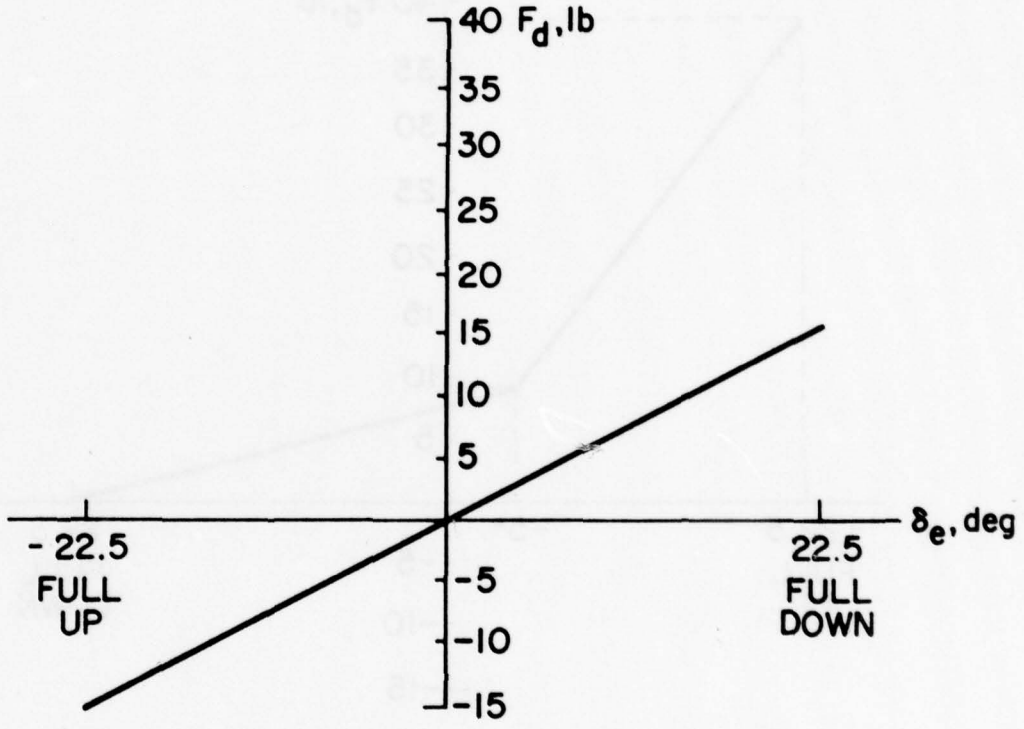

Figure 2-25. $F_d = f(\delta_e)$, Case 5. , Downspring Characteristics:
$F_{d_o} = 0$, $K_d = 38.2$ lb/rad.

Note: Downspring force changes sign for up elevator deflection.

- Case 2 (Figure 2-22)

  Downspring force varies linearly with elevator deflection from F_d = 15 lb for full up elevator to F_d = 0 for full down elevator.

- Case 3 (Figure 2-23)

  Downspring force varies linearly with elevator deflection from F_d = 0 for full up elevator to F_d = 15 lb for full down elevator.

- Case 4 (Figure 2-24)

  Segmented downspring force curve, with sharp change in force gradient for large negative elevator deflections.

- Case 5 (Figure 2-25)

  Downspring force varies linearly with elevator deflection and changes from positive to negative for large elevator deflections.

Calculation of Control Force Trim Curves - The trim curve calculation again begins with the equation,

$$F_c = - GH_e - F_d \quad , \tag{2-12}$$

If the downspring force is a linear function of elevator position,

$$F_d = F_{d_o} + K_d \delta_e \tag{2-13}$$

where, F_{d_o} = downspring force for $\delta_e = 0$

K_d = slope of F_d vs. δ_e curve

The control force equation then becomes

$$F_c = - GH_e - F_{d_o} - K_d \delta_e$$

$$= - GS_e \bar{c}_e q \eta_t \left(C_{h_o} + C_{h_\alpha} \alpha_t + C_{h_\delta} \delta_e + C_{h_{\delta_t}} \delta_t\right) - F_{d_o} - K_d \delta_e$$

(2-14)

Substituting the expressions for α_t and δ_e given in Section 2.3, the control force equation becomes

$$F_c = \tfrac{1}{2} K \rho V^2 \left(A + C_{h_{\delta_t}} \delta_t\right) - K \frac{W}{S} \frac{C_{h_\delta}}{C_{m_\delta}} \left.\frac{\partial C_m}{\partial C_L}\right|_{free} - \left(F_{d_o} + K_d \delta_e\right)$$

$$+ \frac{2(W/S)}{\rho} \frac{K_d}{C_{m_\delta}} \left.\frac{\partial C_m}{\partial C_L}\right|_{fixed} \left(\frac{1}{V}\right) \qquad (2\text{-}15)$$

where,

$$K = - GS_e \bar{c}_e \eta_t$$

$$A = C_{h_o} + C_{h_\alpha} \left(\alpha_o - i_w + i_t\right) + C_{h_\delta} \delta_{e_o}$$

Setting $F_c = 0$ and $V = V_t$, Eq. 3-6 can be solved for the trim tab setting for zero control force at the trim speed:

$$\left(A + C_{h_{\delta_t}} \delta_t\right) = \frac{2 (W/S)}{\rho V^2} \frac{C_{h_\delta}}{C_{m_\delta}} \left.\frac{dC_m}{dC_L}\right|_{free} + \frac{2\left(F_{d_o} + K_\delta \delta_{e_o}\right)}{K \rho V_t^2}$$

$$- \frac{4(W/S)}{K \rho^2 V_t^4} \frac{K_d}{C_{m_\delta}} \left.\frac{dC_m}{dC_L}\right|_{fixed} \qquad (2\text{-}16)$$

Substituting this value of $(A + C_{h_{\delta_t}} \delta_t)$ into Eq. 3-6 and simplifying:

$$F_c = \left[K \frac{W}{S} \frac{C_{h_\delta}}{C_{m_\delta}} \left. \frac{\partial C_m}{\partial C_L} \right|_{free} + (F_d + K_d \delta_e) - \frac{2(W/S)}{\rho V^2} \frac{K_d}{C_{m_\delta}} \left. \frac{\partial C_m}{\partial C_L} \right|_{fixed} \left(\frac{V^2}{V_t^2} + 1 \right) \right] \left(\frac{V^2}{V_t^2} - 1 \right) \qquad (2\text{-}17)$$

A special precaution must be observed in using Eq. (2-17). When calculating F_c at a given airspeed, the downspring characteristics F_d and K_d at the airspeed V must be the same as the downspring characteristics at the trim airspeed. In the case of a segmented downspring characteristic, such as Case 4 shown in Fig. 2-24, this may not be the case. If the downspring characteristics at the airspeed of interest are different from the downspring characteristics at the trim airspeed, Eq. (2-15) and (2-16) must be used to calculate the central force, F_c. First, Eq. (2-16) is used in conjunction with the downspring characteristics at the trim point to calculate the trim tab setting. This trim tab setting is substituted into Eq. (2-15), which is used in conjunction with the downspring characteristics at airspeed V to calculate the control force at that speed.

Equations (2-15), (2-16), and (2-17) were used to calculate the trim curves of Fig. 2-26 through 2-30.

Dynamics Considerations - In Section 2.3 it was pointed out that variations in c.g. position and trim speed could lead to destabilization of the phugoid mode in airplanes equipped with classical, constant-force downsprings. Downsprings whose force varies

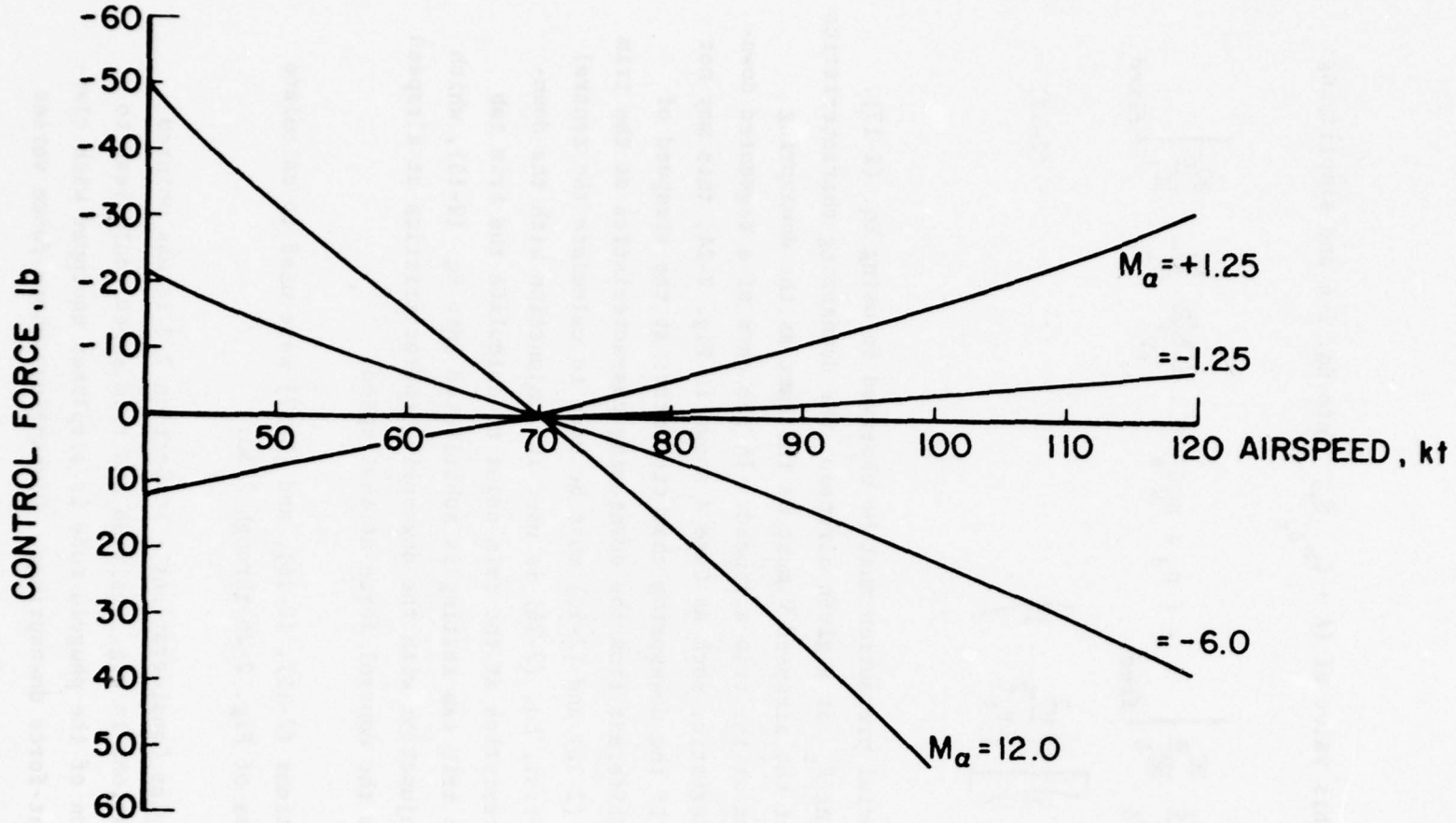

Figure 2-26. Trim Curves: $F_d = f(\delta_e)$, ($F_{d_o} = 0$, $k_d = -25.5$ lb/rad).

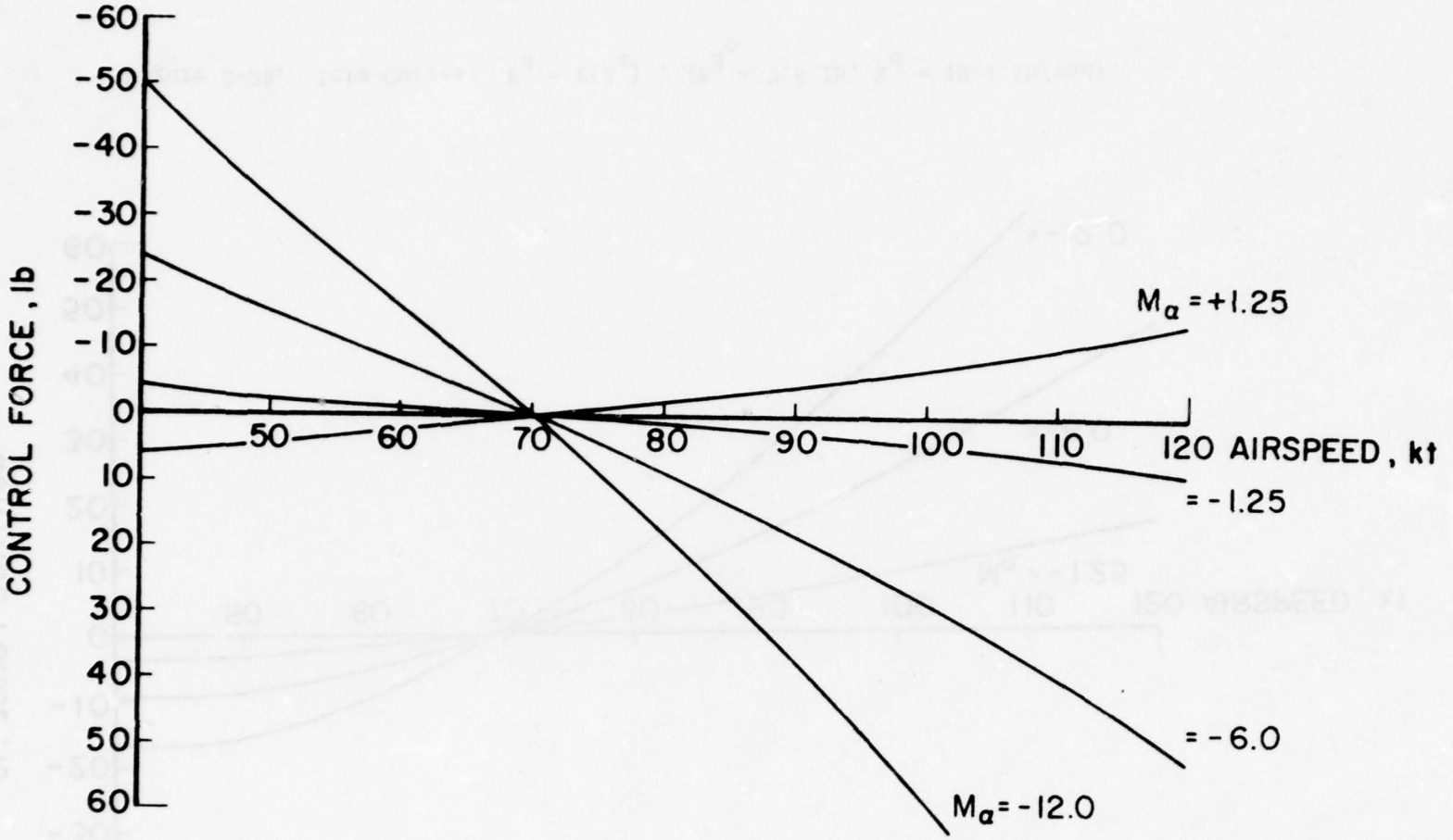

Figure 2-27. Trim Curves: $F_d = f(\delta_e)$, (F_{d_o} = 7.5 lb, k_d = - 19.1 lb/rad).

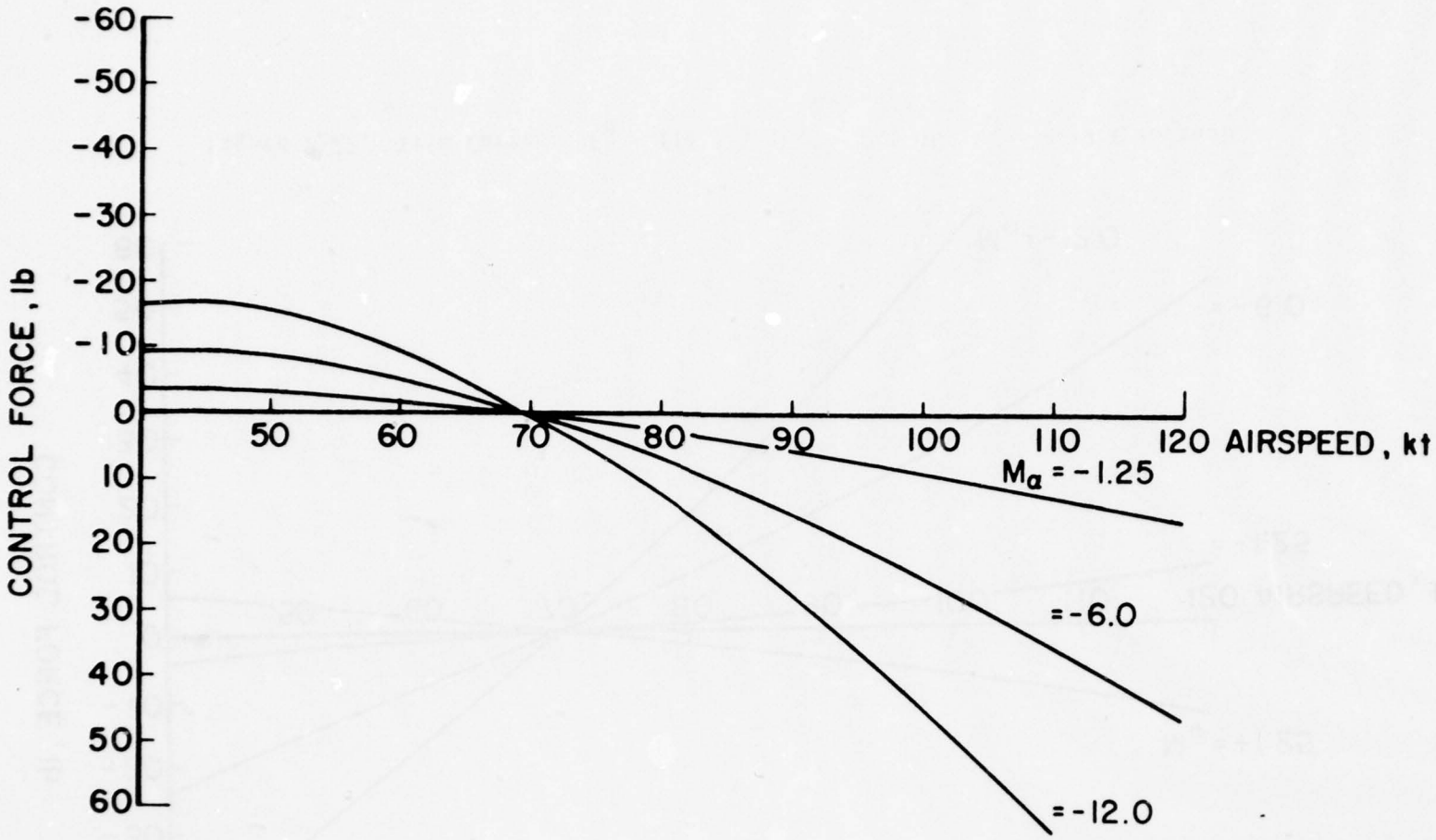

Figure 2-28. Trim Curves: $F_d = f(\delta_e)$, (F_{d_o} = 7.5 lb, k_d = 19.1 lb/rad).

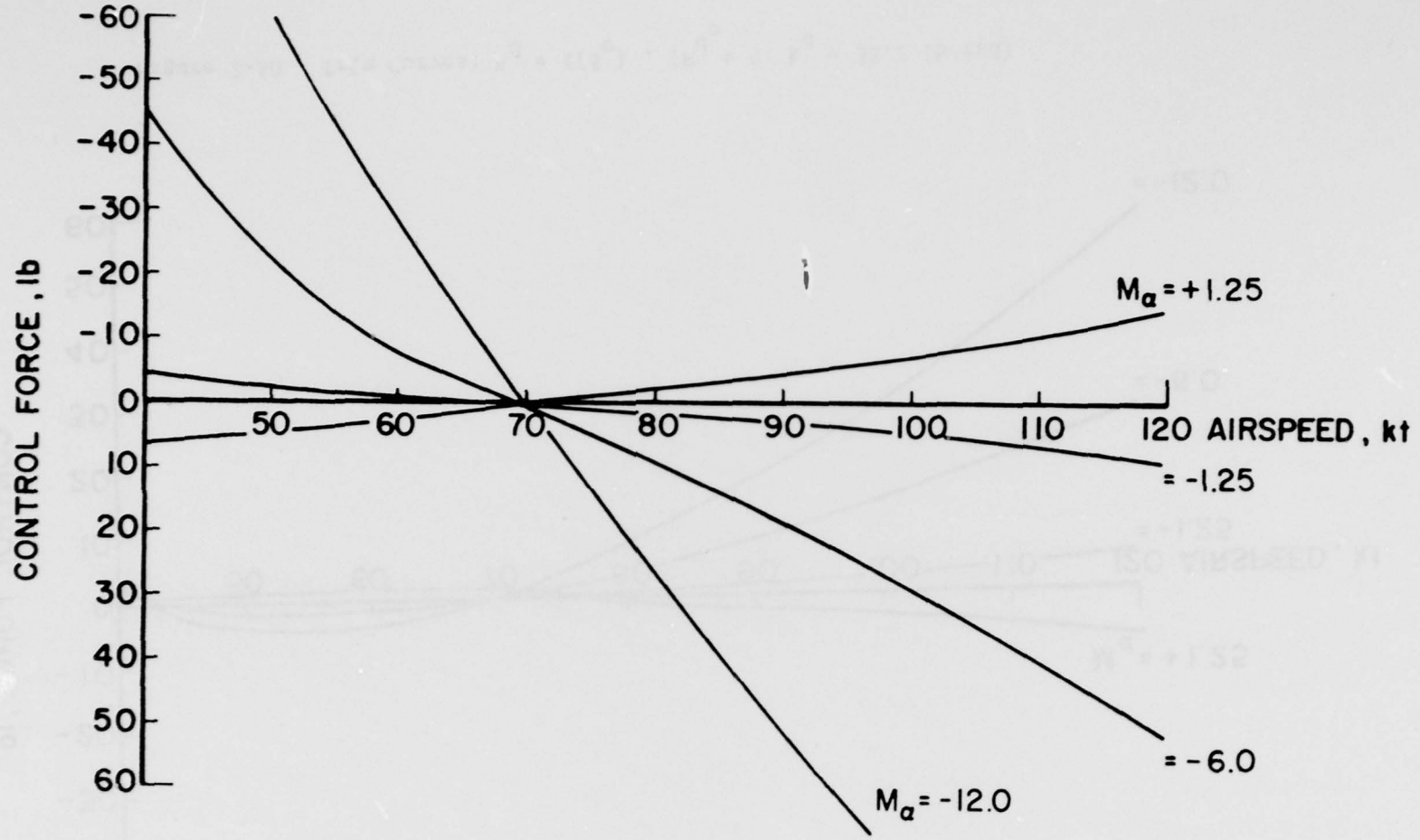

Figure 2-29. Trim Curves: Two Segment Downspring Characteristic (See Figure 3-16).

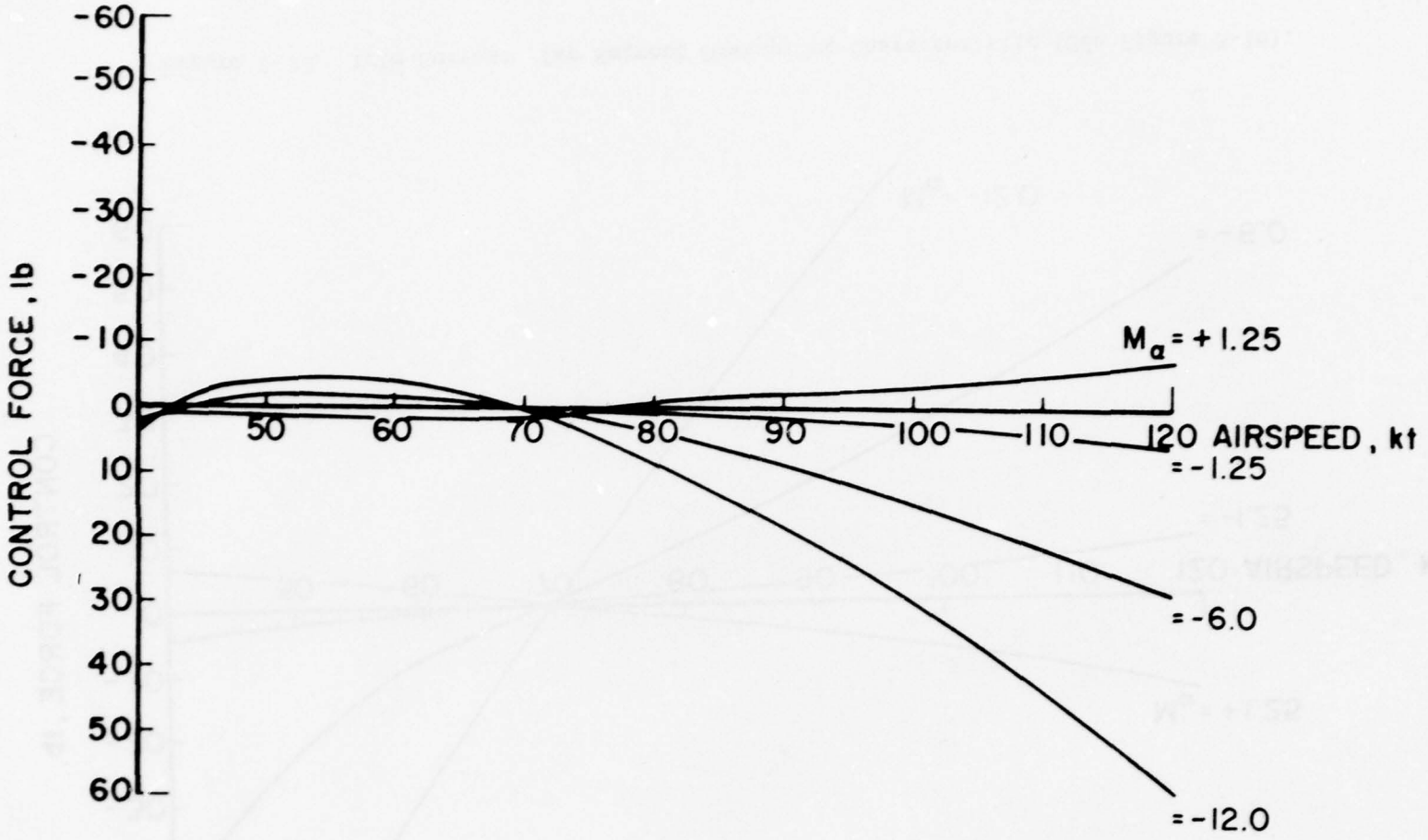

Figure 2-30. Trim Curves: $F_d = f(\delta_e)$, ($F_{d_o} = 0$, $k_d = 38.2$ lb/rad)

with control position add another complication, in that the downspring force itself varies with trim speed. Hence, if low trim speed is coupled with large downspring force, as in the case shown in Fig. 2-22, unstable phugoid dynamics could result. In such a case, the minimum acceptable phugoid damping might become the design condition limiting maximum downspring force at low trim speed.

2.3.3 Non-Classical Downspring: Downspring Force a Function of Angle-of Attack

Background Discussion - Some general aviation airplanes are equipped with systems which vary downspring force as a function of angle of attack in order to achieve desired static control force characteristics. In order to investigate the characteristics of such devices, three cases were selected for analytical evaluation. Trim curves were calculated for each of these cases at the four levels of static stability (M_α = + 1.25, - 1.25, - 6.0, - 12.0). The downspring force vs. angle of attack profiles chosen for evaluation are illustrated in Fig. 2-31 through 2-33. The trim curve equation is developed and the curves are plotted in the next section.

As always with downsprings, the worst case condition for phugoid destabilization must be kept in mind, as this may determine the maximum allowable downspring force. The downspring force vs. α curve of Case 1, for example, gives a 30-lb downspring force for any trim speed less than 70 kt, which would give a very unstable phugoid for the baseline airplane of this study (see Section 2.3).

Calculation of Control Force Trim Curves - The control force derivation again begins with the equation,

$$F_c = - GH_e - F_d \quad . \qquad (2\text{-}18)$$

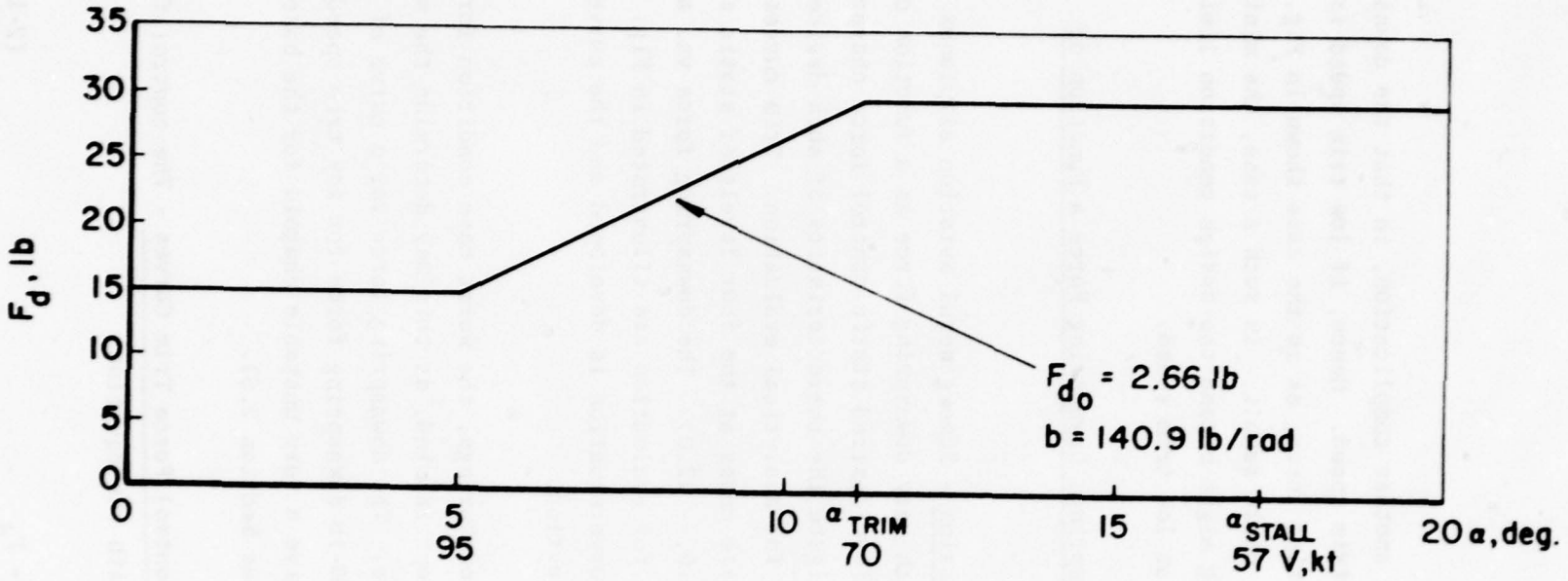

Figure 2-31. $F_d = f(\alpha)$, Case 1.

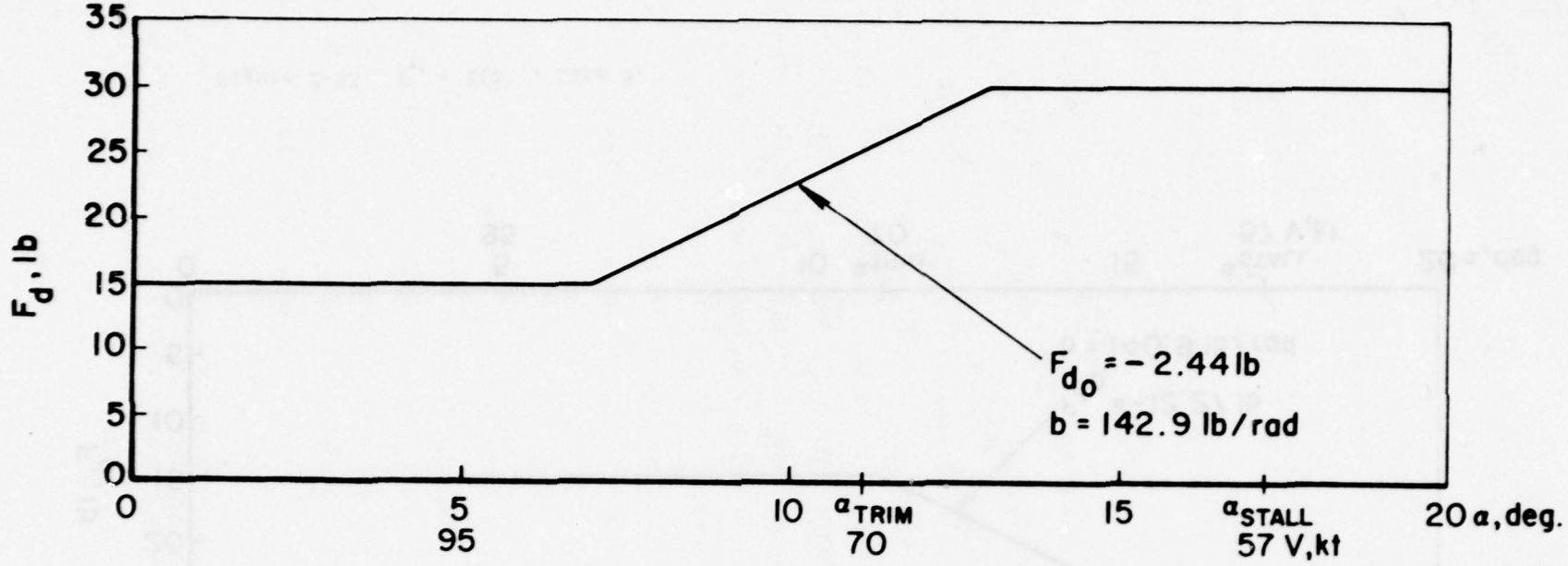

Figure 2-32. $F_d = f(\alpha)$, Case 2.

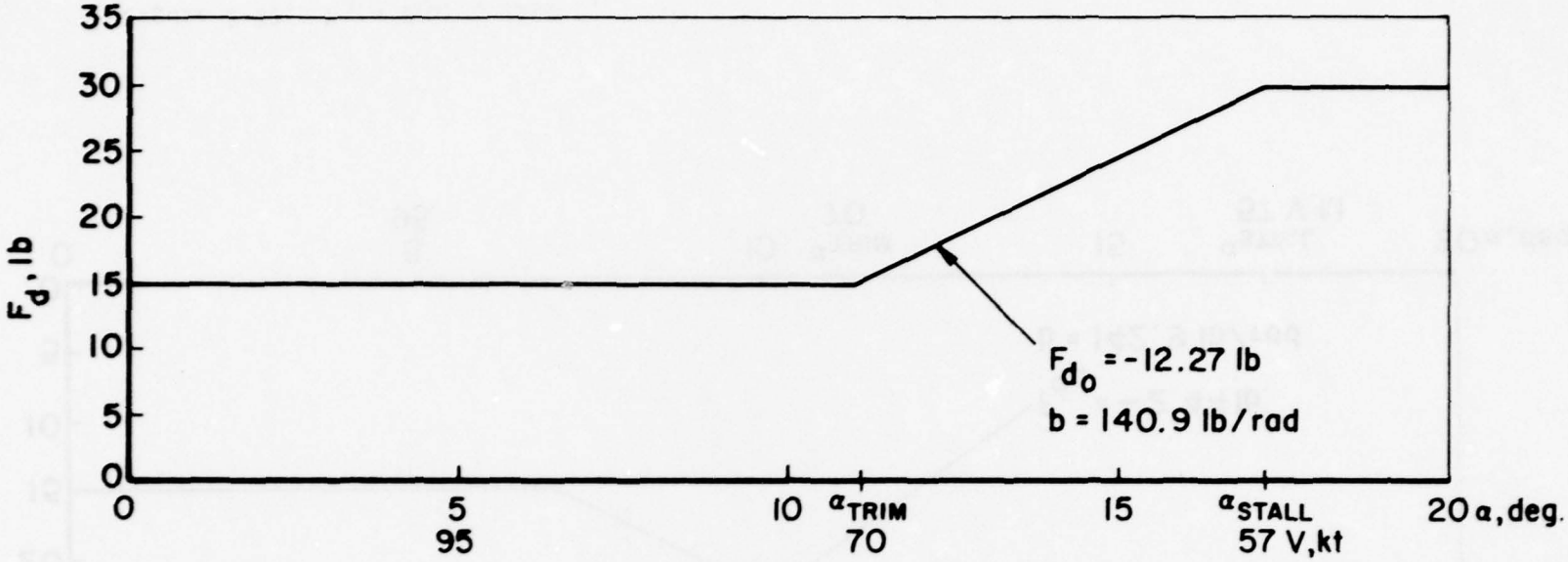

Figure 2-33. $F_d = f(\alpha)$, Case 3.

In this case, the downspring force is a linear function of airplane angle of attack,

$$F_d = F_{d_c} + K_\alpha \alpha_w \tag{2-19}$$

where,

F_{d_c} = downspring force for $\alpha_w = 0$

K_α = slope of the F_d vs α_w curve.

The control force equation becomes,

$$F_c = - GH_e - F_{d_c} - K_\alpha \alpha_\omega \tag{2-20}$$

$$= - GS_e \bar{c}_e q \eta_t \left(C_{h_o} + C_{h_\alpha} \alpha_t + C_{h_{\delta_e}} \delta_e + C_{h_{\delta_t}} \delta t\right) - F_{d_o} - K_\alpha \alpha_w$$

The following equations will be needed:

$$\alpha_t = \alpha_o + \frac{C_L}{a_w} \left(i - \frac{\partial \varepsilon}{\partial \alpha}\right) - i_w + i_t \tag{2-21}$$

$$\delta_e = \delta_{e_o} - \left.\frac{\partial C_m}{\partial C_L}\right|_{\text{fixed}} \frac{C_L}{C_{m_\delta}} \,. \tag{2-22}$$

$$\alpha_w = \alpha_o + \frac{C_L}{a_w} \tag{2-23}$$

Substituting the last three equations into Eq. (2-20) leads to

$$F_c = \tfrac{1}{2} K \rho V^2 \left(A + C_{h_{\delta_t}} \delta_t\right) - K \frac{W}{S} \frac{C_{L_\delta}}{C_{m_\delta}} \left.\frac{dC_m}{dC_L}\right|_{\text{free}} - \left(F_{d_o} + K_\alpha \alpha_o\right) - \frac{2(W/S)}{\rho} \frac{K}{a_w} \frac{1}{V^2} \tag{2-24}$$

Substituting this equation into Eq. (2-24) and simplifying leads to the following form of the control force equation:

$$F_c = \left[K \frac{W}{S} \frac{C_{h_\delta}}{C_{m_\delta}} \left.\frac{dC_m}{dC_L}\right|_{free} + \left(F_d + K_\alpha \alpha_o \right) + \frac{2(W/S)}{V^2} \frac{K_\alpha}{a_w} \left(\frac{V^2}{V_t^2} + 1 \right) \right] \cdot \left(\frac{V^2}{V_t^2} - 1 \right) \qquad (2\text{-}26)$$

This gives the control force as a function of airspeed for the case of linear variation of downspring force with angle of attack.

The precaution mentioned previously for use of Eq. (2-17) applies here also. When calculating control force, the downspring characteristics F_{d_o} and K_α at the airspeed of interest must be the same as those at the trim speed. If the downspring characteristics at the airspeed of interest differ from those at the trim speed, then Eq. (2-24) and (2-25) must be used to calculate the control force. First Eq. (2-25) is used, along with the downspring characteristics at the trim speed, to calculate the trim tab setting. This is substituted into Eq. (2-24), which is used, in conjunction with the downspring characteristics at the airspeed of interest, to calculate the control force. This procedure was used to calculate the trim curves of Fig. 2-34 through 2-36.

2.4 BOBWEIGHTS AND THEIR EFFECTS ON LONGITUDINAL STABILITY AND CONTROL

2.4.1 Classical Constant-Force Bobweights

Like the downspring, the bobweight is a familiar device for augmenting the control-free static stability of an airplane. Physically, the bobweight is attached to the longitudinal control system so as to

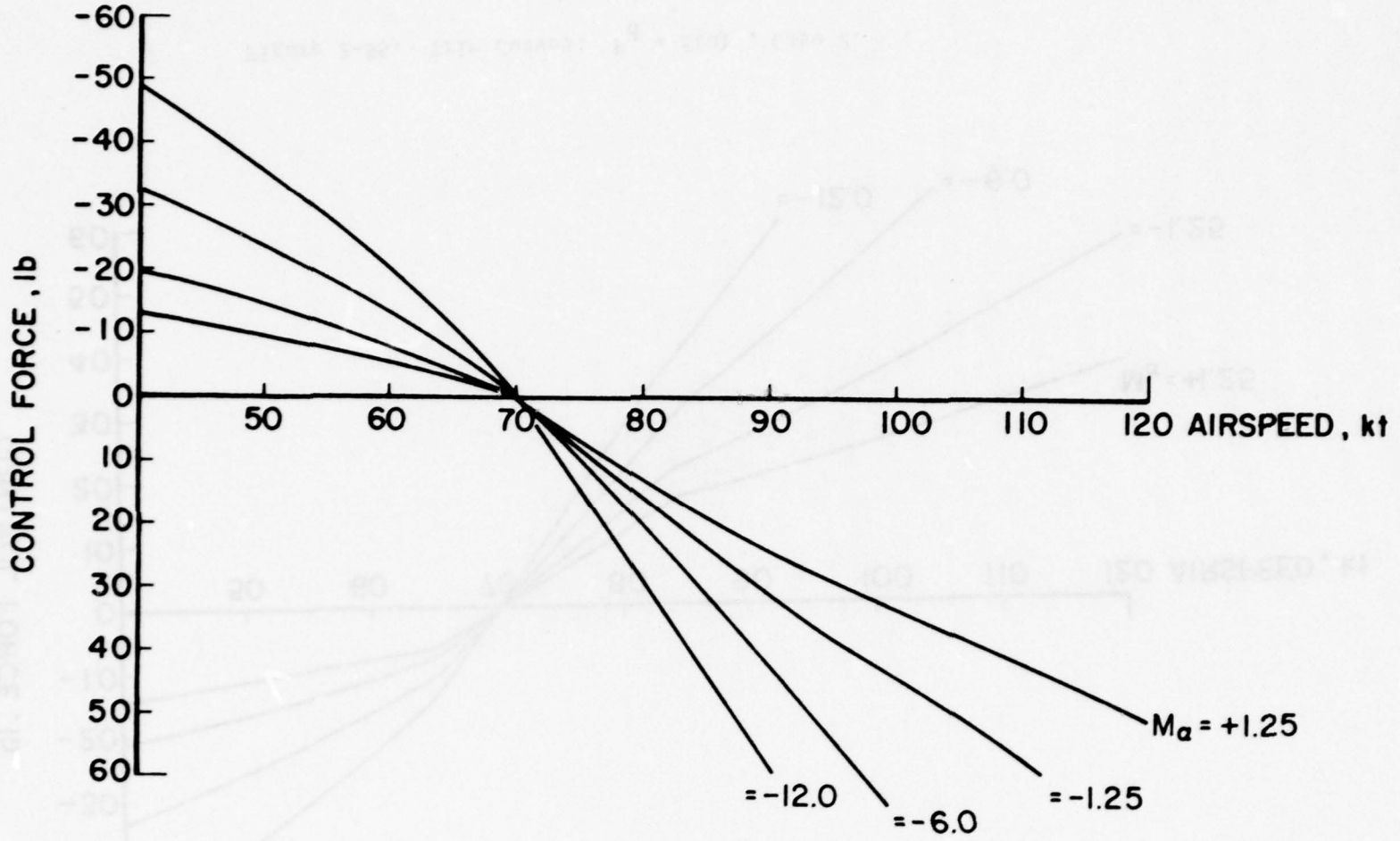

Figure 2-34. Trim Curves: $F_d = f(\alpha)$, Case 1.

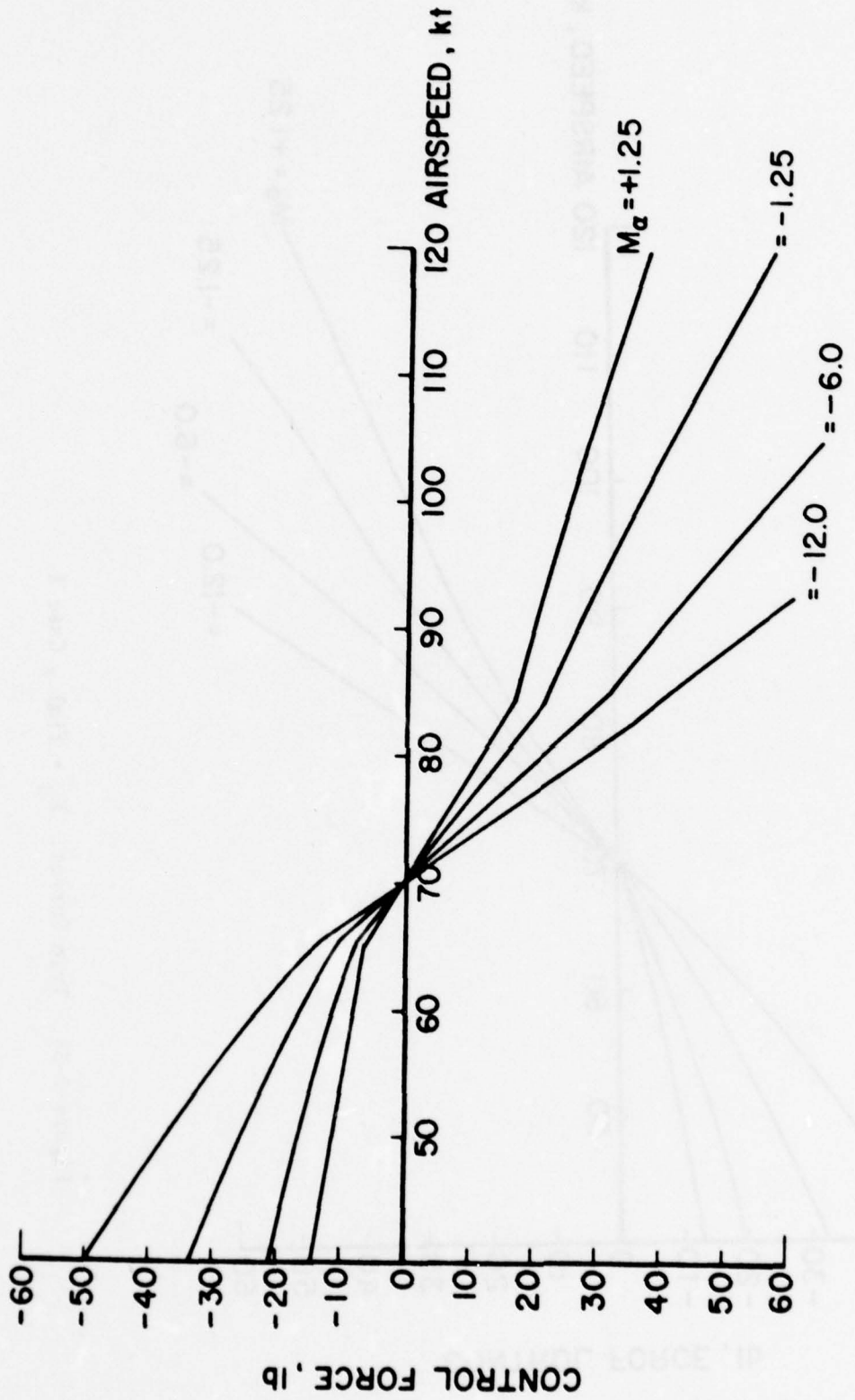

Figure 2-35. Trim Curves: $F_d = f(\alpha)$, Case 2.

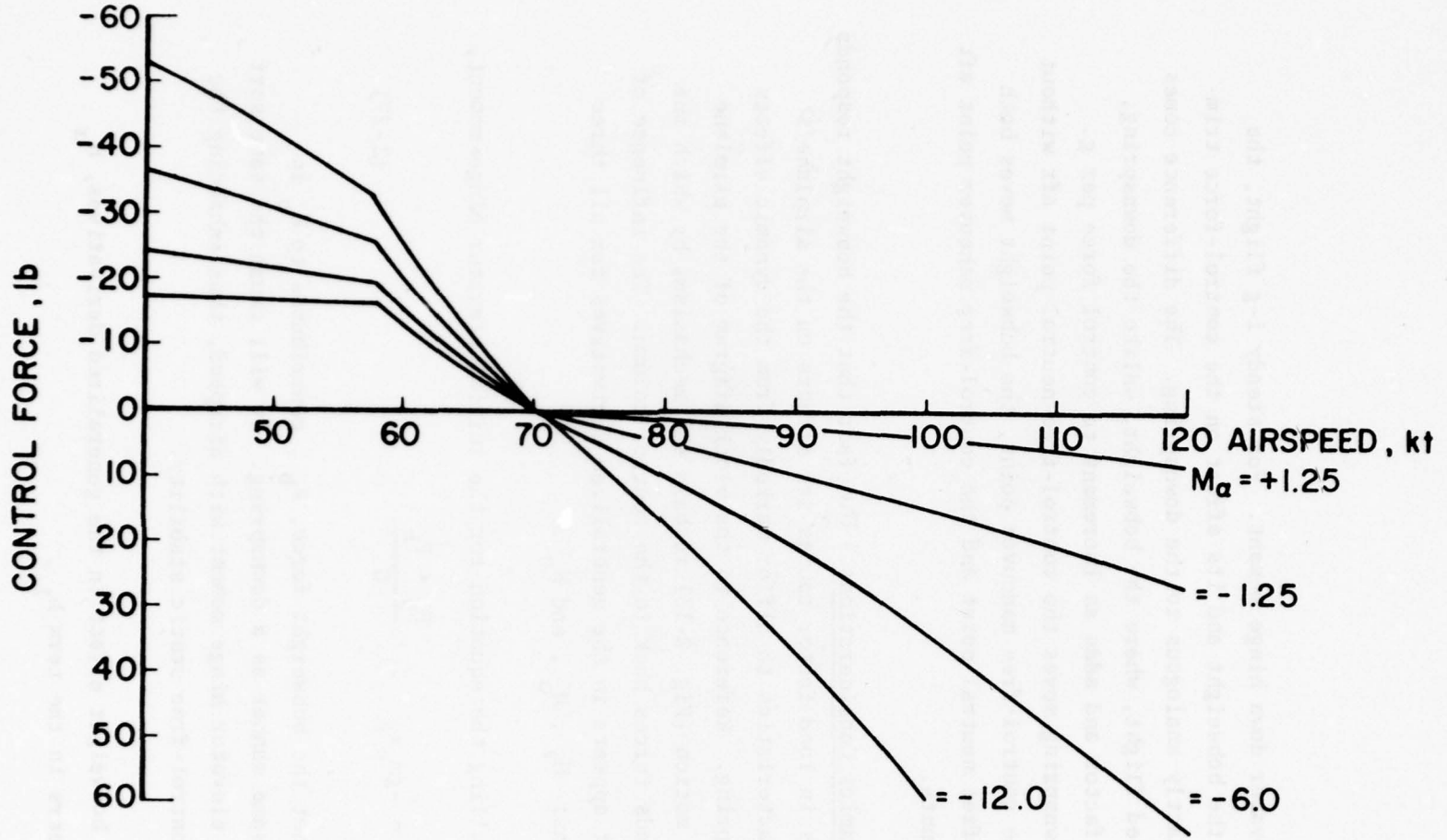

Figure 2-36. Trim Curves: $F_d = f(\alpha)$, Case 3.

exert an elevator down hinge moment. For steady 1-g flight, the function of the bobweight and its effect on the control-force trim curve are exactly analogous to the downspring. The difference comes in accelerated flight, where the bobweight, unlike the downspring, senses load factor and adds an increment to control force per g. While the downspring moves the control-free neutral point aft without affecting the control-free maneuver point, the bobweight moves both the control-free neutral point and the control-free maneuver point aft by equal amounts.

Dynamics Considerations - The fact that the bobweight responds to variations in load factor causes its effects on the airplane's dynamic characteristics to differ markedly from the dynamic effects of the downspring. Reference to the block diagram of the airplane equations of motion (Fig. 2-13) reveals the mechanisms by which the bobweight feeds forces back to the control column. The influence of the bobweight appears in the generalized derivatives for all three feedback paths: H_V , H_α , and H_θ .

Recalling the equation for the initial elevator hinge moment,

$$H_o = -gm_e x_e - \frac{F_d + F_b}{G} \qquad (2-27)$$

It is seen that the bobweight force, F_b , contributes to H_o in exactly the same manner as a downspring. It will cause the same sort of change in elevator hinge moment with airspeed, thus enhancing the airplane's control-free static stability.

The bobweight effect in the generalized derivatives, H_α and H_o , appears in the term h_1 ,

$$h_1 = z\left(C_{h_b} + \Delta C_{h_b}\right) \qquad (2-28)$$

where,

$$C_{h_b} = \frac{F_b}{G\, S_e\, \bar{c}_e\, (W/S)} \quad ,$$

C_{h_b} is an elevator hinge moment parameter due to bobweight, and

$$\Delta C_{h_b} = \frac{W_e\, x_e}{S_e\, \bar{c}_e\, (W/S)} \quad , \qquad (2\text{-}29)$$

This is an elevator hinge moment parameter due to elevator mass unbalance. Note that ΔC_{h_b} could be due to a bobweight mounted on the elevator. Returning to the block diagram of the equations of motion (Fig. 2-13), isolating the force feedback terms representing the influence of the bobweight confirms that a force is fed back to the control column proportional to incremental load factor:

$$h\ (\Delta\dot{\theta} - \Delta\dot{\alpha}) + = h_1 \Delta\dot{\gamma}$$
$$= h_1 \frac{g}{V} \Delta n \qquad (2\text{-}30)$$

The root locus plot in Fig. 2-37 illustrates the effect of the bobweight on the dynamic characteristics of the baseline airplane for nominal control-fixed static stability, $M_\alpha = -6.0$. The root locus indicates that a bobweight of any reasonable magnitude can be employed without encountering problems with dynamics. The phugoid mode is insensitive to the use of a bobweight, while the short period frequency increases.

Figure 2-38 shows the effect of a bobweight far aft of the c.g., $M_\alpha = +1.25$. For a sufficiently large bobweight, the airplane not only becomes statically stable but also takes on conventional phugoid and short period characteristics. Figure 2-39 shows an expanded view of the low-frequency region, giving the change in the phugoid roots for increasing bobweight force.

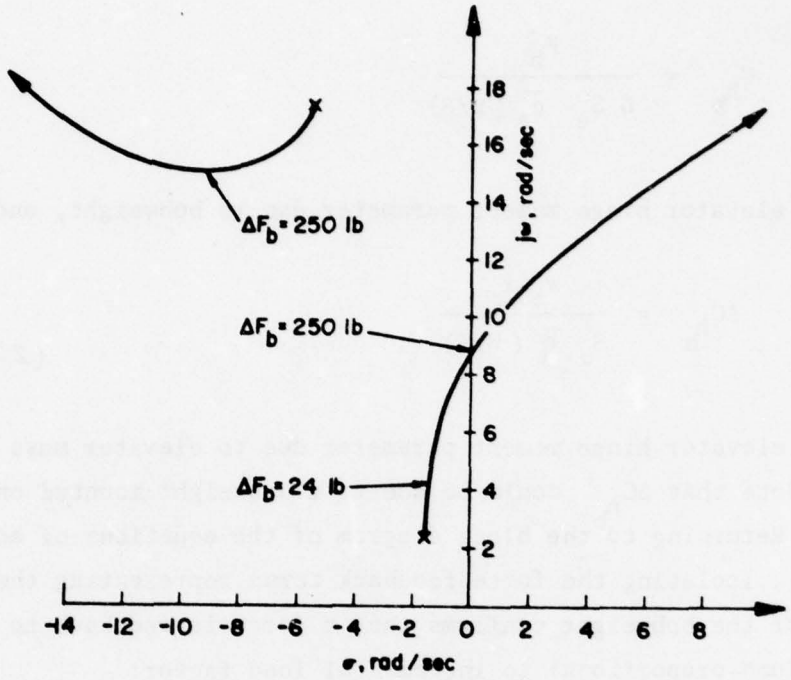

Figure 2-37. Root Locus: Variable Bobweight Positive ΔF_b .

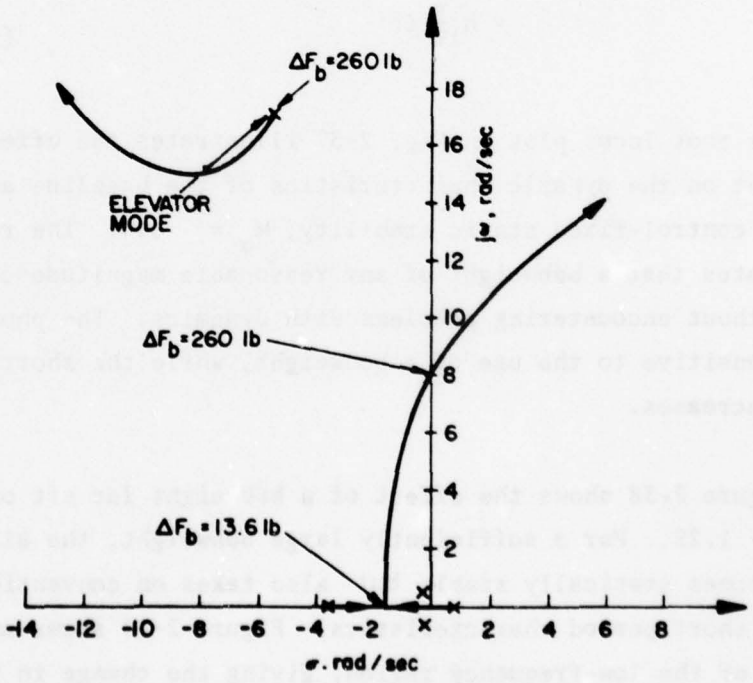

Figure 2-38. Root Locus: Variable Bobweight Positive ΔF_b M_α = + 1.2.

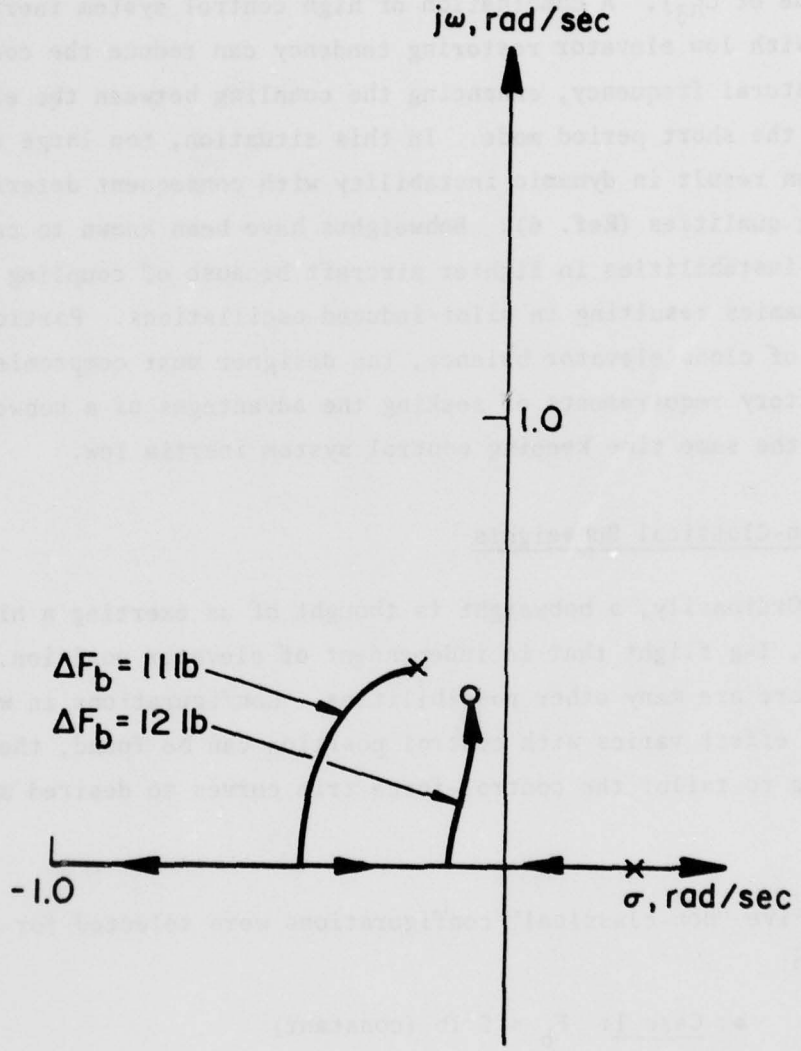

Figure 2-39. Root Locus: Variable Bobweight Positive ΔF_b $M_\alpha = +1.25$. Expansion of Phugoid Region of Figure 4.2.

The root loci shown are for the baseline airplane nominal restoring tendency, C_{h_δ} = - 0.60 rad^{-1}. A potential complication arises when the use of a bobweight is coupled with a closely balanced elevator (low value of C_{h_δ}). A combination of high control system inertia, coupled with low elevator restoring tendency can reduce the control system natural frequency, enhancing the coupling between the elevator mode and the short period mode. In this situation, too large a bobweight can result in dynamic instability with consequent deterioration of flying qualities (Ref. 6). Bobweights have been known to cause catastrophic instabilities in fighter aircraft because of coupling with aircraft dynamics resulting in pilot-induced oscillations. Particularly in cases of close elevator balance, the designer must compromise between contradictory requirements of seeking the advantages of a bobweight while at the same time keeping control system inertia low.

2.4.2 Non-Classical Bobweights

Ordinarily, a bobweight is thought of as exerting a hinge moment in steady, 1-g flight that is independent of elevator position. In actuality, there are many other possibilities. Configurations in which the bobweight effect varies with control position can be found, their objective being to tailor the control-force trim curves to desired specifications.

Five "non-classical" configurations were selected for analytical evaluation:

- Case 1: F_b = 5 lb (constant)
- Case 2: F_b = 10 lb (Constant)
- Case 3: Bobweight force varies linearly with elevator deflection from F_b = 5 lb for full up elevator to F_b = 0 for full down elevator. (Fig. 2-40).

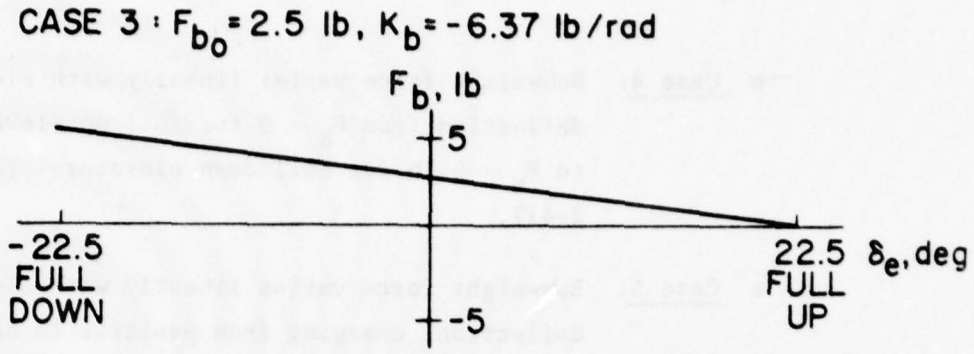

Figure 2-40. Case 3 : F_{b_o} =2.5 lb, K_b=-6.37 lb/rad

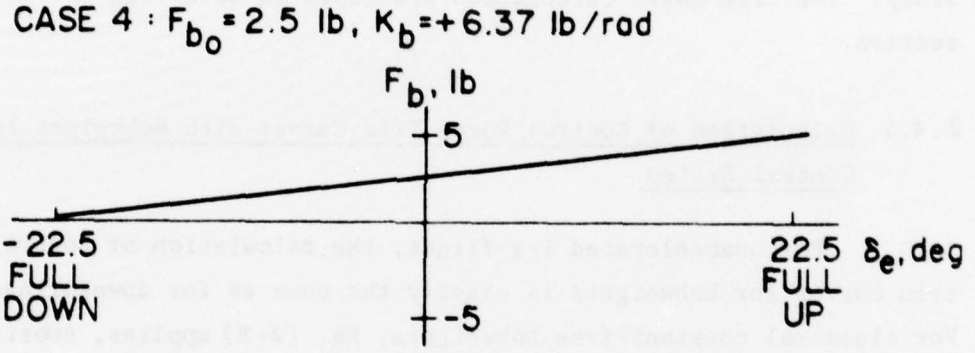

Figure 2-41. Case 4 : F_{b_o} =2.5 lb, K_b=+6.37 lb/rad

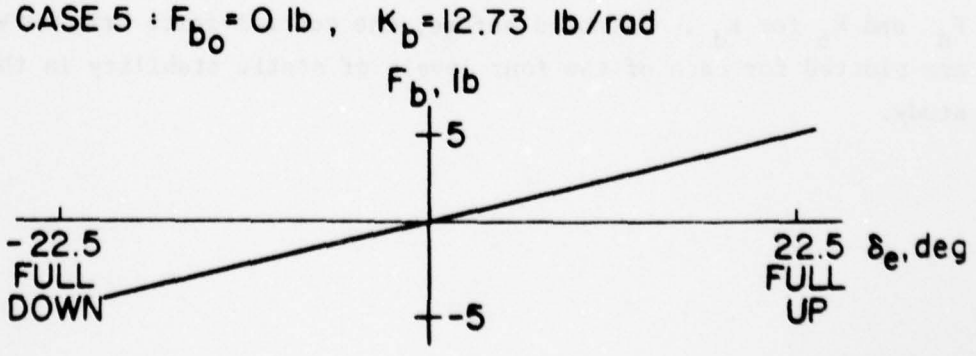

Figure 2-42. Case 5 : F_{b_o} = 0 lb, K_b=12.73 lb/rad

- Case 4: Bobweight force varies linearly with elevator deflection from F_b = 0 for full up elevator to F_b = 5 lb for full down elevator. (Fig. 2-41).

- Case 5: Bobweight force varies linearly with elevator deflection, changing from positive to negative for large elevator deflection. (Fig. 2-42).

Control-force trim curves for these cases are plotted in Fig. 2-43 through 2-47 for the four values of M used previously in this study. The trim curve calculation procedure is described in the next section.

2.4.3 Calculation of Control Force Trim Curves with Bobweight in Control System

For unaccelerated 1-g flight, the calculation of control force trim curves for bobweights is exactly the same as for downsprings. For classical constant-free bobweights, Eq. (2-8) applies, substituting bobweight force F_b for downspring force F_d. When the bobweight force varies linearly with elevator deflection,

$$F_b = F_b + K_b\delta_e \qquad (2\text{-}31)$$

The trim curve is calculated using Eq. (2-17), substituting F_b for F_d and K_b for K_d. As noted before, the control-force trim curves are plotted for each of the four levels of static stability in this study.

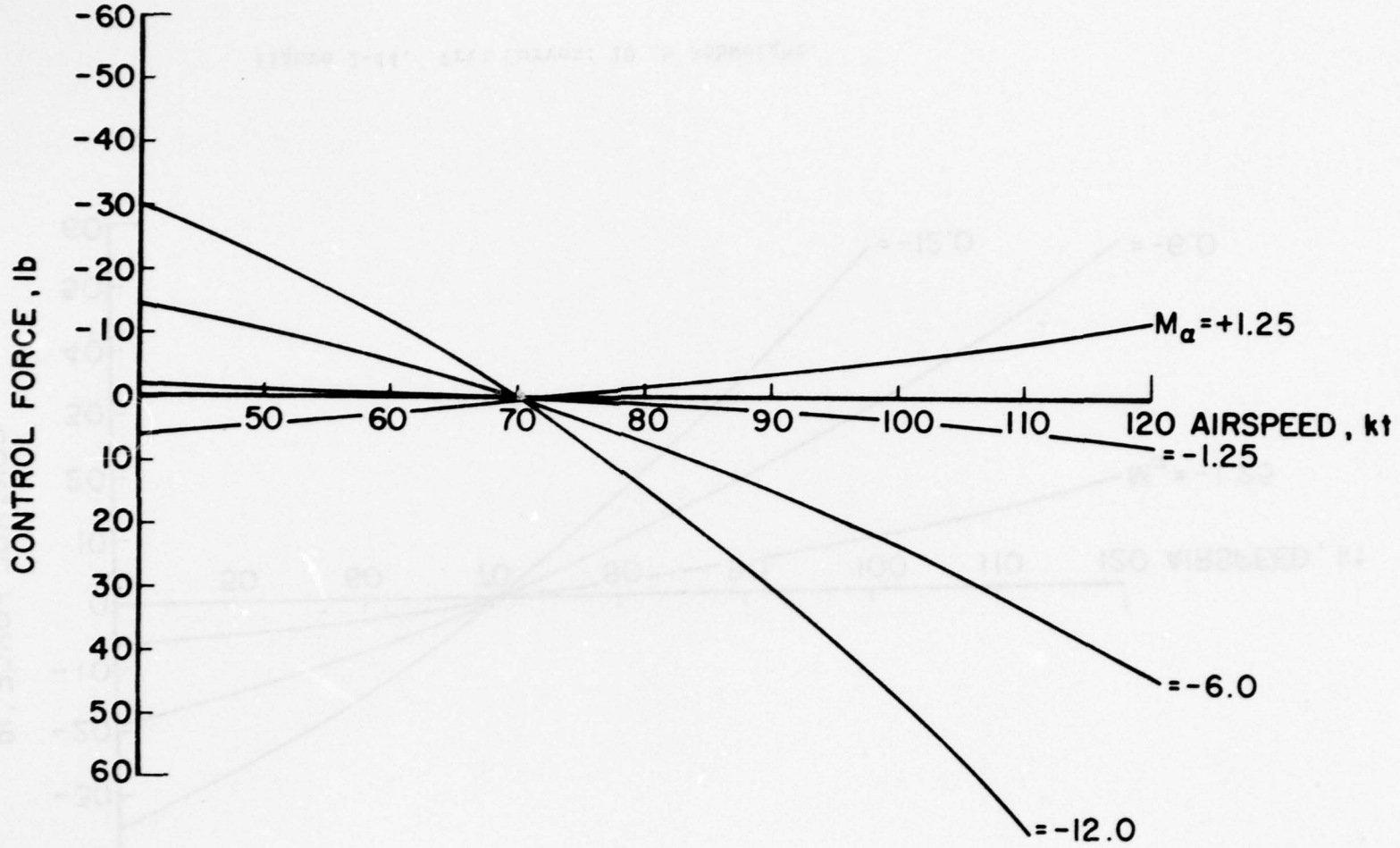

Figure 2-43. Trim Curves: 5 lb Bobweight.

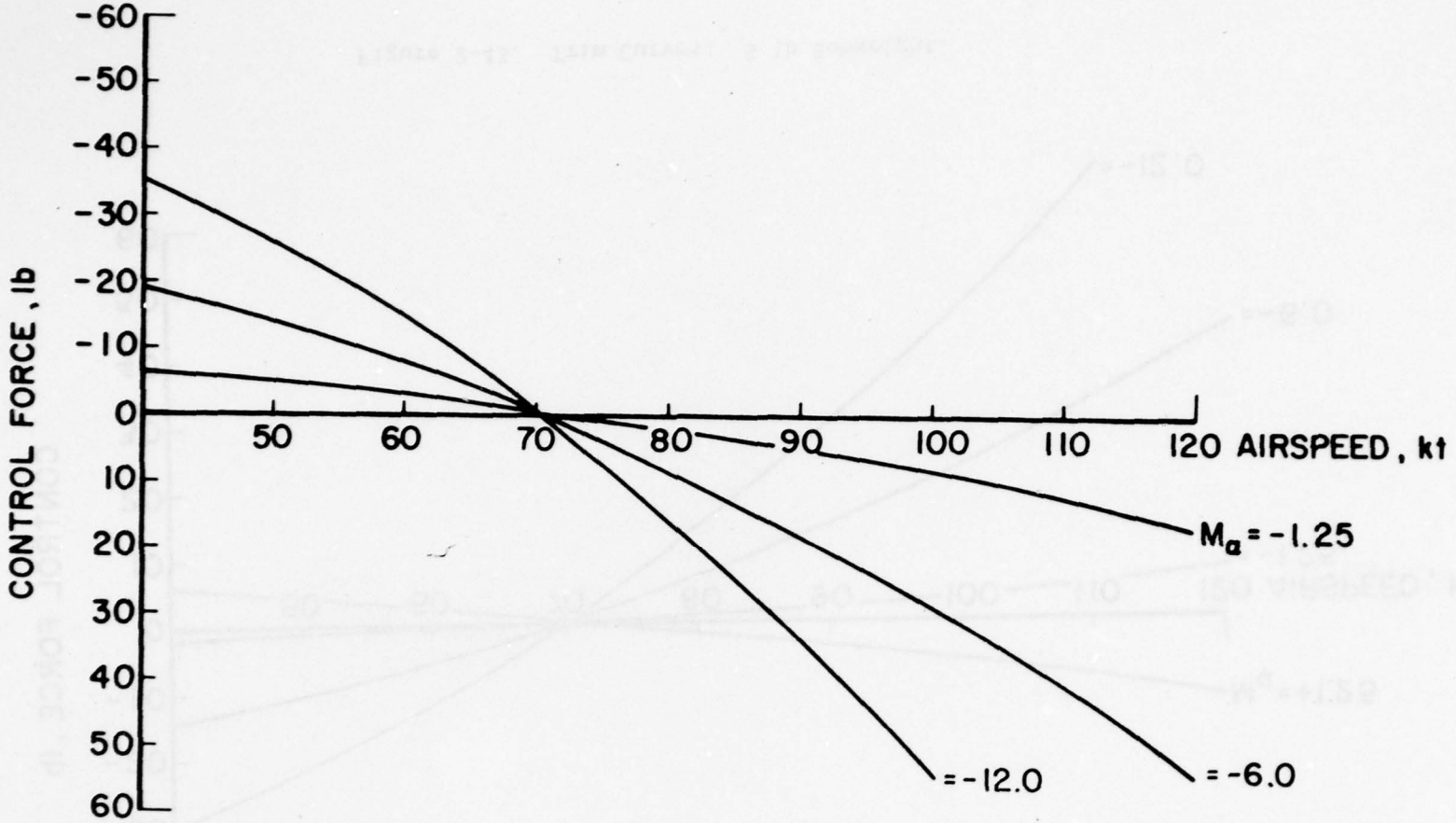

Figure 2-44. Trim Curves: 10 lb Bobweight.

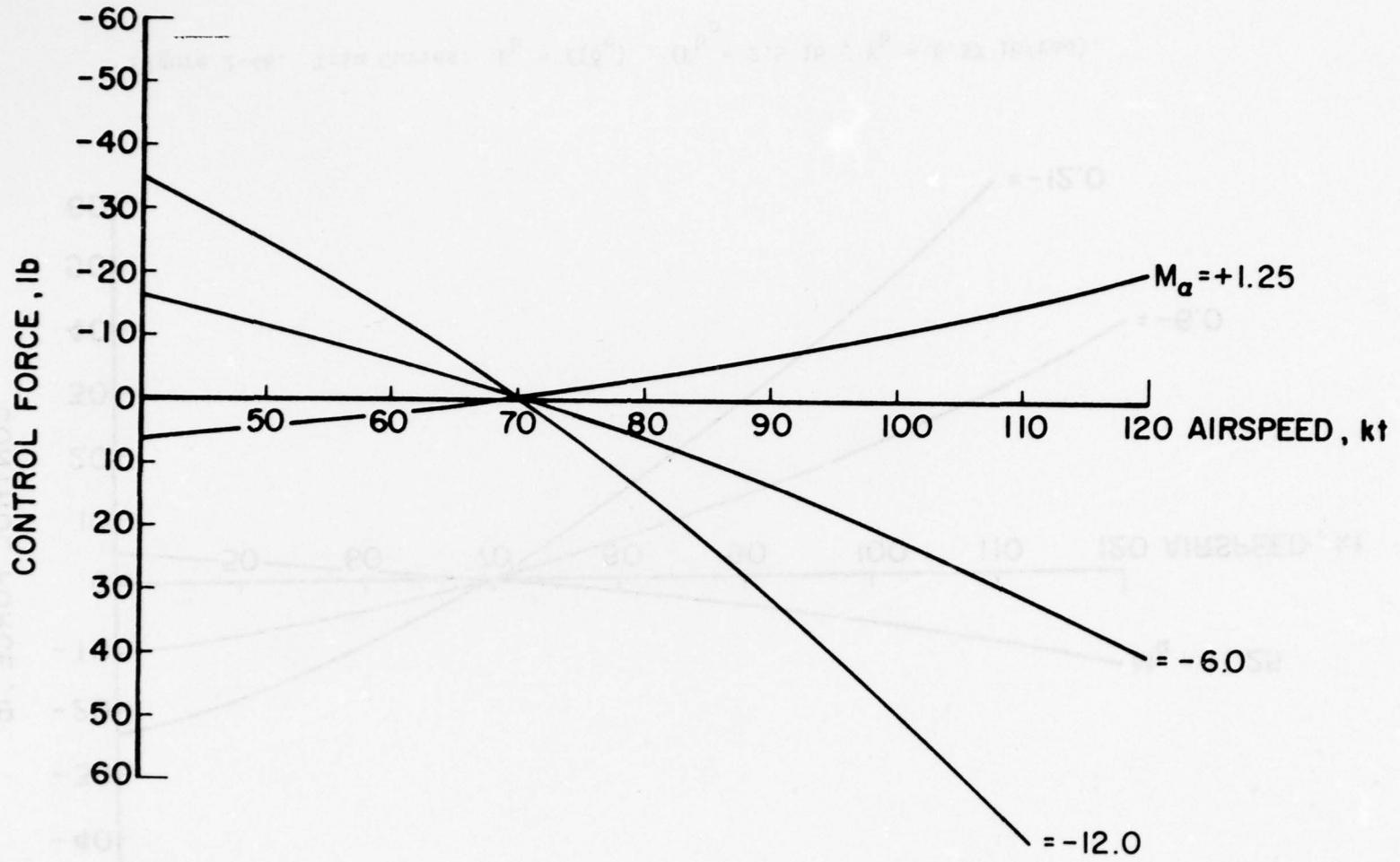

Figure 2-45. Trim Curves: $F_b = F(\delta_e)$, (F_{b_o} = 2.5 lb, K_b = -6.37 lb/rad)

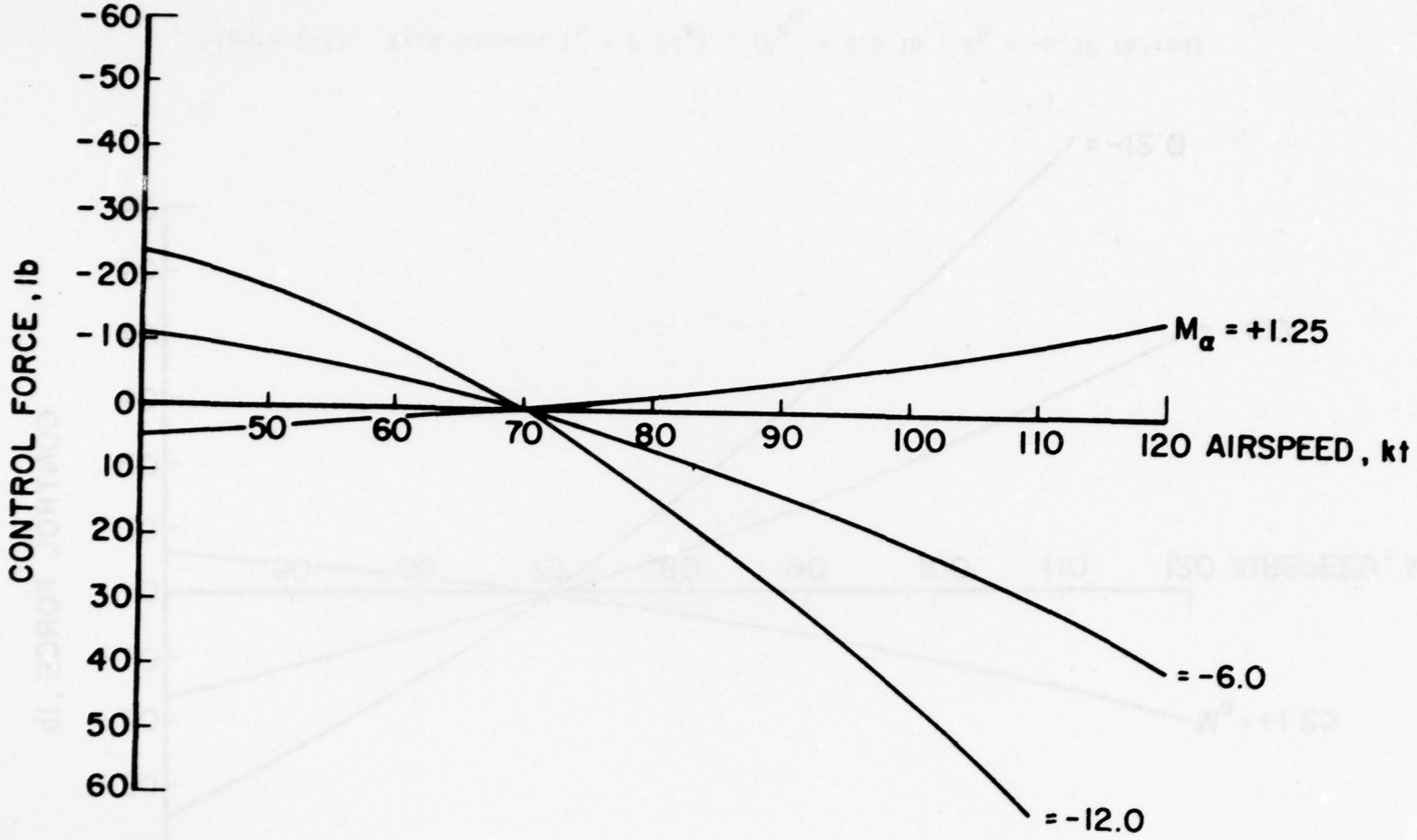

Figure 2-46. Trim Curves: $F_b = f(\delta_e)$, (F_{b_o} = 2.5 lb , K_b = 6.37 lb/rad).

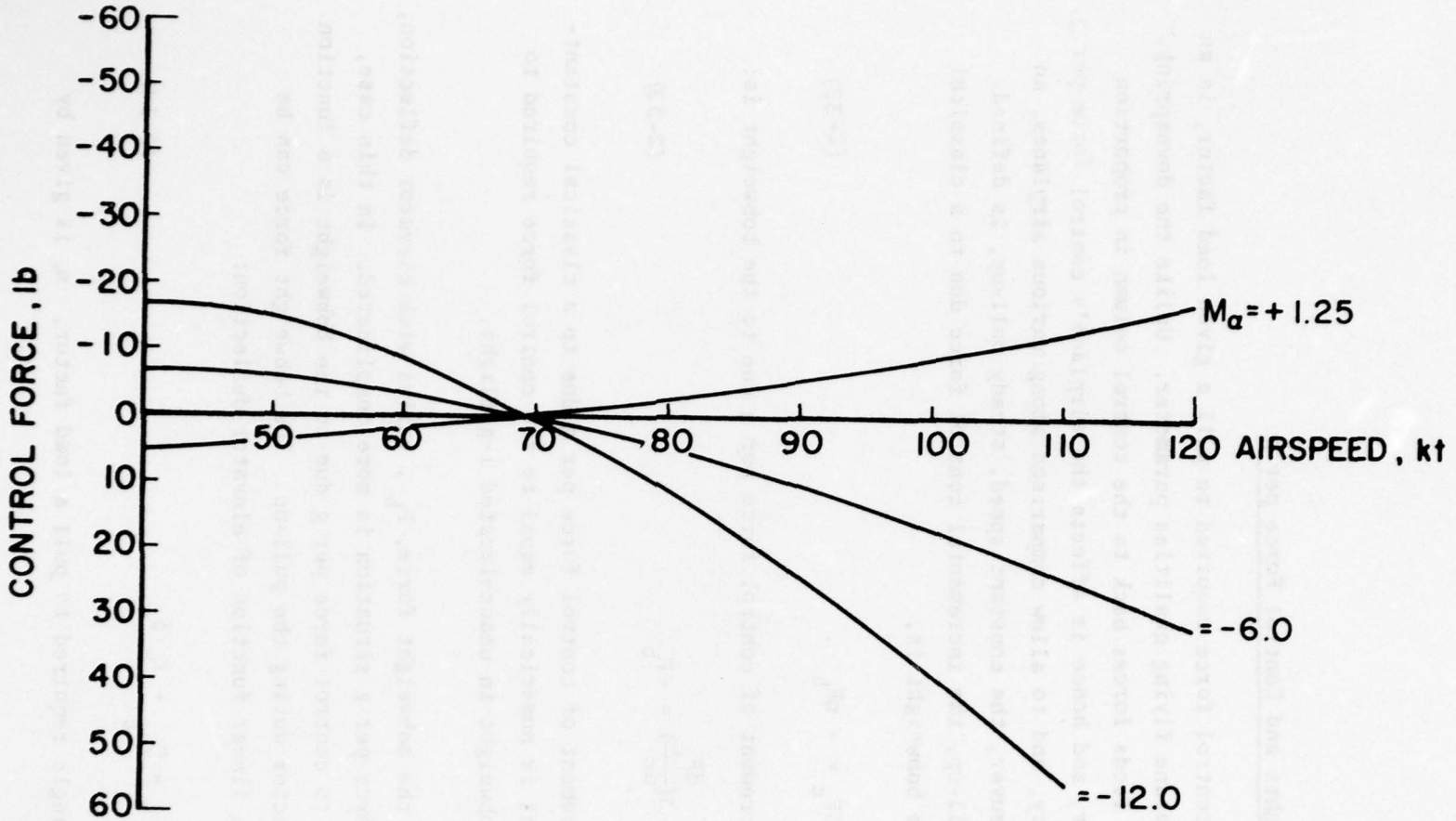

Figure 2-47. Trim Curves: $F_b = f(\delta_e)$, ($F_{b_o} = 0$, $K_b = 12.73$ lb/rad)

2.4.4 Bobweights and Control Force per g

The control force required to pull a given load factor, is an important airplane flying qualities parameter. Unlike the downspring, the bobweight feeds forces back to the control column in proportion to load factor, and hence it affects the airplane's control force per g. For consistency, and to allow comparison among various airplanes, an idealized maneuver, the constant speed, steady pull-up, is defined. For such a pull-up, the incremental control force due to a classical constant force bobweight is,

$$\Delta F_c = - nF_b \quad . \tag{2-32}$$

Hence, the increment of control force per g due to the bobweight is:

$$\Delta\left(\frac{dF_c}{dn}\right) = -F_b \tag{2-33}$$

Thus, the increment of control force per g due to a classical constant-force bobweight is numerically equal to the control force required to balance the bobweight in unaccelerated 1-g flight.

When the bobweight force, F_b , varies with elevator deflection, the control force per g situation is more complicated. In this case, the increment to control force per g due to the bobweight is a function of the load factor during the pull-up. The bobweight force can be expressed as a linear function of elevator deflection:

$$F_b = F_{b_c} + K_b \delta_e \quad . \tag{2-34}$$

The elevator angle required to pull a load factor, n, is given by (Ref. 7):

$$\delta_e = \delta_{e_o} - \frac{2n(W/S)}{V^2 C_{m_\delta}} \cdot \left.\frac{\partial C_m}{\partial C_L}\right|_{fixed} - \frac{1.1\, g l_t (n-1)}{\tau V^2} \qquad (2\text{-}34)$$

Using the above two equations, the incremental control force during the pull-up due to bobweight can be expresses as

$$\Delta F_c = - nF_b = - n \left(F_{b_o} + K_b \delta_e \right)$$

$$= - n \left[F_{b_o} + K_b \delta_{e_o} - \frac{2nK_b (W/S)}{\rho V^2 C_{m_\delta}} \left.\frac{\partial C_m}{\partial C_L}\right|_{fixed} - \frac{1.1\, K_b g l_t (n-1)}{\tau V^2} \right] \qquad (2\text{-}35)$$

Differentiating with respect to n yields the incremental control force per g, due to bobweight. For the case of bobweight force varying linearly with elevator deflection,

$$\Delta\left(\frac{\partial F_c}{\partial n}\right) = - F_{b_o} - K_b \delta_{e_o} + \frac{4(W/S)}{\rho C_{m_\delta}} \frac{nK_b}{V^2} \left.\frac{\partial C_m}{\partial C_L}\right|_{fixed} + \frac{1.1 g l_t}{\tau} \frac{(2n-1) K_b}{V^2} \qquad (2\text{-}36)$$

Substituting baseline airplane values for the constants in this equation yields

$$\Delta \left(\frac{\partial F_c}{\partial n}\right) = - F_{b_o} - (0.145) K_b - (21{,}800) \frac{nK_b}{V^2} \left.\frac{\partial C_m}{\partial C_L}\right|_{fixed} + \frac{(1100)(2n-1) K_b}{V^2} \qquad (2\text{-}37)$$

Hence, calculation of the incremental control force per g requires knowledge of:

- Load factor time history during pull-up: (defined L = nW)
- Airspeed during steady pull-up: V
- Control fixed static stability: $\left.\frac{\partial C_m}{\partial C_L}\right|_{\text{fixed}}$
- Bobweight characteristics: F_{b_c} and K_b

2.5 CHAPTER SUMMARY

Based on the analytical work described in the preceding chapters, the following summary statements may be made:

- Angle of attack static stability, M_α, is directly related to control force gradient through trim, and is an important determinant of dynamic response characteristics.
- As elevator floating tendency, C_{h_α}, becomes increasingly negative, control-free static stability decreases relative to control-fixed static stability. Dynamic response characteristics are favorable for a large range of negative C_{h_α}, but positive values can lead to unfavorable dynamic response and control-feel characteristics.
- Elevator restoring tendency, C_{h_δ}, must be negative for control system stability but can vary over a wide range of negative values without dynamic complications.
- Classical constant-force downspring causes the control-free neutral point to move aft, thus augmenting control-free static stability of the airplane. A downspring has no effect on control-fixed stability, and its use to mask a control-fixed instability could be dangerous

in case of insufficient elevator control power. A downspring tends to destabilize the phugoid, this effect being worse at low trim speeds; a downspring has little effect on short period characteristics.

- In actual practice, downspring force may vary with elevator position. This variation may be the result of a short spring, or the downspring may be geared for a particular variation of downspring force with control position in order to tailor the control force trim curve to desired specifications. Expressions have been derived for calculating control force trim curves for cases of linear or piecewise-linear variation of downspring force with elevator position.

- Systems which vary downspring force with angle of attack are in use, allowing adjustment of the control force trim curve. Expressions have been derived for calculating control-force trim curves for cases of linear or piecewise-linear variation of downspring force with angle of attack.

- The effect of a bobweight on the control-force trim curve is identical to the effect of a downspring. As with a downspring, a bobweight may be mounted so as to yield a particular variation of bobweight force with control position. With the substitution of F_b for F_d, the trim curve equations derived for downsprings are applicable to bobweights.

- Since the bobweight senses load factor, it adds an increment to control force per g. A bobweight moves both the control-free neutral point and the control-free maneuver point aft by equal amounts; it increases short period frequency but has little effect on the phugoid

mode. An expression has been derived for incremental control force per g for the case of a linear variation of bobweight force with elevator position.

AD-A060 467 PRINCETON UNIV N J DEPT OF AEROSPACE AND MECHANICAL--ETC F/G 1/3
A STUDY OF LONGITUDINAL CONTROLLABILITY AND STABILITY REQUIREME--ETC(U)
AUG 78 D R ELLIS, C L GRIFFITH DOT-FA75WA-3679
UNCLASSIFIED AMS-1369 FAA-RD-78-113 NL

2 OF 2
AD A060 467

END
DATE FILMED
1-79
DDC

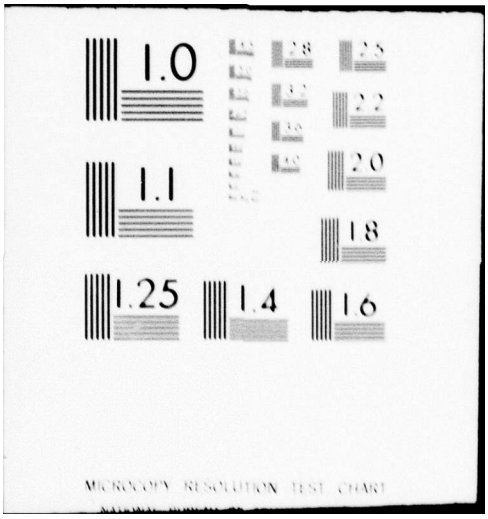
1.0
1.1
1.25
1.4
1.6
2.0
2.2
2.5
MICROCOPY RESOLUTION TEST CHART

3. DESCRIPTION OF EXPERIMENTS

3.1 VARIABLE-RESPONSE RESEARCH AIRCRAFT

The experimental phases of the study made use of the Princeton 5-DOF Variable-Response Research Aircraft, described in detail in Appendix A. For purposes of understanding this and subsequent sections of the report, it is sufficient to note that the evaluation pilot operates a set of "fly-by-wire" controls which provide electrical signals to command electro-hydraulic actuators at the engine and at each control surface. The cockpit control signals are summed with those from various sensors, such as angle-of-attack vanes, rate gyros, and accelerometers. These sensor-derived signals serve to alter the static stability and damping characteristics of the basic airframe. By means of specialized calibration techniques, any desired combination of characteristics may be simulated.

For this study, a special cockpit control wheel unit was developed which provides for in-flight changes in the longitudinal force vs. displacement characteristics. The following variable features are pertinent to this study:

- Control column-to-elevator gearing
- Force at wheel vs. displacement
- Control system damping
- Coulomb (sliding) friction
- Simulated downspring (constant force, variable with elevator deflection, variable with angle of attack)
- Simulated bobweight (constant or variable force with elevator deflection)
- Stick-force-per- g gradient decrease at specified load factor.

Details of the system may be found in Appendix B.

3.2 TEST PROCEDURES AND CONDITIONS

3.2.1 Static Stability Tests

The experiments involving static stability focused on terminal area flight phases, which tend to be critical from the standpoint of precision path and speed control. The choice was dictated,in large part,by the longitudinal flying qualities experiments of Ref. 9, which strongly suggested that airplanes which are marginally acceptable on the approach might not be acceptable for flare and touchdown. A second important factor is that the condition of lowest static stability for many airplanes is the low-speed, high-power climb.

The test procedure featured continuous circuits of the airfield (Princeton's Forrestal Airport) with a combination of simulated IFR and VFR approach segments, landing flare with actual (not simulated) touchdown, and maximum performance climb after takeoff. Typically, a sequence would go as follows:

- Evaluation pilot assumes control on either the downwind or base leg of the pattern at 800-ft AGL, in trim at 70-75 kt.
- At an appropriate point, the safety pilot calls for a turn to a heading which will intercept the localizer of a TALAR MLS; localizer and a 3-deg glideslope are tracked down to an altitude of 200-ft AGL.
- Upon looking up, the evaluation pilot continues the approach and executes a flare and touchdown.
- Full throttle is applied (for simplicity,this is maximum continuous climb power),and take off and transition to a 70-kt climb are accomplished.
- Either a climbing turn is made to the downwind leg by the evaluation pilot, or the safety pilot takes control in order to reconfigure the airplane.

Testing was limited to smooth air or light natural turbulence; this usually corresponded to winds of less than 10 kt.

Pilot ratings and commentary were requested for each configuration flown. The number of runs on each configuration varied; at least two or three generally were needed in order to give an assessment. Pilots were asked to give separate ratings and comments for the various flight phases and, if they wished, an overall rating for terminal area operations. They were briefed to rate and comment upon at least the following specific items:

Phase	Rating Basis or Comment
APPROACH	• Path and speed control, "trimmability" • Control forces, quality of off-speed cue
FLARE AND TOUCHDOWN	• Precision of control • Control forces, proper variation during maneuver
CLIMB	• Speed control, "trimmability" • Can attention be diverted

3.2.2 Maneuvering Stability Tests

Since factors such as stick force per g tend to assume a secondary role for low-speed terminal area operations, a low-speed cruise condition was simulated in the maneuvering-stability phase of the experiments. (A high-speed cruise condition would have been preferable for realism and to attain higher incremental load factors, but in order to avoid inadvertent overstressing with marginal configurations, speed was limited to slightly below the maneuvering value of 108 kt).

The particular evaluation maneuvers were the following:

- Visual pull-up from a shallow dive (as from a stall recovery situation, or from a collision avoidance maneuver)
- Pull-up by reference to instruments (recovery from unusual attitude)
- Steep turn (possible collision-avoidance maneuver, where pitch attitude and pitch rate cues are not as evident as in the wings-level cases).

In each case, the evaluation pilot assumed control with the airplane trimmed at 105 kt. He was briefed to perform two or three of each of the maneuvers before rating and commenting on the configuration.

3.2.3 Additional Details

In addition to the collection of pilot commentary and ratings (accodring to the Cooper-Harper scale of Ref. 10), airplane motion variables and cockpit control activity were recorded on the ground via a telemetry link. One Princeton and one FAA pilot shared the evaluation flying. The former flew all configurations; the latter flew those judged to be most significant.

3.3 TEST CONFIGURATIONS

This section covers the general aspects of the test matrix, with specific test points being identified as they occur in the discussion of results.

3.3.1 Static Stability Tests

Basic Airframe Variables - The primary airframe variable was

the static angle of attack stability, M_α , since, with other factors fixed, it largely governs the stick force vs. speed characteristics, and changes in the parameter correspond physically to moving the center of gravity fore and aft. Key test values are shown in Table 3-1:

TABLE 3-1
TEST CONFIGURATIONS

M_α, rad/sec^2/rad	dF_s/dV @ V_{trim} (no friction) lb/kt.	Description
-12.	0.425	Very stable, forward c.g.
-6.	0.33	Nominal stable value, typical for approach or climb
-.6	-0.04	Marginal stable value, aft c.g.
+.6	-0.04	Slightly unstable value, aft c.g.
+2.4	-0.15	Moderately unstable

The second airframe variable was the pitch control effectiveness, M_δ . An experiment was conducted to select a nominal satisfactory value for the baseline stable case (M_α = -6), which was then retained for the other levels of static stability. Data are shown in the section on results.

Trim changes with power generally were set at zero, although a few tests were run with moderate variations of both signs to explore the significance of this parameter at low levels of static stability.

Both manual and electric simulated pitch trim systems were available; trim rate was not a test variable, but was pilot-adjusted to a satisfactory level for the nominal configuration.

Other airplane longitudinal characteristics were fixed at the research aircraft's nominal levels for the sake of convenience.

For a nominal approach speed of 70 kt (pilots were briefed to fly within the range 70 - 75 kt), the stability derivatives are the following (nomenclature of Ref. 6):

$(D_v - T_v) = 0.16\ sec^{-1}$ $\qquad$ $M_v = 0$

$(D_\alpha - g) = -12\ ft/sec^2/rad$ $\qquad$ $M_{\dot{\alpha}} = -0.82\ sec^{-1}$

$L_v/V_o = .0046\ ft^{-1}$ $\qquad$ $M_{\dot{\theta}} = -1.7\ sec^{-1}$

$L_\alpha/V_o = 1.2\ sec^{-1}$

The combination of the above derivatives with the previously discussed M_α variations give the following range of modal characteristics for the basic airplane:

M_α	Characteristic Roots or Eigenvalues
-12	- .071 ± 0.349j ; -1.869 ± 3.246j
-6	- .067 ± 0.325j ; -1.873 ± 2.137j
-0.6	-0.101 ± 0.159j ; -2.77 ; -0.907
+0.6	-0.355 ± 0.318j ; -3.288; +0.119
+2.4	-0.224 ± 0.435j ; -3.821; +0.389

Lateral-directional characteristics were those of the research aircraft, with roll and yaw control sensitivities set to pilot-selected favroable values; the basic qualities are good (Ref. 11) and did not distract the pilot in performing longitudinal evaluation.

Control System Variables - In order to retain a physical feel for the problem and to obtain information which will relate directly

to control system design, these variations are described in terms of real devices.

Downspring Variations:

- Constant-force downsprings from 0 to 30 lb.
- Downsprings varying with elevator deflection - linear change with δE from full down to full up, 30 lb to zero and zero to 30 lb (15 lb at the trim point, V_t = 70 kt).
- Downsprings with a pronounced change in gradient for nearly full-up elevator - one increasing, one changing sign from down-force to up-force.
- Downsprings varying with angle of attack - various ranges of α-tensioning.

Bobweight Variations:

- Constant-force bobweights, 0 to 10 lb.

Control System Dynamics - Three variations in control system dynamic characteristics (that is, the frequency and damping of the free control system apart from the rigid airframe modes) were flown:

Description	ζ_c	ω_c, rad/sec	Gradient, lb/in
L (Light)	0.7	15	2.5
N (Normal)	0.7	10	5
H (Heavy)	0.7	7	7.5

Good quantitative information on control system dynamics is sparse; the above range was based on measurements of the research aircraft and consultations with manufacturers.

A fixed, low level of coulomb friction, (about 1 lb) simulating

cable/pulley interaction was used. A small breakout force would have been desirable, but this aspect of the force-feel simulation was not available for the program. By lightplane standards,the control system displayed low-friction characteristics.

3.3.2 Maneuvering Stability Tests

Baseline Configuration - A baseline configuration was established with the following longitudinal characteristics:

- Nominal lightplane short period pitch dynamics (M_α= -6, ω_{sp}= 2.84 rad/sec, ζ_{sp}= 0.66) at a speed of 105 kt.

- Nominal wheel-type pitch control system (ω_{sp}=10 rad/sec,ζ_{sp}= 0.7, static gradient=10 lb/in at 105 kt, no imbalance or bobweight, low friction)

This combination of characteristics gave a basic stick force per g gradient of 20 lb/g, a value well above the absolute minimum for normal category of 7.14 lb/g and slightly above the "need not exceed" minimum value of 17.9 lb/g discussed in Chapter 1. (The 20-lb-per-g level is, however, not small by most current production airplane standards, as indicated by Ref. 12 measurements. Even with aft c.g., most trainers exhibit force gradients in the neighborhood of 20 lb/g, with other popular light airplanes as high as 65 lb/g; forward c.g. figures are considerably higher.)

As in the static stability tests, lateral-directional characteristics were non-interfering, being those of the research aircraft with favorable control sensitivities.

$F_{s/n}$ Variations - The primary issue addressed was the question of how much variation from linearity should be allowable. Preliminary trials indicated that the evaluations were best done at fairly low

incremental load factors to avoid excessive speed loss and exaggerated attitudes, and the following variations were selected:

Gradient, Linear portion	Slope Reduction at n = 1.5g
Nominal: 20 lb/g	0 to 100 percent
Low: 7 lb/g	0 to 100 percent

The focus of the experiment was on identification of the minimum detectable reduction in gradient.

4. RESULTS AND DISCUSSION

4.1 STATIC STABILITY EXPERIMENTS

4.1.1 General Observations

As noted in the previous section, the piloting task in this phase involved several elements: approach (both head-down on the MLS and head-up), flare and touchdown, and climb. In general, it was observed that the climb phase was the most demanding, for the following reasons:

- Since the climb followed a touch-and-go landing, there was a transient period in which the airplane was accelerating and out of trim (the trim most likely having been left at the approach setting during the landing), and the pilot was seeking the proper pitch attutude to hold the specified climb speed. By contrast, the long approach phase was relatively steady once the localizer and glide slope were acquired.

- Because of the high power used in the climb, the level of stability was slightly lower than it would be for level flight or descent conditions. This was not measured precisely, but qualitatively it seemed to reduce a slightly stable airplane (M_α = -0.60) to about neutral stability. In contrast, the most stable condition occurred during flare and touchdown, due to combined effects of low power and ground effect, and in fact a slightly unstable level-flight case (M_α = +0.60) would appear to be noticably "stiffer" longitudinally during the landing. On the other hand, the change in stability due to leaving ground effect during take off was hard to detect, most likely due to the transients of rotation and seeking a climb attitude

- Control of pitch attitude using "out the windshield" cues was notably more difficult during the climb than in the other phases, most likely because the pitch attitude was high and the sky scene usually did not

present the fixed panorama which the ground scene did on approach and landing. One pilot commented that he usually felt most confortable flying instruments shortly after breaking ground in order to quickly establish a steady climb condition by cross-checking attitude and airspeed.

All of the above effects are evident in real airplane operations, of course, and it was felt that a more realistic simulation was obtained by allowing the stability to change rather than by adjusting the systems to maintain constant characteristics. Even so, actual operations can be even more demanding than this simulation task, with power adjustments (here only a check that full power was being developed was required), trim changes due to gear and flap retraction (fixed gear; no take-off flap simulated due to questions of what levels to use and how to generalize the results), radar vectors, frequency changes, and communications. At least in its initial, more transient stages (whether originating from a take off, a missed approach, or a balked landing), the climb is an inherently high-worked situation and one in which the pilot does not have the benefit of an engaged autopilot. These general observations suggest that the climb case warrants special consideration in design and in setting standards.

4.1.2 Control Effectiveness Selection

Initial tests focused on selection of a satisfactory level of control effectiveness to be used with the baseline configuration described in Section 3.3.1. The results, based on the data from three pilots shown in Fig. 4-1, favored the value $M_\delta = .35$. Bars on the average ratings for individual pilots indicate the range of rating assigned for the various phases : approach, landing, and climb. For pilots A and B, the best rating was given to the approach phase, the worst to the climb; pilot C was not consistent in his relative rankings, but the range is small.

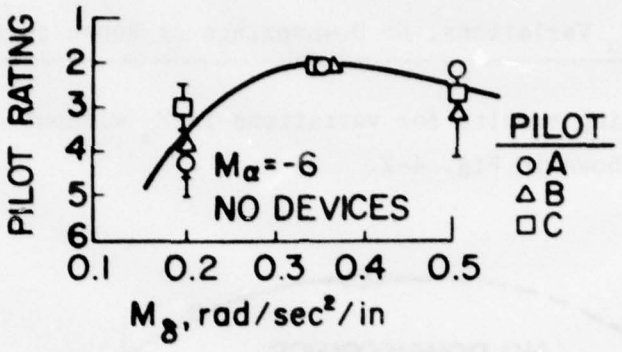

Fig. 4-1 Selection of Pitch Control Effectiveness, M_{δ_c}.

The low value of M_δ was not favored because of the relatively large control motions required, which tended to make small, quick attitude adjustments difficult. Adequate control power ($M_\delta \ \delta_{max}$) was available for lift off rotation on take off and for the landing.

Additional trials which did not involve all three pilots indicated that the selected M_δ would be satisfactory over a wide range of stable and unstable M_α ; on the other hand, ratings degrade only about 1 to 2 units for sensitivities two and one-half times as high. For high stable values of M_α , of course, the higher values of M_δ are favored in order to have adequate control power with normal cockpit control movement.

Finally, a few runs were made with the "light" and "heavy" control system configurations described in Section 3.3.1; it was found that M_δ = 0.2 was adequate for those cases, ratings remaining better than 3.5 for both.

4.1.3 Effect of M_α Variations, No Downsprings or Bobweights

Pilot rating results for variations in M_α without downspring or bobweight are shown in Fig. 4-2.

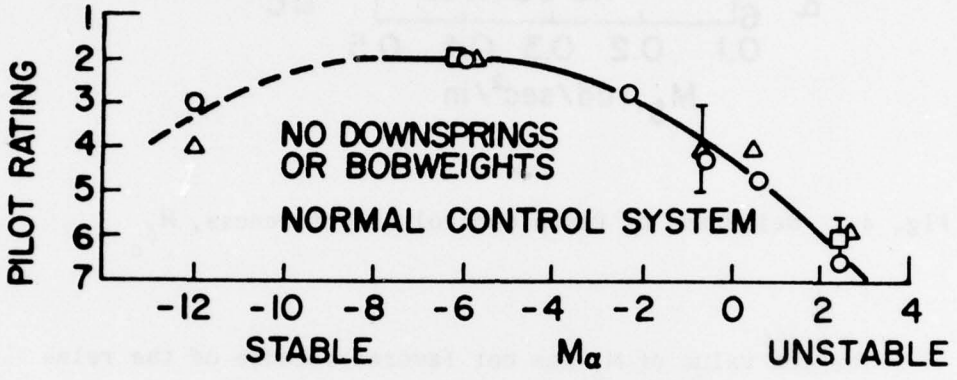

Figure 4-2. Results of M_α Variations.

The trends are the expected ones: there is little change about the very favorable baseline value, then gradual degradation as the static stability decreases. The finding that the airplane is considered unsatisfactory but acceptable with $M_\alpha = 0$ agrees with past approach tests (Ref. 9) and more recent work in which the same baseline configuration was used (Ref. 13).

Commentary indicated that airspeed and precise attitude control became progressively more difficult as M_α became positive. In the unstable cases, the pilots described their control activity as "jabbing" at the airplane to stop the frequent unwanted attitude excursions. If full attention is available, however, performance remains acceptable; the only noticeable degradation usually being in the climb case, when trouble was often experienced in stabilizing on the desired speed.

The small degradation in rating for the very stable M_α is not

too significant; it mainly is a result of being, in a comparative sense, less pleasant to flare and land due to larger stick forces.

It should be noted that the bulk of the testing was done under conditions of little wind and turbulence, and the curve certainly would shift downward somewhat under less favorable conditions. Judging by the discussion of this point in Ref. 13, past experience with the basic airplane, and a few trials carried out in moderate turbulence, the downward shift would probably be about 1.5 rating units for the low M_α end of the curve.

4.1.4 Downspring Variations

Constant Force and Elevator Deflection - Dependent Downsprings - Presented in this section are the results of flight experiments in which the various forms of downspring described in Section 3.3.1 were applied to the basic (no control system devices) airplane configurations. In particular, results will be shown for variations of -6, -0.6, +0.6, and +2.4 in M_α. Downspring variations are shown in Fig. 4-3.

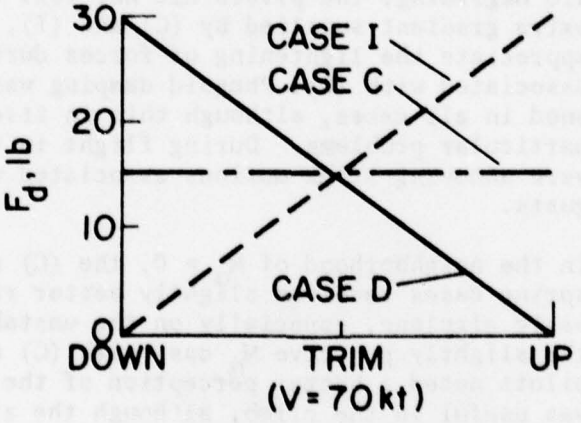

Figure 4-3. Downspring Variations with Elevator Deflection.

The three variations -- constant-force (C), increasing with up-elevator (I), and decreasing with up-elevator (D) -- are idealized versions of devices found in current airplanes. As implied in the sketch, the

force supplied by the downspring at the normal trim speed is the same for all three, and thus the local force gradient for very small elevator deflections about trim will be the same; however, as soon as any appreciable deflection takes place, the gradients will start to differ in the manner discussed in Chapter 2. In particular, type (I) will increase the gradient compared to (C), and (D) will decrease it.

Pilot rating results are shown in Fig. 4-4 for the three individual downspring cases, using data from three pilots. As in earlier figures, the bars represent the spread of ratings between approach, landing, and climb tasks; the climb generally is the critical case, especially for low M_α, due to altitude and speed-control problems.

The various downspring cases are best considered in a comparative sense, referring to Fig. 4-5, where the faired data of the previous figure are overlaid on the faired curve of Fig. 4-2, the no-downspring case. The following points are noteworthy:

- For the stable (M_α = -6) airplane, all downspring cases are degrading; the pilots did not feel the need for the extra gradient supplied by (C) and (I), and did not appreciate the lightening of forces during the flare associated with (D). Phugoid damping was noticably lightened in all cases, although this in itself did not cause particular problems. During flight in turbulence, there were annoying stick motions associated with fore-and-aft gusts.

- In the neighborhood of M_α = 0, the (C) and (I) downspring cases received slightly better ratings than the basic airplane, especially on the unstable side. For the slightly positive M_α case with (C) and (I), the pilots noted a better perception of the trim point which was useful in the climb, although the airplane would still tend to diverge if unattended even for a very short time.

- For a very unstable airplane, all three varieties of downspring help to define the trim speed and thus improve the handling of the airplane. The constant and increasing

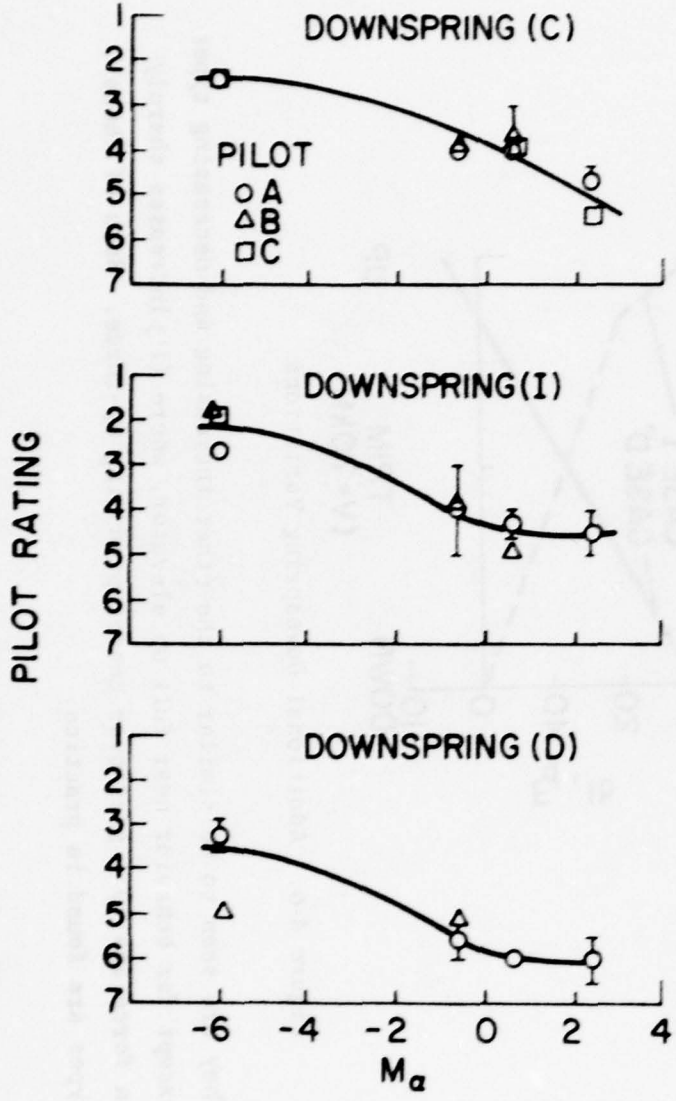

Figure 4-4. Pilot Ratings for Three Types of Downspring.

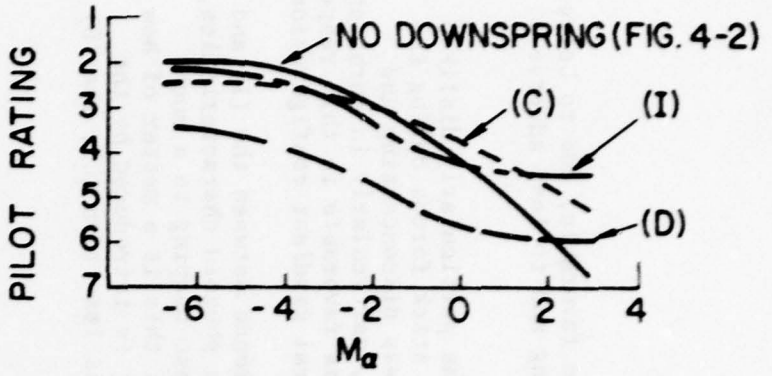

Figure 4-5. Direct Comparison of Pilot Ratings of Downspring and No-Downspring Case.

force types are clearly more favorable, due to better feel in the flare and landing and to less adverse affect on phugoid damping.

- The decreasing downspring was particularly disliked for its tendency to lighten stick forces during the flare and touchdown. This was disconcerting and sometimes led to ballooning, particularly in turbulence. The increasing downspring was favorable in this respect, especially for the low natural gradient configurations.

- There is a pronounced difference between the (I) and (D) cases in their effect on phugoid characteristics, the latter tending to decrease damping to a much greater extent. Physically, this is a matter of how much velocity stability (M_V) is introduced by the system; the (I) case produces less than (C), the (D) case more (see Chapter 2).

Other Variations - In addition to the three major downspring variations discussed above, two other minor cases were tested, as sketched in Fig. 4-6.

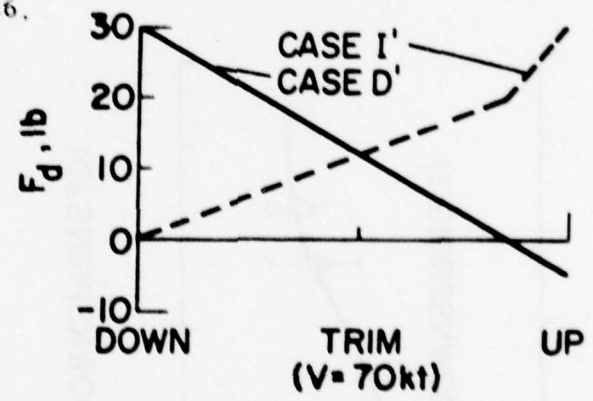

Figure 4-6. Additional Downspring Variations

They are seen to be similar to the other increasing and decreasing types except for behavior near full up elevator, where (I') increases sharply in force and (D') goes over center producing up-force. Both of these types are found in practice.

The findings for these two cases were very similar to those

for (I) and (D). Where increasing gradients were favorable, (I') was as satisfactory as (I), and vice versa. Where lightening of forces during landing was unfavorable, (D') was slightly worse than (D). In any case, the rating differences were no more than one-half unit.

Heavy and Light Control Systems - As noted in Section 3.3.1, most of the flying was done with so-called normal control system characteristics. However, some tests were repeated with the heavy and and light variations. The results were as one might predict -- if in a given situation gradients were already somewhat light, then the light system was unfavorable, and the heavy favorable. Conversely, the heavy system was not appreciated when large gradients were already present. The rating differences tended to be generally within ½ to 1 units at most.

The downspring results might be summarized as follows:

- Because of its degrading effects at normal stability levels, the smallest possible downspring should be installed if an improved force gradient at aft c.g. is needed.
- Constant or increasing-force downsprings should be used in preference to decreasing downsprings.

Angle of Attack-Tensioned Downspring - A short generalized study was made of α- tensioned downsprings. Although at least one current production airplane has such a device, the experiment did not set out to duplicate those particular characteristics. Rather, attention was focused on assessing the significance of operating points and actuator rates.

In an actual installation, the system consists of an elevator downspring attached to a servoactuator in a manner which allows extension or relaxation over a limited range. The actuator itself is

commanded by an electrical signal from an angle of attack sensor, and begins to increase spring tension at a pre-set point, thus applying a nose-down moment as speed is decreased.

The particular configurations chosen for study are sketched below (Fig. 4-7).

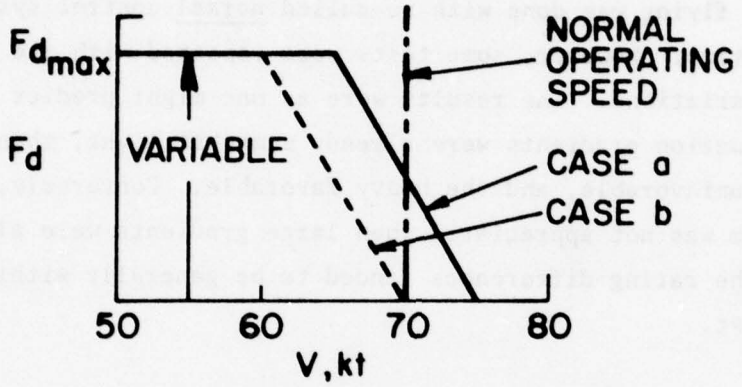

Figure 4-7. Downspring Force vs. Airspeed.

Here, F_d is the downspring contribution to the force which must be trimmed out, in a sense which increases the force-vs.-velocity gradient; the curves represent steady-state forces. The difference in the two cases is simply the position of the onset point with respect to the normal operating speed. The solid-line case (a) has one-half the available downspring force in effect at 70 kt, while the dotted-line system (b) comes into effect as speed decreases below that point.

Preliminary trials with <u>case (a)</u> immediately pointed up the significance of the rate of the (simulated) actuator. If the actuator is assumed to operate without lag or rate limit, then at any trim point between 75 and 65 kt (or any time the α-sensor is on the range which moves the actuator), there is a direct feedback of angle of attack to elevator; this results in annoying transient control forces and column motions, particularly during the landing flare and flight in turbulence (in the simulation, the angle-of-attack sensor was not "gust-proofed" in

any way). In steady flight above 75 kt, there is no input, of course, and below 65 kt, there is simply the impression of a constant downspring. In the actuation range, however, with a strong spring (30 lb, for example) the apparent "stick-pumping" action is quite undesirable.

A fast spring extension is obviously not needed if the intent is to increase the static force gradient over a particular speed range, and two approaches to slowing the simulated actuator were tried:

- First-order time lag in the actuator motion.
- Rate-limited operation of the actuator.

For the first-order time lag with case (a) above, and either a 15-lb or 30-lb maximum downspring in the M_α = - 6 airplane, it was found that a time constant of at least 3 sec was needed in order for the fast-stick transients noted above not to be at an annoying level. With τ = 5 sec, the spring force was not evident for quick maneuvering about trim, but it was obviously "catching-up" during long-term α-change maneuvers, such as the landing flare.

Although not enough data were gathered to make a complete picture, a few runs with the M_α = + 0.6 airplane and the 16-lb maximum downspring indicated that with low stability, the shorter time constants(τ=2.5 sec) imparted a favorable stiffening effect (M_α augmentation) in spite of disagreeable transients. In this case, the "catching-up" phenomenon was evident at τ = 3 sec.

The trials with case (b) (onset of spring at 70 kt), indicated that even with a favorable time delay of τ = 3 sec, the force build-up (or catching-up) was more evident than for (a), particularly during the landing.

It should be noted that where the first-order lag is used with

the actuator, the time to 63 percent of the commanded travel--the definition of the time constant-- is the measure of the speed of response regardless of input size. This was not the case with the second simulated actuator which was rate limited, so that the time to fully respond to an angle-of-attack command was proportional to the size of the input. The time to travel through the full actuator range, assuming a sufficiently large input of α, was adustable.

This rate-limited actuator arrangment conforms more closely to what is likely to be found in an actual installation. Simulation results are given below for case (a), in the middle of the tension range of the 70-kt arrangement with a 30-lb maximum downspring:

Time Required to Respond to Five-Deg α Input	Result
T_a = 10 sec	Too slow in getting to trim point; system "catching-up" all of the time.
T_a = 5 sec	Better indication of trim point due to faster actuator; still aware of delay, however.
$T_a \leq$ 4 sec	Forces build too quickly; causes pitch transients if stick position not held firmly.

As this indicates, it was difficult to find a completely satisfactory setting, although the faster ones could probably be improved by smoothing the simulated starting and stopping action. Comparative rating results for two levels of M_α and downsprings which were equivalent in size at the steady 70-kt trim point are shown in Table 4-1. The tensioned spring is seen to give the poorest results, reflecting the pilot's awareness of the system transients. It might be noted that the pilot felt that the M_α = - 6 airplane had adequate feel already, and that the degradation of the long-period mode due to either downspring

was unfortunate. The marginally stable airplane, on the other hand, was slightly improved by the constant spring which imparted better feel for the trim point, particularly during climb; although this also was true with the α-downspring, the dynamics were too noticable to consider it an improvement over the no-spring case.

TABLE 4-1

CONFIGURATION	PILOT RATING		
	No Downspring	Constant 15-lb Downspring	α - Downspring* 30-lb max, 15-lb @70kt
M_α = -6 (stable)	2	2.5	4
M_α = -0.6 (slightly stable)	4	3.5	4.5

* Actuator rate T_a = 5 sec for full travel after step α.

Trials with the constant-rate actuator and case (b) were even less satisfactory, particularly in the landing flare, where the pilot objected to the sharp onset and lagging build-up of force.

In summary, the variations of the α-downspring simulated were difficult to adjust so as to remove an awareness of transients, and although they did indeed improve the static force gradient, they seemed less satisfactory than constant downsprings of equivalent size.

4.1.5 Bobweight Variations

The discussion in Chapter 2 indicates that a bobweight of comparable size will have the same influence on the trim curves as a

downspring but will not undamp the phugoid. Constant-force bobweights were flown back-to-back with constant downsprings and confirmed the same favorable effect of trim-point definition at low M_α ; phugoid characteristics were not much of a factor in these tightly-flown tasks.

The main difference noted was in the area of turbulence response, where the bobweight system seemed to be somewhat more active, though not seriously so. Control column motions due to normal accelerations on a rough runway could be quite annoying, however.

4.2 MANEUVERING STABILITY EXPERIMENTS

4.2.1 General Observations

Although a useful evaluation routine was devised after a few preliminary trials, this sort of experiment is difficult to do for the following reasons:

- Due to a desire not to exceed maneuvering speed for the basic airplane (108 kt), the test maneuvers were initiated at 105 kt; at that speed, pitch and turn rates are high for a given load factor, and it required some planning to avoid speed bleed-off before reaching the desired stick force or incremental load factor. (A useful technique was to trim in level flight to 105 kt, then slow to a lower speed, reaccelerate toward 105 kt in a shallow dive, and initiate the maneuver as that speed was reached.)
- The evaluation must be completely subjective, since the task is not realistic as it is in approach-and-landing simulations, for example, and the pilot must try to extrapolate from contrived maneuvers to real situations.

Nevertheless, the experiment is felt to have shed light on the question of allowable nonlinearity in the stick force per g curve.

4.2.2 F_s vs. n Variations

Two basic configurations were tested, one with a nominal linear gradient F_s/n = 20 lb/g and one with a minimum (for Normal Category airplanes) gradient of 7 lb/g. Starting at an incremental load factor of about 0.5 g, variations in slope were introduced up to a complete flattening of the curve (Fig. 4-8).

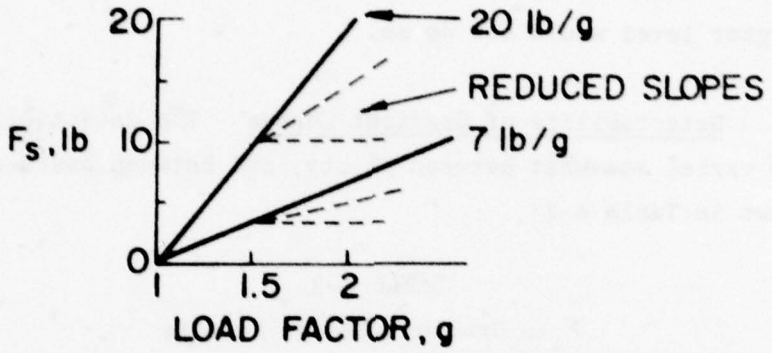

Fig. 4-8. Range of Experimental Stick Force per g

The break in the curve was intentionally kept as well-defined as the electronics would allow, since the major objective was to examine how small a slope change could be detected by the pilot.

Influence of Basic F_s/n Level - As noted in the section on configurations, the basic short-period pitch dynamics were conventional and of favorable frequency and damping ratio. The basic linear (no reduction) gradients were evaluated to be satisfactory:

Basic F_s/n	Rating	Comment
20 lb/g	3	Satisfactory; forces large enough to be useful load factor cue.
7 lb/g	3-3.5	Light, but pleasant for maneuvering; sensing Δn directly as well as force for load factor cue.

It has been suggested that at some level of F_s/n , the forces are so light that direct g sensing is the most useful cue for judging load factor. This is an interesting possibility, but not enough testing could be done at intermediate levels to determine where the crossover might be. The rating, it should be emphasized, applies to the maneuvers as flown; it does not represent a judgement as to whether or not it would prevent inadvertant overloading in a stressful situation. The feeling of at least one evaluation pilot is that even the higher level would not do so.

Detectability of Gradient Change - The detectability of slope change varied somewhat between pilots, and between basic configurations, as shown in Table 4-2:

TABLE 4-2

F_s/n Gradient Change Results

Baseline $F_s/$	Percent Gradient Reduction	Can Detect/ Acceptable or Unacceptable		
		Pilot A	Pilot B	Pilot C
20 lb/g	0	No /A	No /A	-
	20	No /A	No /A	
	40	No /A	Yes/A	
	50	Yes/A	Yes/A	
	60	-	Yes/A	
	80	Yes/U	Yes/(A)	
	100	Yes/U!	Yes/U!	
7 lb/g	0	No /A		No /A
	25	No /A		No /A
	50	No /A		Yes/A
	75	Yes/A		Yes/U
	100	Yes/(U)		Yes/U!

As indicated in the table, a gradient reduction in the neighborhood of 50 percent is detectable in both cases but also acceptable, in terms of having enough to serve as a useful indication of increasing load factor. And although there is some disagreement, it appears that

reductions in the neighborhood of 75 to 80 percent are definitely unacceptable (the parenthesis on the Pilot B rating in the 20 lb/g 80 percent reduction case indicates that although he judged it to be unsatisfactory, he would accept it; in the 7 lb/g 100 percent reduction case, Pilot A commented that it was a little hard to judge the amount of reduction; he thought he was depending on g sensing rather than force anyway, so the unacceptable rating is qualified).

4.2.3 Concluding Remarks

The question of how a higher onset load factor would affect the picture perhaps needs to be explored, the concern being that while a 50-percent reduction in gradient might be acceptable at low load factor, a sharp change of that magnitude while maneuvering very near limit load factor might induce transient overstressing.

Another concern is with cases of lower pitch damping than the heavily-damped example flown. Light short period damping is rarely seen in conventional small airplanes, but unconventional configurations and the growing trend toward high altitude flight could lead to situations where control over load factor is less precise. This line of thinking leads, of course, to the broader question of whether or not the civil standards should have quantitative rather than simple qualitative criteria for short period characteristics.

Except for these two areas, however, it would appear that there is no reason to require linearity in the F_s vs n curve, and the military specification allowance of 50-percent variation in slope is a reasonable one. However, it would appear advisable to require testing to limit load factor rather than extrapolating low-g data if there is any reason to suspect that a greater change or reversal might occur.

5. CONCLUSIONS

The following conclusions are based upon the background study and in-flight simulation experiments described in the report. The experiments were carried out in the context of typical small airplane operations in low levels of turbulence, with continuous pilot attention; the evaluators were experienced test pilots.

5.1 STATIC STABILITY

- Pitch control effectiveness, M_δ, may be as low as 0.2 rad/sec^2/in and still be satisfactory, provided M_α is in the moderately stable range. Generally, levels of M_δ greater than 0.3 are preferred, particularly if the static stability is high.

- Moderate levels of static stability are preferred for the terminal area tasks involved in these tests. High levels of M_α lead to objectionable forces during landing; low (moderately unstable) levels are associated with problems of attitude and speed control, particularly in climbing flight.

- There is little perceptible difference in flying qualities between a slightly statically stable and a slightly unstable airplane, and both are found to be acceptable for terminal area operations; however, with even small instability, there is room for concern over the possible consequences of pilot distraction.

- Installation of a constant-force device (downspring or bobweight) to steepen the stick force vs velocity gradient tends to improve controllability for unstable M_α at the expense of degrading the stable cases; in general, the spring or bobweight gradient will not provide the same level of flying qualities as a natural gradient of the same magnitude because of unfavorable changes in the airframe dynamic modes.

- A downspring which increases tension with increasing up-elevator deflection generally provides the same level of flying qualities as a constant-force spring (both providing the same force level at some nominal operating point). A decreasing-force (with up elevator) spring is decidedly less favorable due to its introducing a larger increment of velocity stability, M_V, (and hence less phugoid damping) and lightening of control forces during landing.

- The type of downspring which increases tension with increasing angle of attack is effective in improving the static force gradient over a desired speed range, but it is sensitive to actuation rate and onset point; high rates result in fluctuating stick forces, low rates to noticeable lagging or "catching-up" action. The transient nature of the system is more noticeable if the nominal operating speed coincides with the actuation onset point.

5.2 MANEUVERING STABILITY

- A 50-percent reduction in slope of the stick force vs. load factor curve, can be detected during maneuvering, but for the cases tested (good pitch damping, 20-and 5-lb/g basic gradients),this was not considered to be degrading. Though pleasant for intentional maneuvering, such low F_s/n levels are unlikely to prevent inadvertent overstressing.

- At low basic stick force levels ($F_s/n = 10$), there is some evidence that force itself is not a reliable load factor cue, and the pilot must resort to direct sensing of normal acceleration.

- A 70-to-80 percent reduction in F_S/n gradient is unacceptable and may lead to an inadvertent increase in load factor during a maneuver. This suggests that if such behavior is noted or suspected, compliance with FAR 23.155 should not be based upon extrapolation of F_s/n determined at low load factor.

APPENDIX A
THE IN-FLIGHT SIMULATOR

A.1 GENERAL DESCRIPTION

The In-Flight Simulator (Fig. A-1) is based upon a modified Ryan Navion airframe; the power plant is a Teledyne-Continental IO-520B engine of 212.6 kw (285 hp) driving a Hartzell reversing propeller. Gross weight has been increased from the original 12,230 to 14,010 N (2570 to 3150).

Two externally noticeable airframe modifications have been made to improve the research capability of the machine. The flap hinging and actuation have been changed to allow up, as well as down,

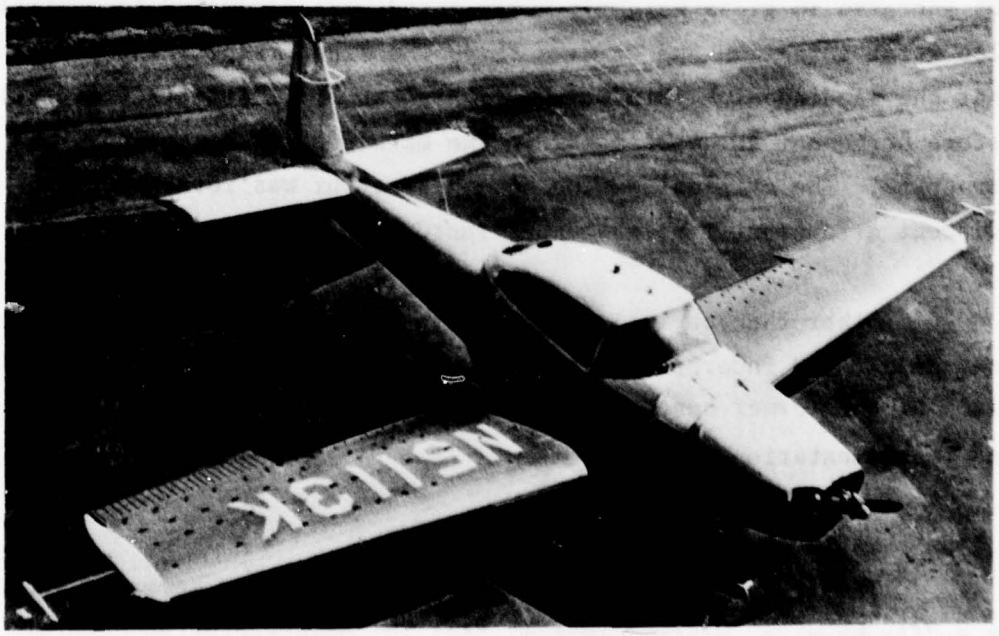

Figure A-1 Five-Degree-of Freedom (5-DOF) In-Flight Simulator, Navion N5113K.

deflection over a ±30-deg range, resulting in increased lift modulation authority and smaller drag changes compared to the previous 0-40 deg down-only flap. Aerodynamics of the basic airframe and of this flap arrangement were explored in the full-scale wind tunnel tests reported in Ref. 15 and 16. The second change is an increase in vertical tail area which was made necessary by serious losses in directional stability when operating in the reverse thrust range. This was predicted by the wind tunnel tests and confirmed in flight. A 35.6 cm (14 in) extension, added to the base of the fin and bottom of the rudder, increased vertical tail area by nearly 50% and solved the problem, at the expense of increased gust response and high rudder pedal forces in forward-thrusting flight.

The normal Navion main landing gear struts have been replaced with those from a Camair twin (Navion conversion with nearly 40% increase in gross weight). Drop tests were conducted to optimize oleo strut inflation and orifice size, the final results indicating that the landing sink rate may be as high as 3.8 m/sec (12.5 ft/sec) before permanent set will occur in the main gear or attaching structure. The original Navion nose gear strut was retained, but adjacent attachment fittings and structure have been strengthened.

Other changes included redesign and relocation of the instrument panel, and incorporation of a single rear seat arrangement in place of the former bench seat in order to accomodate electronics and instrumentation equipment.

A.2 VARIABLE-RESPONSE CONTROL SYSTEM

The In-Flight Simulator utilizes what is now commonly known as a "fly-by-wire" control system, that is, power-actuated control surfaces commanded by electrical signals. The signals come from the various cockpit controllers and motion sensors; when appropriately processed and summed, they provide net signals to the servo-actuators,

changing airplane response as desired. In this case, the servos are hydraulic, supplied by an engine-driven hydraulic pump delivering about .03 m^3/min at 5 x 10^6 N/m^2 (9 gpm at 725 psi pressure). Independent control over the three angular and two of the three linear degrees of freedom is provided; independent side-force control is not provided.

Moment Controls - Control over pitching, rolling, and yawing is obtained from conventional elevator, aileron, and rudder control surfaces. The full authority (that is, maximum travel) of each surface is available, and the maximum deflection rate in each case is about 70 deg/sec. At a typical low operating speed of 70 kt, the available control powers are, respectively:

Pitch: ± 4.4 rad/s^2 (from trim)
Roll: ± 4.1 rad/s^2
Yaw: ± 1.3 rad/s^2

The presently available inputs to each of these controls are shown in Table A-1.

Normal Force Control - Independent control over normal acceleration is exercised through the Navion flap, modified to deflect up, as well as down, through a ± 30-deg range. The upward motion provides increased lift modulation authority and tends to minimize the problems of drag and angle-of-zero-lift changes. Actuation is hydraulic, with a maximum available surface rate of 110 deg/sec. At 70 kt, the available authority is slightly more than ± 5 g. Inputs presently available are shown in Table A-2.

Thrust Control - Thrust and drag modulation is by direct control of the blade pitch on the Hartzell reversing propeller, with the engine governed at 2300 ± 30 rpm by means of a tachometer feedback and throttle servoactuator. This system allows precise control

TABLE A-1. INPUTS OF MOMENT CONTROLS

CHANNEL	INPUT	FUNCTION VARIED
Pitch	Control column displacement	Control sensitivity
	Thrust lever	Simulated moment due to thrust
	Column thumbwheel	Simulated DLC moment
	Radar altitude	Ground effect moment
	Airspeed	Speed stability
	Angle of attack	Static stability, pitching at stall
	Pitch attitude	Attitude hold sensitivity
	Pitch rate	Pitch damping
	Flap angle	Trim change from flap
	Flap rate	Moment from flap rate (Approximately $M_{\dot{\alpha}}$)
	Propeller pitch	Moment due to thrust
	Integral of column displacement	Rate command gain
	Simulated turbulence	Turbulence response
Roll	Wheel displacement	Control sensitivity
	Sideslip	Dihedral effect
	Roll rate	Roll damping
	Yaw rate	Roll due to yaw rate
	Rudder pedal displacement	Roll due to rudder
	Simulated turbulence	Turbulence Response
Yaw	Rudder pedal displacement	Control sensitivity
	Sideslip	Directional stability
	Yaw rate	Yaw damping
	Roll rate	Yaw due to roll rate
	Wheel displacement	Yaw due to aileron
	Simulated turbulence	Turbulence response

over thrust and drag at flight path angles and/or deceleration rates well beyond the capability of the basic airplane with normal powerplant and closed throttle.

Propeller blade pitch is commanded through an electro-hydraulic actuator connected to the mechanical-feedback servo which normally drives the reversing propeller when it is operating in its "Beta" mode. The blade pitch range presently used is +25 to -8 deg. With the engine governed at 2300 rpm, this provides performance ranging from modest climb (about 152 m/min or 500 ft/min) to steep descent ($\gamma \simeq -18$ deg with V = 70 kt). Maximum blade actuation rate is about 20 deg/sec. Inputs to the thrust/drag modulation system are shown in Table A-3.

Interconnects - It may be noted in the lists of inputs for the system (Tables A-1 to A-3) that several coupling functions are provided. For some experiments, it is desirable to remove interacting effects in the basic airframe. Lift and moment changes from thrust may be eliminated with interconnects between the propeller pitch sensor and the flap and elevator. Pitching moments due to flap angle and flap rate are countered with inputs to the elevator.

Simulated interacting effects are handled by using inputs from the various cockpit controllers. Pitching moments and lift changes due to power are provided by interconnecting the elevator and the flap with the thrust lever (M_{δ_T}, L_{δ_T}). Lift and drag changes due to pitch controller displacement are represented in L_{δ_S} and D_{δ_S}. Other controllers may be similarly interconnected.

TABLE A-2. INPUTS TO NORMAL FORCE CONTROL

INPUT	FUNCTION VARIED
Control column displacement	Lift due to control (simulates elevator lift, or direct lift control integrated with column)
Thrust lever displacement	Lift due to thrust, direct lift control integrated with throttle
Column thumbwheel	Separate direct lift control
Radar altitude	Ground effect lift; wind gradients
Airspeed	Lift change with speed
Angle of attack	Lift response to angle of attack, lift change at stall
Propeller pitch	Lift due to thrust
Simulated turbulence	Turbulence response

TABLE A-3. INPUTS TO THRUST/DRAG MODULATION SYSTEM

INPUT	FUNCTION VARIED
Control column displacement	Drag due to control (simulated control surface drag; drag due to direct lift controls integrated with column)
Thrust lever displacement	Thrust command/throttle sensitivity
Column thumbwheel	Drag change due to direct lift control (separate controller)
Radar altitude	Ground effect drag change; wind gradients
Airspeed	Drag change with speed
Angle of attack	Drag change with angle of attack

A.3 COCKPIT AND EVALUATION PILOT CONTROLS

The instrument panel and controls are shown in Fig. A-2. The right seat is occupied by the safety pilot, who operates the normal Navion wheel and rudder and the power plant controls which have been relocated on the right side of the cockpit. Simulation system controls occupy the right side of the panel and the lower and middle consoles.

The evaluation pilot is seated on the left and is provided with a standard flight instrument layout and conventional column, rudder, and throttle controls. Linear force gradients with no significant nonlinearities are provided for the roll and yaw controls. The values shown in Table A-4 are currently being used. The throttle control features adjustable friction and travels over a total range of 13.3 cm (5.25 in).

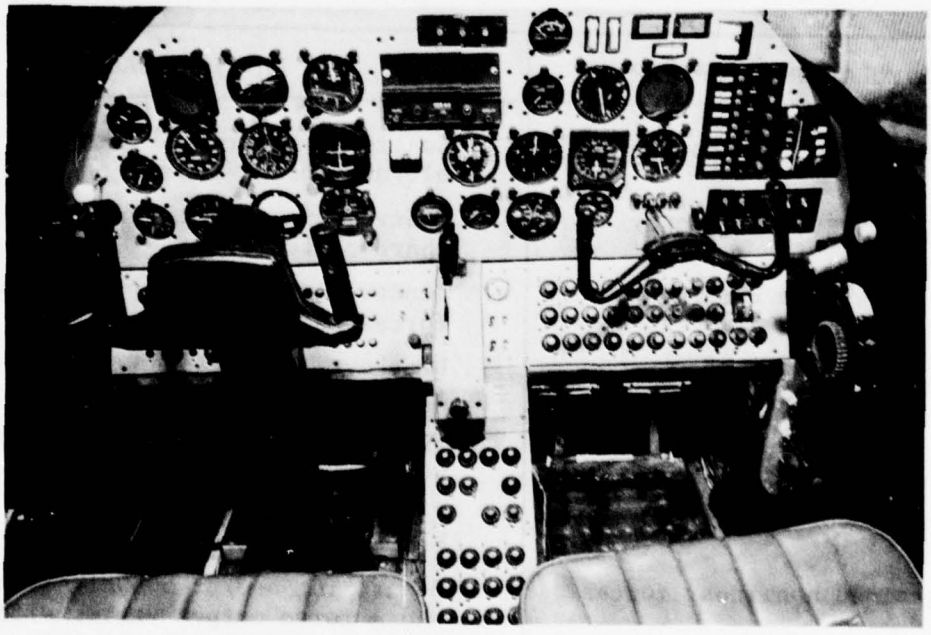

Figure A-2 Instrument Panel and Controls of the 5-DOF In-Flight Simulator

TABLE A-4. ROLL AND YAW CONTROL FORCE GRADIENTS

CONTROL	TRAVEL	GRADIENT
Wheel (Roll)	±18.7 cm (±7.35 in) ±80°	3.3 N/cm (1.9 lb/in)
Pedals (Yaw)	±6.3 cm (±2.5 in)	44 N/cm (25 lb/in)

A variable force-feel system is provided in the pitch axis. The functional details are covered in Appendix B; here it is sufficient to note that cockpit controls are provided for the parameters listed in Table A-5.

TABLE A-5. LONGITUDINAL FEEL SYSTEM PARAMETERS

SIMULATION PARAMETER	PHYSICAL PARAMETER
Column force gradient	Control geometry and gearing; elevator hinge moments
Control system frequency	Control system mass and inertia characteristics
Control system damping	Linear damping due to aerodynamic forces on control surface
Friction	Breakout (static) and sliding friction forces
"q" - feel	Force variations due to airspeed change
Force-producing devices	Constant-force downspring and bobweight
Programmed nonlinear forces	Downspring and/or bobweight whose force output varies with elevator deflection or angle of attack.

Special controls presently installed include the following:

- Direct Lift - Thumbwheel separate controller; integrated with pitch column; integrated with throttle. Adjustable moment and drag interconnects are available.
- Pitch Attitude Command - Proportional to column displacement, with trimmable attitude hold.
- Pitch Rate Command - Proportional to column displacement with attitude hold.

Attitude hold may also be selected with any portions of the direct lift system engaged.

A.4 DATA ACQUISITION

Data acquisition is through telemetry, with 43 channels available. Airframe motion parameters (linear accelerations, angular rates, attitude, and heading), control inputs, and performance measures, such as localizer and glide-slope deviation, are normally recorded. Altitude and altitude rate are available from the radar altimeter.

Correlation of touchdown time with the other parameters is obtained through a recording of fore-and-aft acceleration of the main landing gear strut. Wheel spinup loads produce enough strut motion to record even very smooth landings.

A.5 SAFETY CONSIDERATIONS

By its very nature, landing research involves repeated exposure to minimum-speed, low-controllability situations, so special consideration was given to providing sufficient airframe strength and simulation system reliability to make the risk of damage from occasional hard touchdowns or control system failures acceptably low. The matter of strengthened landing gear was mentioned in an earlier section; the control system aspects are discussed here.

Safety Pilot Function - Fundamental to the operation of an in-flight simulator is the concept that a safety pilot will continually follow the movements of the basic airplane controls, monitor the systems and the flight path, and be ready to disengage or override the evaluation pilot in case of a malfunction or unsafe condition. For disengaging, a disconnect switch on the control wheel is the primary cutout, with the main electrical and hydraulic controls providing secondary means of deactivating the system.

Manual override of the hydraulic servoactuators is possible for all controls except the flap. The force required is set through an adjustable poppet valve on each servo, 178 N(40 lb) being a typical value.

Warning of system failures is provided by a flashing master warning light on the upper edge of the instrument panel in front of the safety pilot, with individual channel disengage warning indicators on a panel slightly lower and to the right.

Redundant Control Channels - The elevator, aileron, and throttle systems incorporate redundant control channels. The philosophy here is that hard-over control inputs resulting from system failures are particularly dangerous in this low-speed, low-altitude situation and should be guarded against if possible. With the redundant channels, any substantial error between the commanded and actual control position is detected, and a switchover to a second servo is made. The evaluation pilot retains control during this process, but all inputs to the switched channel, except those from the control column, are eliminated, thus reducing the possibility that a defective transducer or signal path is causing the problem. Redundant sensors for the control input signal are incorporated; the other transducers are not duplicated. The fact that a channel

has switched to the secondary servo is communicated to the safety pilot by the aforementioned warning lights; he can then disengage the system and assume control.

The elevator is clearly critical with regard to failures which result in sudden full deflection, with the ailerons only slightly less so. Redundancy was incorporated in the throttle channel to reduce the possibility of a failure, which would apply power with the propeller blade pitch below the normal low-pitch stop, a condition which would overspeed the engine. Redundancy was not incorporated in the rudder or propeller pitch channels, because inadvertent disengagements were felt to be less critical. Since he follows pedal and Beta motions continuously, the safety pilot can very effectively override large-deflection failures. The flap channel was not duplicated because most failure modes are not hazardous -- the surface trails aerodynamically at a 10-deg down position; upon disengagement, its return to this position from up-deflection is rapid. Down-flap deflections clearly pose no safety problem; up-flap hardovers could be hazardous due to the large lift loss, but this has proved to be a failure mode so instantly recognizable by the safety pilot that a disengagement (with subsequent down-float of the flap) can be effected with very small altitude loss.

Waveoff Automation - To aid the safety pilot in recovering from an excessive sink rate situation, an "abort mode" system disengagement can be used. Activated by pressing the disengage thumb switch, the flap travels at maximum rate to a 20-deg down position, and power is automatically advanced to a climb setting; primary control reverts to the safety pilot. Using this system, recovery from a 70-kt, 6-deg approach (sink rate of 3.8 m/sec or 12.5 ft/sec with a simulated up-flap failure) can be made with less than 3-m (10-ft) altitude loss.

APPENDIX B

LONGITUDINAL FORCE-FEEL STICK SYSTEM

The key element in the force-feel stick system is a hydraulic servomechanism. Pilot input (stick force) is sensed by strain gages; this signal then becomes the input to the stick force model, which electronically computes what the corresponding stick displacement should be. The output of the model is a commanded stick position; it is the input to a stick positioner device (i.e., a servo with position feedback). This appendix shows how the stick force equation is modeled.

The forces felt by a pilot can be grouped in the following four types:

- Forces due to aerodynamic hinge moments on the control surfaces
- Forces due to mechanical-inertial properties of the stick elevator, and cable system
- Bobweight and downspring forces
- Servo actuator force feedback

This section presents the assumptions and simplifications used in the 5-DOF In-Flight Simulator's force-feel system.

B.1 FORCE-FEEL STICK MODEL FOR IN-FLIGHT SIMULATOR

Stick Force Due to Aerodynamic Hinge Moments - The stick force due to the aerodynamic hinge moment is

$$F_a = -GH \qquad \text{(B-1)}$$

where G is a constant representing the elevator stick gearing and H

represents the sum of all aerodynamic hinge moments. Hinge moments may be nondimensionalized according to

$$H = 1/2\rho V^2 S_e c_e C_H \tag{B-2}$$

or

$$H = q\, S_e c_e C_H \tag{B-3}$$

S_e represents the surface area of the elevator, and c_e is the elevator chord. C_H depends mainly on elevator deflection, angle of attack of the tail, and tab deflection. C_H also depends on elevator deflection rate (or $\dot{\delta}_e$), as well as $\dot{\alpha}_t$, $\dot{\Theta}$, and $\dot{V}$; these effects were ignored. Therefore, the stick force due to aerodynamic hinge moments may be represented by

$$F_a = - qS_e c_e G(C_{h\alpha}\cdot\alpha_t + C_{h\delta_e}\cdot\delta_e + C_{h\delta_{tab}}\cdot\delta_{tab}) \tag{B-4}$$

assuming a linear relation for the parameters $C_{h\alpha}$, $C_{h\delta_e}$, and $C_{h\delta_{tab}}$. For simplicity, assume that

$$K_a = - S_e c_e G(C_{h\alpha}\cdot\alpha_t + C_{h\delta_e}\cdot\delta_e + C_{h\delta_{tab}}\cdot\delta_{tab}) \tag{B-5}$$

Then,

$$F_a = K_a \cdot q \tag{B-6}$$

Stick Forces Due to the Mechanical-Inertial Properties of Control System - These forces can be expressed as the sum of three terms: inertia force, viscous friction force, and Coulomb friction force:

$$F = I_{eff}\ddot{\delta}_s + B\dot{\delta}_s + F_c \tag{B-7}$$

I_{eff} represents the effective control system moment of inertia, B is the viscous friction coefficient (constant), and F_c, represents Coulomb friction, which can be expressed as a function of the Coulomb friction magnitude, C:

$$F_c = C\,|\dot{\delta}_s|/\dot{\delta}_s \qquad \text{(B-8)}$$

Bobweight and Downspring Forces - Mass unbalance in the control system of the airplane has the same effect as a bobweight. It is expressed generally as

$$F_b = K_b \cdot n_z \qquad \text{(B-9)}$$

or

$$F_b = N_b(\alpha \text{ or } \delta_e)n_z \qquad \text{(B-10)}$$

Here, K_b is a linear bobweight constant, N_b is a nonlinear coefficient (when the nonlinear control system is employed), and n_z equals normal acceleration. The downspring force may be represented by either of the following equations:

$$F_d = K_d \qquad \text{(ordinary downspring)} \qquad \text{(B-11)}$$

or

$$F_d = N_d(\delta_s \text{ or } \alpha) \qquad \text{(nonlinear downspring, in which force depends on stick position or angle of attack)} \qquad \text{(B-12)}$$

Servo Actuator Force Feedback - When fully powered control systems are employed, there exists servo actuator force feedback, such as a force due to hydraulic flow in the valve and valve force, etc.; these forces are neglected, as they can be "lumped" with the other forces in the model.

Synthesis of Force-Feel System - From the above analysis, the stick force to be simulated in the force-feel system, can be expressed by the following equation:

$$F_s = I_{eff}\ddot{\delta}_s + B\dot{\delta}_s + F_c + K_a \cdot q + K_b \cdot n_z + K_d \qquad \text{(B-13)}$$

This model assumes that normal downsprings and bobweights are employed. The block diagram representation of this stick force model is shown in Fig. B-1.

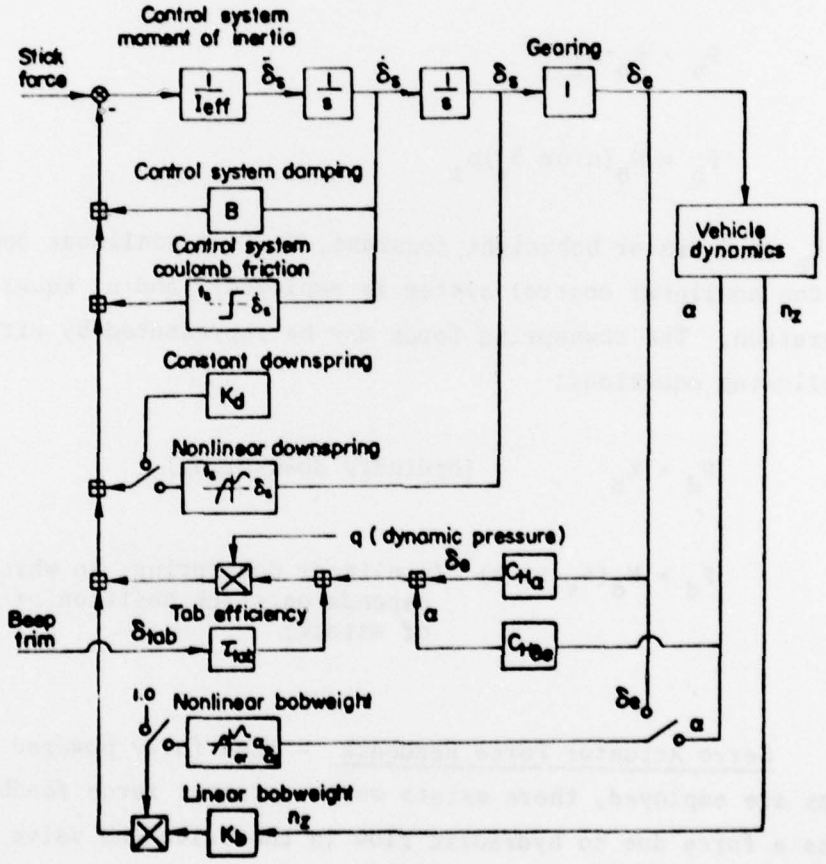

Figure B-1. Block Diagram Representation of Force Feel Stick System.

B.2 FORCE-FEEL STICK SYSTEM FOR FIXED-BASE SIMULATOR

The previous section shows the total stick force to be,

$$F_s = I_{eff}\ddot{\delta}_s + B\dot{\delta}_s + F_c - \frac{1}{2}\rho V^2 S_e c_e G\,(C_{h\alpha}\cdot\alpha_t + C_{h\delta_e}\cdot\delta_e + C_{h\delta_{tab}}\cdot\delta_{tab}) + F_b + F_d \qquad \text{(B-14)}$$

Assume that the force due to the bobweight and downspring are from ordinary bobweights and downsprings:

$$F_b = K_b\cdot n_z \text{ and } F_d = K_d \qquad \text{(B-15)}$$

Neglecting the term $C_{h\alpha}$, which is typically about zero, and the Coulomb friction term results in

$$F_s = I_{eff}\ddot{\delta}_s + B\dot{\delta}_s + KV^2(C_{h\delta_e}\cdot\delta_e + C_{h\delta_{tab}}\cdot\delta_{tab}) + K_b\cdot n_z + K_d \qquad \text{(B-16)}$$

where $K = -\frac{1}{2}\rho S_e c_e G$

To make the stick force equation suitable for an analog computer, it is convenient to linearize about an equilibrium condition. Expansion of the stick force equation begins with

$$F_s = I_{eff}(\ddot{\delta}_{s_o} + \Delta\delta_s) + B(\dot{\delta}_{s_o} + \Delta\dot{\delta}_s) + K(V_o + \Delta V)^2\, C_{h\delta_e}(\delta_{e_o} + \Delta\delta_e) + C_{h\delta_{tab}}(\delta_{tab_o} + \Delta\delta_{tab}) + K_b\left[n_{z_o} + \Delta n_z\right] + K_d \qquad \text{(B-17)}$$

By neglecting second-order terms (e.g., $\Delta V^2 \cdot \Delta\delta_e$ or $\Delta V \cdot \Delta\delta_e$), the stick force equation becomes

$$F_s = I_{eff}(\ddot{\delta}_{s_o} + \Delta\ddot{\delta}_s) + B(\dot{\delta}_{s_o} + \Delta\dot{\delta}_s) + KV_o^2 \left[C_{h\delta_e} \cdot \delta_{e_o} + C_{h\delta_e} \cdot \Delta\delta_e \right.$$

$$\left. + C_{h\delta_{tab}} \cdot \delta_{tab_o} + C_{h\delta_{tab}} \cdot \Delta\delta_{tab} \right] + 2KV_o\Delta V \left[C_{h\delta_e} \cdot \delta_{e_o} + C_{h\delta_{tab}} \cdot \delta_{tab_o} \right]$$

$$+ K_b \left[n_{z_o} + \Delta n_z \right] + K_d \qquad \text{(B-18)}$$

Since the initial condition was one of trim flight, $\ddot{\delta}_{s_o}$ and $\ddot{\delta}_s$ are both zero. For trim flight, the following also must be true:

$$K_b(n_{z_o}) + K_d = KV_o^2 \left[C_{h\delta_e} \cdot \delta_{e_o} + C_{h\delta_{tab}} \cdot \delta_{tab_o} \right] \qquad \text{(B-19)}$$

This simply says that <u>initially</u> any force due to downspring and bobweight must be balanced by the sum of the initial aerodynamic hinge moments. Therefore, the stick force equation becomes

$$F_s = I_{eff}\Delta\ddot{\delta}_s + B\Delta\dot{\delta}_s + KV_o^2 \left[C_{h\delta_e} \cdot \Delta\delta_e + C_{h\delta_{tab}} \cdot \Delta\delta_{tab} \right]$$

$$+ 2KV_o\Delta V \left[C_{h\delta_e} \cdot \delta_{e_o} + C_{h\delta_{tab}} \cdot \delta_{tab_o} \right] + K_b(n_z) \qquad \text{(B-20}$$

This equation can be rewritten by noting that

$$2KV_o\Delta V \left[C_{h\delta_e} \cdot \delta_{e_o} + C_{h\delta_{tab}} \cdot \delta_{tab_o} \right] = \frac{2 \cdot \Delta V \cdot V_o^2 K}{V_o} \left[C_{h\delta_e} \cdot \delta_{e_o} + C_{h\delta_{tab}} \cdot \delta_{tab_o} \right]$$

and

$$V_o^2 K \left[C_{h\delta_e} \cdot \delta_{e_o} + C_{h\delta_{tab}} \cdot \delta_{tab_o} \right] = F_d + F_b$$

Therefore, Equation B-20 can be expressed as

$$F_s = I_{eff}\ddot{\Delta\delta}_s + B\dot{\Delta\delta}_s + G(H_{\delta e}\cdot\Delta\delta_e + H_{\delta_{tab}}\cdot\Delta\delta_{tab}) + K_b(\Delta n_z) + 2(F_d+F_b)\Delta V/V_o \quad \text{(B-21)}$$

Since $G\cdot\Delta\delta_e = \Delta\delta_s$,

$$F_s = I_{eff}\ddot{\Delta\delta}_e + B\dot{\Delta\delta}_s + H_{\delta e}\cdot\Delta\delta_s + GH_{\delta tab}\cdot\Delta\delta_{tab} + K_b(\Delta n_z) + 2(F_d+F_b)\Delta V/V_o \quad \text{(B-22)}$$

or

$$\left[F_s - GH_{\delta tab}\cdot\Delta\delta_{tab} - K_b(\Delta n_z) - 2(F_d+F_b)\Delta V/V_o\right] 1/H_{\delta e} = I_{eff}\ddot{\Delta\delta}_s/H_{\delta e} + (B/H_{\delta e})\dot{\Delta\delta}_s + \Delta\delta_s$$

$$\left[F_s - GH_{\delta tab}\cdot\Delta\delta_{tab} - K_b(\Delta n_z) - 2(F_d+F_b)\Delta V/V_o\right] 1/H_{\delta e} = \ddot{\Delta\delta}_s/\omega^2 + 2\zeta\dot{\Delta\delta}_s/\omega + \Delta\delta_s \quad \text{(B-23)}$$

where

$$\omega^2 = H_{\delta e}/I_{eff} \quad \text{(B-24)}$$

$$2\zeta\omega = B/I_{eff} \quad \text{(B-25)}$$

The above equation represents the stick force equation as it might be modeled for simulation purposes. The right-hand side is a second-order differential equation which may be represented as in Figure B-2.

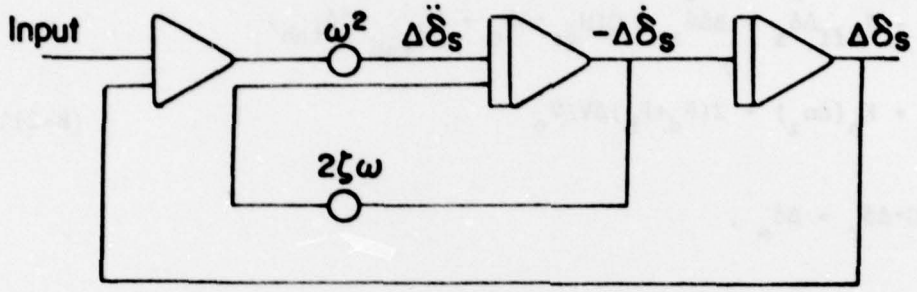

Figure B-2. Second-Order Stick-Force Model.

Assuming no input, the model is a representation of

$$\Delta\ddot{\delta}_s/\omega^2 + 2\zeta\Delta\dot{\delta}_s/\omega + \Delta\delta_s = 0 \qquad \text{(B-26)}$$

or

$$\Delta\ddot{\delta}_s/\omega^2 = (-2\zeta/\omega)\ \Delta\dot{\delta}_s - \Delta\delta_s \qquad \text{(B-27)}$$

Multiplying both sides by ω^2,

$$\Delta\ddot{\delta}_s = -2\zeta\omega\Delta\dot{\delta}_s - \Delta\delta_s\omega^2 \qquad \text{(B-28)}$$

exactly the representation shown above.

The model which was tested used only a force input; inputs due to tab, n_z, downspring, and bobweights were neglected. This gives

$$F_s = \Delta\ddot{\delta}_s/\omega^2 + 2\zeta\Delta\dot{\delta}_s/\omega + \Delta\delta_s \qquad \text{(B-29)}$$

The corresponding block diagram is shown in Fig. B-3.

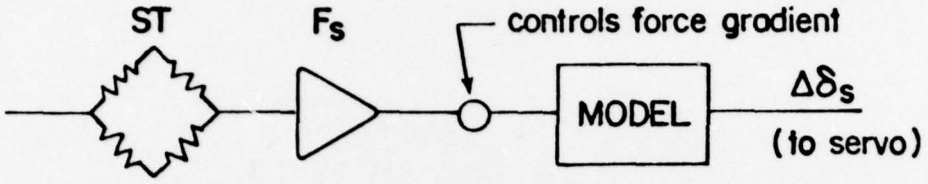

Figure B-3. Block Diagram Representation Force-Feel Model for Analog Computer System.

The potentiometer shown represents the force gradient and may be varied to give different levels.

REFERENCES

1. Smith, C. B., "The Effect of Bobweight and Downspring on the Longitudinal Dynamic Stability of an Airplane", Princeton University Aeronautical Engineering Report No. 229, May 1953.

2. Goldberg, J. H., "Effects of Spring and Inertia Device on the Longitudinal Stability of Aircraft", Princeton University Aeronautical Engineering Report No. 236, 1953.

3. Anon., "Federal Aviation Regulations, Part 23, Airworthiness Standards: Normal, Utility, and Aerobatic Category Airplanes", Department of Transportation, June 1974.

4. Anon., "Military Specification, Flying Qualities of Piloted Airplanes", MIL-F-8785B(ASG), 7 Aug. 1969.

5. Chalk, C. R. et.al, "Background Information and User Guide for MIL-F-8785B(ASG), Military Specification-Flying Qualities of Piloted Airplanes", August 1969.

6. Seckel, E., Stability and Control of Airplanes and Helicopters, Academic Press, New York, 1964.

7. Perkins, C. D. and Hage, R. E., Airplane Performance, Stability, and Control, J. Wiley and Sons, New York, 1949.

8. Eshelby, M. E., "The Influence of Short Springs on Longitudinal Static Stability", Cranfield Institute of Technology, Cranfield Report Aero No. 29, March 1975.

9. Ellis, D. R., "Flying Qualities of Small General Aviation Airplanes: Part 4, Review of Recent In-Flight Simulation Experiments and Some Suggested Criteria", FAA-RD-71-118, Dec. 1971.

10. Harper, R. P. and Cooper, G. E., "The Use of Pilot Rating in the Evaluation of Aircraft Handling Qualities", NASA TN D-5152, April 1969.

11. Ellis, D. R. and Tilak, N. W., "An In-Flight Investigation of Lateral Control Nonlinearities", NASA CR-2625, November 1975.

12. Ellis, D. R., "A Study of Lightplane Stall Avoidance and Suppression", FAA-RD-77-25, February 1977.

13. Joslin, R. and Ohmiya, H., "A Study of an Open-Loop System for Decoupling Airspeed and Flight Path Control", Princeton University Report No. 1324, March 1977.

14. Neal, T. P., "The Influence of Bobweights and Downsprings on Flying Qualities", SAE Paper 710388, March 1971.

15. Seckel, E., and Morris, J. J., "Full-Scale Wind Tunnel Tests of a Low-Wing, Single-Engine, Light Plane with Positive and Negative Propeller Thrust and Up and Down Flap Deflection", NASA CR-1783, August 1971.

16. Shivers, J. P., Fink, M. P., and Ware, G. M., "Full-Scale Wind Tunnel Investigation of the Static Longitudinal and Lateral Characteristics of a Light Single-Engine Low-Wing Airplane", NASA TN D-5857, June 1970.